Medhani, Rezene Gurmu

STABILIZATION OF PONCA CITY SHALE

The University of Oklahoma PH.D. 1982

PLEASE NOTE:

In all cases this material has been filmed in the best possible way from the available copy. Problems encountered with this document have been identified here with a check mark __√__.

1. Glossy photographs or pages _____
2. Colored illustrations, paper or print _____
3. Photographs with dark background __✓__
4. Illustrations are poor copy __✓__
5. Pages with black marks, not original copy _____
6. Print shows through as there is text on both sides of page _____
7. Indistinct, broken or small print on several pages __✓__
8. Print exceeds margin requirements _____
9. Tightly bound copy with print lost in spine _____
10. Computer printout pages with indistinct print _____
11. Page(s) _____ lacking when material received, and not available from school or author.
12. Page(s) _____ seem to be missing in numbering only as text follows.
13. Two pages numbered _____. Text follows.
14. Curling and wrinkled pages _____
15. Other _____

THE UNIVERSITY OF OKLAHOMA

GRADUATE COLLEGE

STABILIZATION OF PONCA CITY SHALE

A DISSERTATION

SUBMITTED IN THE GRADUATE FACULTY

in partial fulfillment of the requirements for the

degree of

DOCTOR OF PHILOSOPHY

BY

REZENE MEDHANI

Norman, Oklahoma

1982

STABILIZATION OF PONCA CITY SHALE

APPROVED BY

J. Hagood

James M. Robertson

Jim T. Hays

John S. Wickham

DISSERTATION COMMITTEE

ABSTRACT

Preliminary characterization of the Ponca City shale for highway construction purposes, and its amenability to lime, cement, fly ash and conjunctive stabilization were investigated in this study. After numerous screening and evaluation trials it was decided to use 6 percent lime, 14 percent cement, 25 percent fly ash and conjunctively 8 percent cement with 4 percent lime and 18 percent fly ash. The stabilized shale attained a 28-day unconfined compressive strength of 108 psi mininum and its plasticity index was depressed to less than 6 percent. In terms of the strength and plasticity criteria, cement (14%) and conjunctive (8% cement + 4% lime + 18% fly ash) stabilizations were most effective.

Beam action studies were also included and unconfined compressive strength and bending strength values correlated. The correlation equations of the form are helpful in predicting the flexural strength characteristics of stabilized soils and they are considered applicable in the design of multilayered pavement systems.

The strength gain and general amelioration of the

plastic shale were further ascertained and explained by X-ray diffraction and SEM studies. X-ray diffractograms show a significant peak reduction in the major clay minerals and that these reductions may explain the strength enhancements. The main reaction products identified were various forms of hydrated and unhydrated forms of calcium alumina and calcium silicate crystals. The SEM micrographs reveal that stabilization reduced the void areas and depict the silt size aggregations of particles, the spiny crystals (Tobermorites), and the alumina and silica gel, that upon hardening, cement the particles and increase the strength characteristics of the shale-stabilizer-water system.

ACKNOWLEDGEMENT

This investigation was conducted in conjunction with ODOT Study 79-09-2, ORA-158-867. The author wishes to acknowledge the help of Mr. Curtis J. Hayes of the Research and Development Division, Oklahoma Department of Transportation, in the sampling of the shale used in this study.

The author is extremely grateful to his major professor Dr. Joakim G. Laguros for his continuous advice, guidance and supervision of this investigation and for his assistance and friendship. His contributions to the author's educational and personal growth are highly esteemed.

The author expresses his sincere thanks to Dr. James F. Harp, Professor, School of Civil Engineering and Environmental Science, Dr. John Wickham, Professor, School of Geology and Geophysics, Dr. Gene Levy, Professor, Department of Mathematics and Professor James M. Robertson, Professor, School of Civil Engineering and Environmental Science, for their general guidance and their taking time to serve on the author's advisory committee.

Thanks are also due to all those who assisted at various stages of the laboratory work of this study, and to Mrs. Barbara Jones for typing this manuscript.

The author wishes to express his appreciation to his wife and all his friends for their understanding, encouragement and moral support. Finally, the author expresses sincere gratitude to his parents Mr. and Mrs. Medhani for their loyal contribution to the author's education and dedicates this work to them.

TABLE OF CONTENTS

Table of Contents (Continued)

LIST OF TABLES

List of Tables (Continued)

List of Tables (Continued)

List of Tables (Continued)

List of Tables (Continued)

LIST OF ILLUSTRATIONS

List of Illustrations (Continued)

List of Illustrations (Continued)

List of Illustrations (Continued)

List of Illustrations (Continued)

CHAPTER I

INTRODUCTION

Shale, a "soil or rock" like material is widely available on the earth's surface. Shales make up about one-third of the rocks of the earth and about one-half by volume of all sedimentary rocks (Pettijohn 1967). Thus they are often used in many engineering projects, either in their excavated form as construction materials for embankments, bases, subbases or in their natural and undisturbed state, for example, in foundations and in cut slopes. The performance of engineering structures built on shales depends, to a large extent, on the stability and durability of the shale materials.

The Oklahoma Department of Transportation has used shales as foundation materials. Their performance has varied from one area to the other. In some regions the engineering properties of shales did not change as a result of exposure to the action of weathering; thus, they proved sound foundation materials. However, in other areas shales partly lost their initial strength and durability with the result of pavement and structural failures. These varying observations in engineering per-

formance of Oklahoma shales constituted the basis for several studies. The University of Oklahoma, under the direction of Dr. Laguros, in cooperation with the Oklahoma Department of Transportation and the Federal Highway Administration concluded a number of shale studies (Anessi, 1968; Annamalai, 1974; Kumar, 1974; Jha, 1977; Medhani, 1978).

Laguros and Jha (1977) chose eight shales that exhibited typical engineering characteristics of Oklahoma shales. These shales represented a range of geologic, physiographic and geographic provinces and engineering properties. The study focussed on the ammenability of these shales to various stabilizing agents. The most pertinent recommendation was the need for field implementation of the stabilization study.

On the basis of the above recommendation the Oklahoma Department of Transportation and the Federal Highway Administration funded research project ODOT study 79-09-2, ORA-158-867. The research results presented in this report constitute the initial phase of ODOT study 79-09-2, ORA-158-867 and presents the following objectives:

(i) Sampling of the shale and preliminary laboratory testings to determine the engineering properties i.e. gradation, Atterberg limits, moisture-density and soil classification.

(ii) Determining the amounts of stabilizing agents to be adopted for field construction purposes. Evaluation of stabilization effectiveness on laboratory mixed and cured samples for comparative analysis with field stabilized and cured samples.

(iii) Employing the modulus of elasticity as a design parameter. In general, pavements with lime, cement or fly ash treated bases or subbases are designed as flexible pavements. However, stabilized shales when cured properly can develop high modulus of elasticity values which may impart in the pavement enough rigidity to make them perform as a slab or beam rather than as a flexible pavement. Thus, beam strength of stabilized specimens are studied by testing soil-stabilizer beams under flexure.

(iv) Determining the physical changes that occur in stabilized specimens. The improvements that stabilizers impart to soils can be dependably expressed in terms of the reduction in soil plasticity, gradation and strength gains using simple standardized tests. These physical changes are in reality manifestations of modifications in the distribution of pores or voids in a stabilized specimen. Thus, the SEM

(Scanning Electron Microscope) was used to assert these changes at the microscopic level.

(v) Analyzing stabilized specimens by X-ray diffraction techniques for possible clay mineral changes or to identify new crystals that may accompany the strength gains.

CHAPTER II

LITERATURE REVIEW

Classification of Shales:

As the subject of shales has been extensively covered by Jha (1977), this work is limited to an overview of shales and to the presentation of the recent shale classification schemes. The term shale encompases a number of classes of materials. When claystone and/or siltstone are highly indurated and fissile they are equivalent to shales. Twenhofel (1936) designates shales as all argillaceous sediments including claystone, siltstone, mudstone and marl.

The difficulty with the mineral identification and petrologic study of shales has thus far precluded a single classification methodology. Underwood (1967) subdivided shales into compacted or "soil-like" and cemented or "rock-like" classes. He also made a summary of the various classification methods by different authors, and based on the engineering properties (density, natural water content, compressive strength, etc.) and performance of various shales, he grouped shales into the "desirable" and the "undesirable" for engineering purposes.

Gamble (1971) developed a classification system that depended on the slake-durability index of shales and their plasticity index value. Critics of Gamble's approach, argue that plasticity is only a relevant property for the more "soil-like" shales and is difficult or impossible to measure when the shale has a rock-like consistency. Laguros (1972) disaggregated shales by ultrasonic treatment and observed changes in grain size, plasticity and X-ray characteristics. He suggested that a shale be classified as a "problem shale" if after disaggregation by ultrasonic treatment for one hour, the amount of silt and clay is greater than 40 percent.

A classification system that accounts for strength variations and differences in water deterioration characteristics was advanced by Morgenstern and Eigenbrod (1974). A shale rating system (Franklin, 1981) based on the properties of durability, strength and plasticity seems to fit both the "soil-like" and the "rock-like" shales. In this approach a shale is subjected to a cyclic slaking process and is assigned a rating value by first measuring its second cycle slake durability index. Rock-like shales that have durability values greater than 80 percent are further characterized by measuring their point load strength, while soil-like shales with durability values less than 80 percent are further characterized by measuring their plasticity index. Thus, on the

basis of the second cycle durability index and employing either the point load strength or its plasticity index, a shale is given a rating number that ranges from 0 to 9. A shale can be characterized from tentative correlations of these rating numbers and the expected engineering performance. Figure 2.1 presents Franklin's shale rating chart.

Soil Stabilization:

Soil stabilization may be broadly defined as "any regulated process that alters or controls soil properties for the purpose of improving the capacity of soil to perform and sustain an intended function " (Katti, Davidson and Sheeler, 1960). In highway and airport engineering, soil stabilization is the art of mixing soil and other additives in order to produce a low cost, durable paving material that would utilize native soils which would otherwise be considered unsuitable.

The use of admixture stabilization to upgrade certain soil properties is centuries old. The Committee on Soil Placement and Improvement (1978 reports that excavations of the Zoser Pyramid (3000 BC) show that the filler between the stone blocks was found to be composed of clay, limestone powder and quartz. The ancient Greeks and the Romans employed soil stabilization in building their roads and streets. Today, since the beginning of modern road construction, stabilization has been aimed at

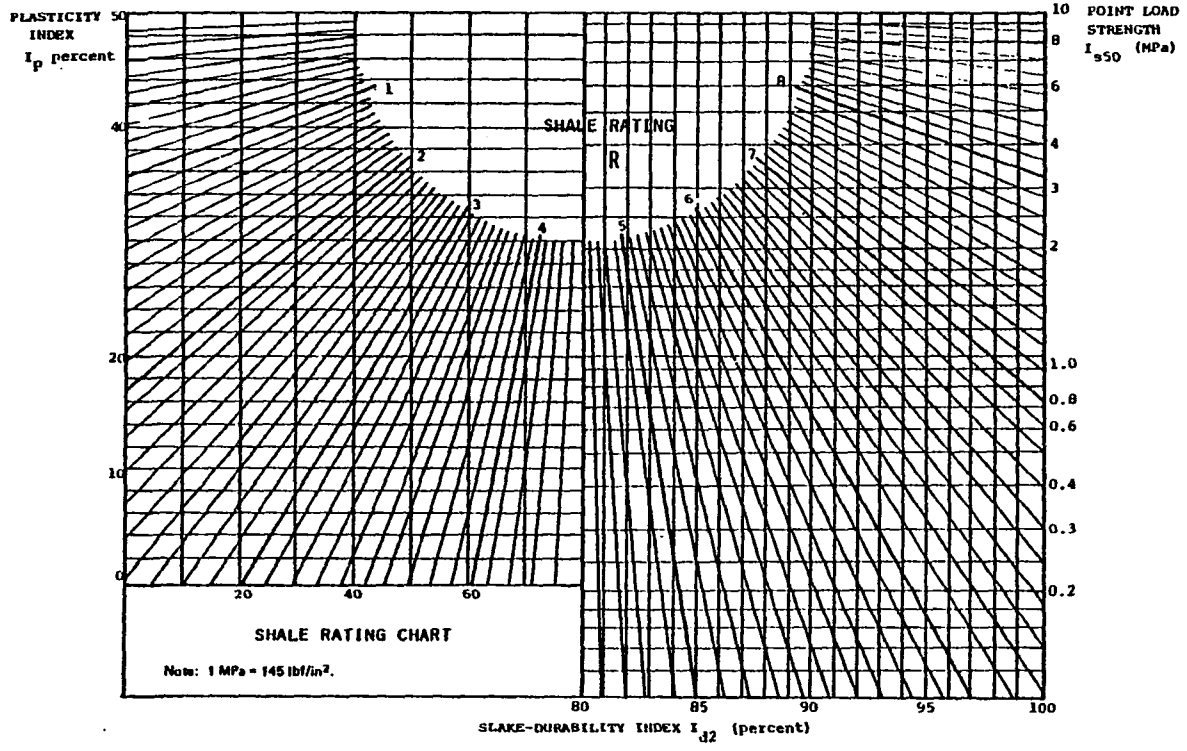

Figure 2.1: Shale rating chart (after Franklin, 1981)

(Yoder and Witczak, 1975) upgrading poor subgrade conditions and border line base materials, to control dust, to control moisture, to salvage old roads and to construct superior bases. Laguros and Jha (1977) also report the major uses of stabilization as:

(i) "Lifting a country or region out of mud or out of sand for better economic developement.

(ii) Providing bases and surfaces for secondary and farm to market roads, where good primary roads are already in existence.

(iii) Providing bases in higher type pavements, where high type rock and crushed gravel normally employed for such bases are not economically available.

(iv) Providing city and suburban streets with certain stabilized soil systems whose noise absorbing and elastic properties possess definite advantages over other construction materials.

(v) Making an area trafficable within a short period of time for military and other emergencies".

The most common techniques of improving soil properties or soil stabilization are chemical and mechanical. However, thermal and electrical methods of stabilizing soils are also occassionaly employed. Chemical stabilization involves mixing with the soil some chemical sub-

stances such as lime, Portland cement, flyash, sodium chloride, calcium chloride and asphalt. Mechanical techniques include the blending of materials, compaction, blasting and vibration. The present study pertains to chemical stabilization. Therefore, a review of chemical stabilization only is presented.

Chemical Stabilization:

Chemical stabilizers can be broadly grouped as per the mechanism of stabilization they exhibit. Some stabilizers, when mixed with the soil water system, foster new chemical products and these new chemical products bring about desired changes in the engineering properties of the soil. The American Society of Civil Engineers (1978) terms these stabilizers "active". Lime is a prime example of active stabilizers. When lime is added to medium to fine grained soils, it reduces soil plasticity and swell, it increases workability and also substantially increases strength.

The chemical properties of the soil, that is, the organic matter content, the natural soil pH and the predominant clay mineral, influence the extent of newly formed chemical products (Laguros and Jha, 1977). The second category of chemical stabilizers are those that do not produce new chemical products and are called "inert" Bitumen is an example of this class of stabilizers. Modifications of the engineering properties of the soil-sta-

bilizer-water system is attained as a result of binding together and/or waterproofing the soil with the stabilizer. Soil physical properties such as gradation, texture and plasticity control the effectiveness of "inert" stabilizers. However, many stabilizers display combinations of active and inert stabilization. Portland cement or lime-flyash may react chemically with the soil to produce a number of desirable reactions such as plasticity reduction, better workability, but the main mechanism of stabilization provided by these agents is the increased strength and durability produced by cementing agents that result from either cement hydration or the pozzolanic reaction between lime and flyash.

Chemical stabilizers include cementing agents, modifiers, waterproofing agents, water retaining agents and miscellaneous chemicals. The behavior of these chemicals vary and each has its particular uses and limitations. In general though, they can be categorized according to the properties they impart upon the soil. Table 2.1 (Yoder, 1975) and Figure 2.2 (Ingles and Metcalf, 1973) present some comparable ranges of applications of various stabilizers.

Several chemical stabilizers are available in the market today, but the most cost effective and extensively used stabilizers are lime, cement, and flyash. This study focusses on the use of these stabilizers, thus a

TABLE 2.1: ADMIXTURE STABILIZATION

	Type	Admix	Primary Mechanics of Stabilization	Use	Situations Best Suited	Approximate Quantity By Weight	Method of Evaluation	Change Soil Property				Construction Procedure	Limitations
								γ	LL	PL	PI		
Increase Strength by Cementing Action	Cementing agents	Portland cement	Principally hydration Some modification of clay minerals	Base and subbase	Sandy soils or lean clays	A-7 9-15% to A-2 5-9%	Durability tests, compression	Decrease	Slight reduction	Increase	Decrease	Pulverize, mix, compact cure	Organic soils
		Lime	Change water film, flocculation, chemical	Some base and subbase, shoulders	Granular materials or lean clays	2-5%	Do	Decrease	Varies	Increase	Decrease	Do	Freeze-thaw may be destructive
		Lime flyash	Pozzolanic action of lime and silica, some modification of clay minerals	Some base and subbase, shoulders	Granular materials or lean clays	2-5% lime 10-20% flyash	Do	Decrease	Varies	Increase	Decrease	Do	Quantity of flyash may be high
		Bitumen		Base and subbase	Granular	2-5%							
Improve Plasticity May or May Not Increase Strength	Modifiers	Cement	Modification of clay Change water film	Improve poorly graded base and subbase	Improve existing road metal, clays	½-4%	Atterburg limits grain size		Varies	Increase	Decrease	Pulverize, mix, compact	Strength increase may be low
		Lime	Change water film, modification of clay minerals	Do	Do	½-4%	Do		Varies	Increase	Decrease	Do	Do
		Bitumen	Retards moisture absorption	Do	Improve existing road metal	1-3%	Absorption tests					Do	Do
Little or No Increased Strength	Waterproofing agents	Bitumen	Retards moisture sorption by coating soil grains	Primarily subbase	Sandy soils or poor quality base materials, some clays	4-6%	Water sorption, compression, volume change	Decrease				Mix, "cure" compact	Limited by soil plasticity
		Membranes	Prevents movement of free water and water vapor	Primarily subbase and subgrades	Soils that may be improved by compaction		Strength of natural soil	None	None	None	None	Compact to high density	Construction may be difficult
	Water retaining agents	Calcium chloride	Deliquescent properties, lowers freezing point, base exchange	Construction expedient, traffic binding	Graded aggregate	½-1½%	Arbitrary	Slight increase	Slight reduction	None		Spread dry or mix with water	Leaches
		Sodium chloride	Deliquescent	Do	Do	½-1½%	Arbitrary	Do	Do	Do		Do	Leaches
Little or No Increased Strength	Water retarding	Organic cationic compounds	Alters clay minerals to act as a hydrophobic agent	Subbases		Trace	Water sorption, compression, volume change					Mix and compact	Mixing very small quantities may be difficult

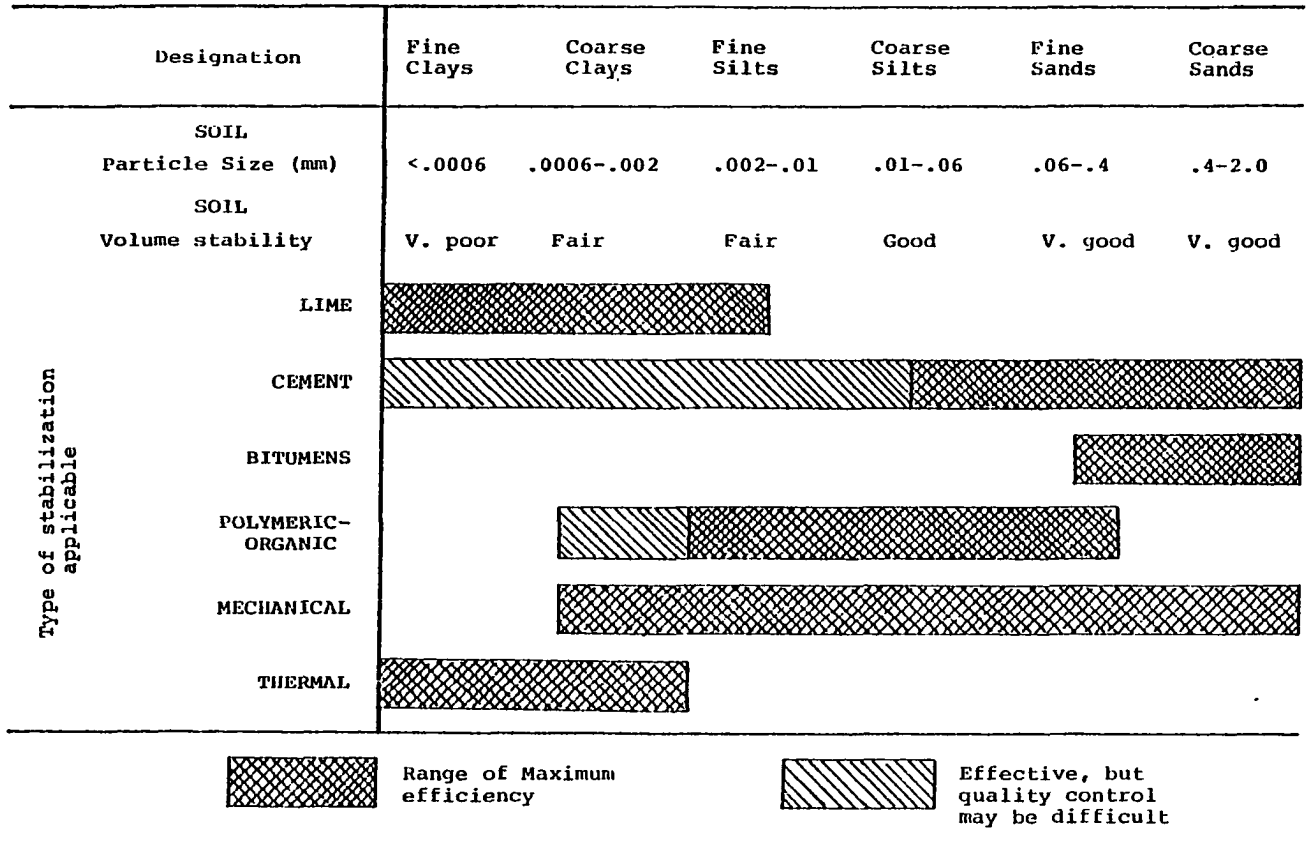

FIGURE 2.2: APPLICABILITY OF STABILIZATION METHODS (after Ingles and Metcalf, 1973)

review of these materials and the mechanisms by which they bring about beneficial changes is in order.

Lime As a Stabilizing Agent. Lime is strictly the oxide of calcium, CaO, but the term is generally used to include all the oxides and hydroxides of calcium and magnesium. Lime is commercially produced by "lime-burning" or calcining crushed limestone. Hot gases supplied by burning gas, coal or oil are passed over the crushed limestone to reduce the calcium carbonate in the stone to the oxide of calcium in the form:

$$\text{heat} + Ca\ CO_3 \longrightarrow CaO + CO_2$$

Also dolomite or dolomitic limestone, a carbonaceous rock similar to limestone but containing some magnesium carbonate ($CaCO_3 + MgCO_3$), is burnt to produce dolomitic lime ($CaO + MgO$). In the stabilization of soils lime is commonly used in one of its two hydrous forms, the hydrated calcium oxide ($Ca(OH)_2$) or the monohydrated and dihydrated dolomitic oxide ($Ca(OH)_2 + MgO$, $Ca(OH)_2 + Mg(OH)_2$). Table 2.2 presents the chemical properties of oxides and hydroxides of calcium.

Lime is widely used to improve the engineering properties of fine grained plastic soils. When lime is added to a fine grained soil several reactions take place. The calcium ions in the lime replace the exchangeable metalic cations in the soil (sodium, Na^+, hydrogen, H^+, potassium, K^+, etc.) and/or crowd themselves around the cations

TABLE 2.2: PROPERTIES OF COMMERCIAL LIMES*

Chemical Composition	Quicklime	
	High Calcium, %	Dolomitic, %
CaO	92.25-98.00	55.50-57.50
MgO	0.30- 2.50	37.60-40.80
CO_2	0.40- 1.50	0.40- 1.50
SiO_2	0.20- 1.50	0.10- 1.50
Fe_2O_3	0.10- 0.40	0.05- 0.40
Al_2O_3	0.10- 0.50	0.05- 0.50
H_2O	0.10- 0.90	0.10- 0.90
Specific Gravity	3.20- 3.40	3.20- 3.40
Bulk Density, pcf	55 - 60	55 - 60

	Hydrates		
	High Calcium	Monohydrated Dolomitic	Dihydrated Dolomitic
Principal Chemical	$Ca(OH)_2$	$Ca(OH)_2$+MgO	$Ca(OH)_2$+$Mg(OH)_2$
Specific Gravity	2.3 - 2.4	2.7 - 2.9	2.4 - 2.6
Bulk Density, pcf	25 - 35	25 - 35	30 - 40

* From "Chemical Lime Facts", Bulletin 214, National Lime Association, 1973.

on clay platelets. These changes result in rapidly lowering the soil plasticity, improve workabiltiy and change the swell properties of the soil-lime mix (Robnett and Thompson, 1969). Furthermore, as a result of the cation exchange the electrical charge is altered which in turn elevates the pore water pH, thus making the soil alumina and soil silica more soluble. The dissolved alumina and silica become available for reactions with calcium ions to produce new products that upon hardening enhance the strength of the stabilized soil by cementing the soil particles.

The second major lime reaction is known as the pozzolanic reaction which results in a slower, long-term cementation of compacted mixtures of lime and moist soil. A third type of lime reaction is carbonation. It is the reversal of the lime producing process. The soil-lime system absorbs carbon dioxide (CO_2) from the air and reacts with the calcium hydroxide ($Ca(OH)_2$) in the lime to produce calcium carbonate ($CaCO_3$). These carbonates are very weak cements, hinder pozzolanic action and thus deter normal strength gain (Herrin and Mitchell, 1961). The soil-lime reactions discussed above cause the following changes in the physical characteristics of clayey soils (Wang and Handy, 1966):

(a) in general, the liquid limit decreases and the plastic limit increases, resulting in sharp

reduction of the plasticity index

(b) soil binder content decreases

(c) lineal shrinkage and swell decrease markedly

(d) clayey soils become more friable and easily workable

(e) excessively moist soils dry faster

(f) lime stabilized bases or subbases form water resistant barriers.

Small amounts of lime, usually not in excess of three percent lime by dry weight of soil fraction, impart the above physical changes without improving the strength and the bearing capacity of the soils (Hilt and Davidson, 1960). However, to ameliorate the strength characteristics additional lime is required. Hilt and Davidson (1961), and Ho and Handy (1963) refer to this small amount of lime added to a soil, which does not contribute to the strength of the soil, as the "lime fixation point" or the "lime retention point". It is thought that the clayey soil has an affinity to fix that much lime before the lime can be free for strength improvement. Pinto, Davidson and Laguros (1962) thought of the same point as the amount of lime at which the floc sizes of the soil-lime mixes become maximum. Eades and Grim (1966) associate it with the pH level required to break down the soil silica, alumina and clay minerals and suggest that it constitutes the basis for the determination of the

amount of lime required to stabilize a soil. Figure 2.3 depicts the relationship between soil-lime pH and amount of lime added.

The pozzolanic or delayed calcium-silica and/or calcium-alumina reactions yield various compounds of hydrated calcium silicates and aluminates.

$$Ca(OH)_2 \longrightarrow Ca^{++} + 2(OH)^-$$

$$Ca^{++} + 2(OH)^- + SiO_2 \text{ (clay silica)} \longrightarrow CSH$$

$$Ca^{++} + 2(OH)^- + Al_2O_3 \text{ (clay alumina)} \longrightarrow CAH$$

where

C = calcium oxide, CaO

S = silicon dioxide, SiO_2

A = aluminum oxide, Al_2O_3

H = water, H_2O

The pozzolanic reactions are controlled by the quantity and type of lime, amount of moisture, degree of densification, soil characteristics and curing temperature and time. For Midwestern United States soils, Thompson (1970), reports that organic content, clay content, clay mineralogy, the pH and natural soil drainage influence the soil-lime reactions in developing a substantial strength gain. All clay minerals are potentially "reactive" but montmorrillonite and the mixed layer clays react more than the rest. High pH soils indicate potentially reactive condition. In so far as the strength increase is concerned most of the factors are interrelated

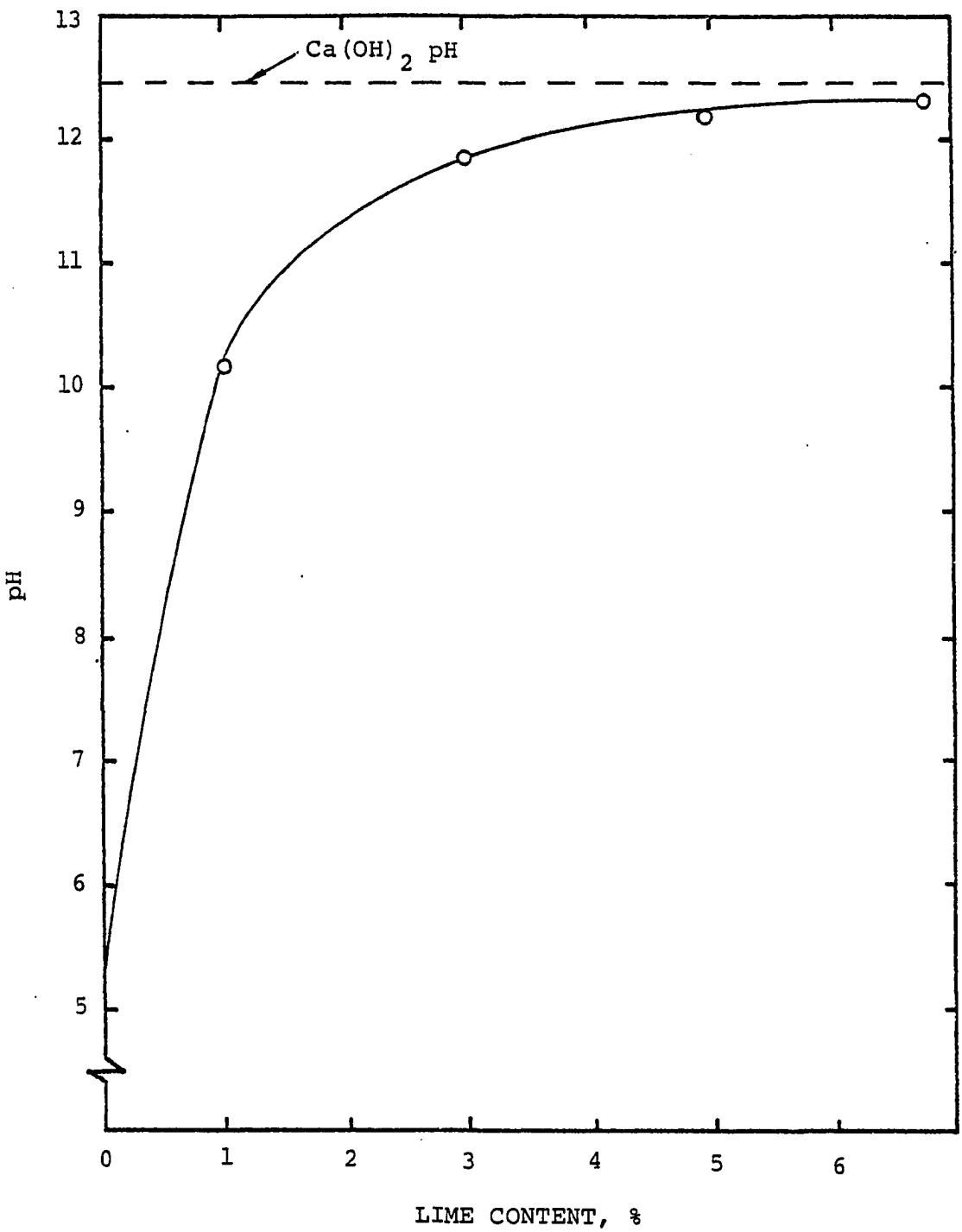

Figure 2.3: Lime determination for soil stabilization (after Jha, 1977)

and except in specific cases, no one of these factors is a great deal more important than another (Herrin and Mitchell, 1961).

Several tests are employed to evaluate the effectiveness of cured soil-lime mixtures. The most common are unconfined compression, triaxial, durability, bearing and Proctor penetration testing (Freeborough, 1947; Whitehurst and Yoder, 1952; Wang, 1966). Lime stabilized soils gain strength with age, usually the strength increase is rapid at the beginning of the curing period, but the rate of increase becomes less and less as the curing period progresses. McDowell (1953) reported that in laboratory conditions, lime stabilized soils increased in strength up to four years. Early strength gains can be accelerated by curing the soil-lime specimens at higher temperatures (Anday, 1963; Diamond, Sidney, White, Dolch, 1963; Ruff, Ho, 1965). The effect of varying the amount of lime added to various soils and the effect of curing time as measured by the unconfined compressive strength can be generalized as shown in Figures 2.4 and 2.5.

The level of strength amelioration of cured soil-lime mixes is dependent upon the type and amount of reaction products formed. For a lime-bentonite ratio of 0.89 and a curing temperature of 104°F, Wang and Handy (1966) identified calcium silicate hydrate (CSH(gel)),

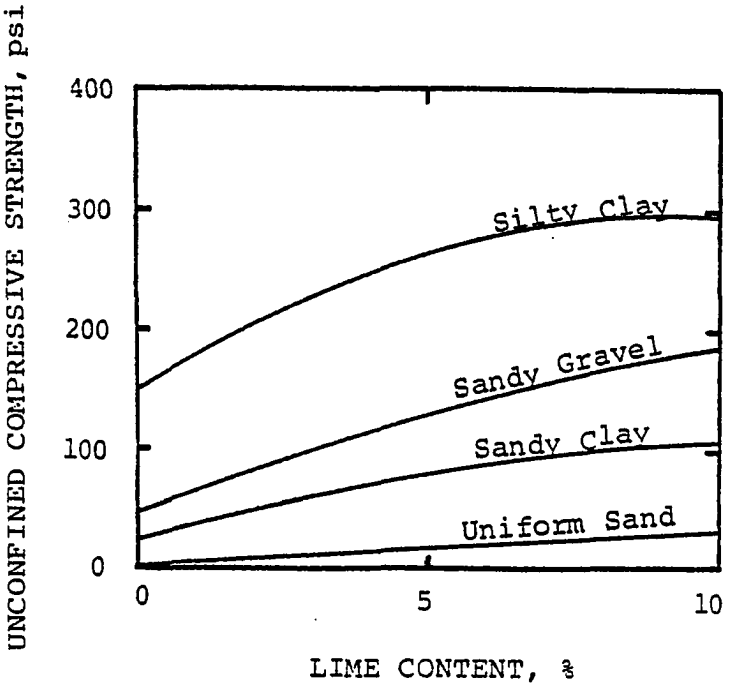

Figure 2.4: Effect of lime content on strength for various soils stabilized with hydrated lime, cured for seven days at 25°C, (after Metcalf, 1973)

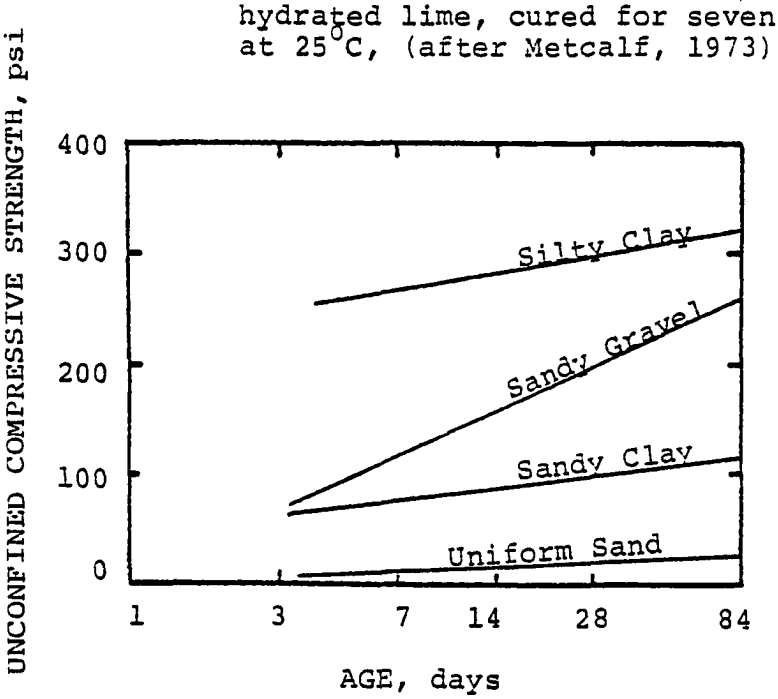

Figure 2.5: Effect of age on strength of various soils stabilized with 5% hydrated lime (after Metcalf, 1973)

calcium silicate hydrate (CSH(I)), hydrogarnet, and tetra-calcium aluminate hydrate (C_4AH_{13}), the products formed being dependent upon the curing time. Also, Ruff and Ho (1966) in a lime-bentonite mixture observed that tetracalcium aluminate hydrate (C_4AH_n), calcium silicate hydrate (CSH(gel)) and calcium silicate hydrate (CSH(II)) were the stable reaction products occuring when cured at 41°F, 73°F and 104°F, respectively. The same reaction products occured at higher curing temperatures (122°F and 140°F) with calcium silicate hydrate (CSH(I)) appearing after several days of curing. Thus, these authors concluded that the lime-clay reaction is a continuous reaction of the form:

lime + clay CSH(gel) CSH(II) CSH(I)

At any given time, depending upon the curing temperature and curing time, there may be more than one phase of the reaction present. The further the reaction progresses to the right, the higher the strength.

Cement Stabilization. Ever since 1935 when the cement stabilized test sections in South Carolina proved that soil and cement were compatible materials, Portland cement has been the widely used chemical stabilizer mixed to soil to form low cost roads. Portland cement and water are mixed with pulverized soil in the construction of base course and subbases for streets, roads, highways, shoulders, airfield pavements and parking areas to pro-

vide a firm, durable pavement layer. Almost any soil with the exception of highly organic materials may be treated with cement and will exhibit an improvement in properties, and increase in strength (Ingles and Metcalf, 1973). The only practical limits to the range of cement utilization are those imposed by clean, well graded gravels or crushed rock materials, where stabilization is not only unnecessary but may, infact, create serious problems of shrinkage cracking. Additional limitations are imposed by the difficulty of incorporating a dry fine cement powder into a moist heavy clay.

The amount of cement needed in soil stabilization varies with the type of soil; it increases with increasing silt and clay content. The proportion of cement to soil can be determined in the laboratory by adding varying amounts of cement to a soil and evaluating the cement requirement on the basis of moisture-density relations, and the Portland Cement Association criteria for weight loss during wet-dry and freeze-thaw tests. The range of the amount of cement needed to meet these criterie, as reported by the Committee on soil-cement stabilization (1961), are presented in Table 2.3. The Oklahoma Department of Transportation set cement requirements for various granular and fine grained soils and they are presented in Table 2.4 (ODOT, 1969).

The prominent effects of Portland cement stabiliza-

TABLE 2.3: CEMENT REQUIREMENT BY AASHTO SOIL GROUPS

AASHTO Soil Group	Cement Content for Wet-Dry and Freeze-Thaw Tests, % by Weight
A-1-a	3-5, 5-7
A-1-b	4-6, 6-8
A-2	5-7, 7-9
A-3	7-9, 9-11
A-4	8-10, 10-12
A-5	8-10, 10-12
A-6	10-12, 12-14
A-7	10-13, 13-15

TABLE 2.4: ESTIMATED CEMENT REQUIREMENT FOR OKLAHOMA SOILS *

AASHTO Class.	% Cement by Dry Weight of Soil							
	% Pass. 200 Sieve							
	0	5	10	15	20	25	30	35
A-1-a	7	7	6	-	-	-	-	-
A-1-b	9	8	8	8	7	7	-	-
A-2-4	9	9	9	8	7	7	8	9
A-2-5	9	9	8	8	8	8	8	8
A-2-6	10	10	9	8	8	8	8	9
A-2-7	11	11	10	9	9	9	10	10

SHALES

A-1, A-2, A-3 --Add 2% cement

A-4, A-5, A-6, A-7 --Add 1% cement

AASHTO Class.	% Cement by Dry Weight of Soil						
	Group Index						
	0-2	3-5	6-8	9-11	12-14	15-17	18-20
A-4	9	10	11	-	-	-	-
A-5	9	10	11	11	12	-	-
A-6	10	11	12	12	13	14	-
A-7-5	11	11	12	13	13	14	16
A-7-6	11	12	13	14	14	15	17

* Research and Development Divison
Oklahoma Department of Highways, 1966

tion are the reduction of soil plasticity and cementation. When moist cohesive soil and Portland cement are intimately mixed, hydration is initiated and the calcium ions released during this process cause a reduction in soil plasticity. These reductions are the result of either a cation exchange or a crowding of additional cations onto the clay. These processes change the electrical charge density around clay particles, thus, causing them to become electrically attracted to one another to form flocullations or aggregations that behave like silt particles.

When a cement stabilized soil is compacted and cured, the various cement constituents are hydrated at different rates. This hydration produces cementitious, amorphous and crystalline products that impart to the soil the early strength and long term strength gains. Cementation is mainly chemical in nature and may be visualized as due to the development of chemical bonds or linkages between adjacent cement grain surfaces, and between cement grain surfaces and the exposed soil particle surfaces.

The effectiveness of cement stabilization is controlled by numerous factors and several studies have been conducted to investigate their influence. Effects of soil type, cement content, moisture content, dry density, curing temperature and time, time elapsed

between mixing and construction and presence of deleterious materials are covered in Highway Research Board Bulletin 292 (1961). Figures A.1 through A.7 in Appendix A graphically summarize the influence of the aforementioned factors on the unconfined compressive strength of cement stabilized soils.

Coal Ash. The technology of coal utilization in coal-fired power plants results in several by-products. When finely ground coal is injected into the boiler furnace, the coal particles burn in a steam of air. The residue that passes through the boiler is a fine cement-like material called "pulverized" fuel ash or fly ash. The residue that settles to the bottom of the furnace is collected as slag or bottom ash. In terms of the size of particles, fly ash is small enough to be entrained in the flue gas and carried away from the site of combustion. Fly ash particles are derived from the melting of mineral matter or the partial combustion of coal. In general, about 70 to 80 percent of the solid wastes derived from the combustion of coal is fly ash (Dvorak, Lewis et al. 1978; and EPRI, 1979). Fly ash is collected in the stacks of power plants by electrical precipitators or mechanical means or combination of the two. A possible schematic arrangement of coal ash collecting devices is presented in Figure 2.6.

As the use of powdered coal by power generating

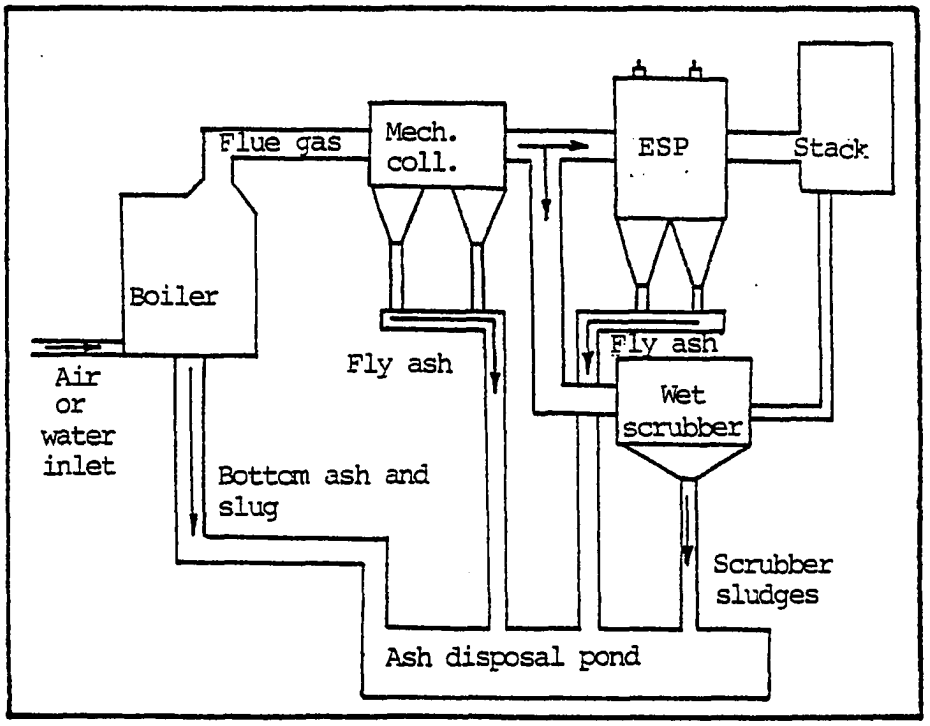

Figure 2.6: Possible arrangement of coal ash collecting devices (after ISGS, 1981)

plants in the United States increased, the regulations to restrict the amount of smoke discharge to the atmosphere became stiffer. This, in turn meant an abundance of fly ash collected in the smoke stacks of coal operated power plants all over the Nation. In 1978 power plant ash was the sixth most plentiful mineral in the United States (Chemical and Engineering News, 1978). During 1977, the electric utility industry in the United States burned 475 million tons of coal that resulted in 48.5 million tons of coal ash. The rate of ash production during the past three decades for the United States is presented in Figure 2.7. By 1990, ash production is expected to increase to 125 million tons (Faber 1979) and is expected to continue increasing (Yuan, 1979) due to:

(i) increased utilization of higher ash coals

(ii) utility companies switch from oil to coal

(iii) increased efficiency of ash collection systems

Chemical and Physical Properties of Fly Ash. Fly ash is a pozzolan and is defined as "a siliceous or siliceous and aluminous material, which in itself possesses little or no cementitious value but which will, in finely divided form and in the presence of moisture, chemically react with calcium hydroxide at ordinary temperatures to form compounds containing cementitious properties".

Fly ash particles are primarily composed of silica and alumina. Secondary ingredients are carbon and oxides

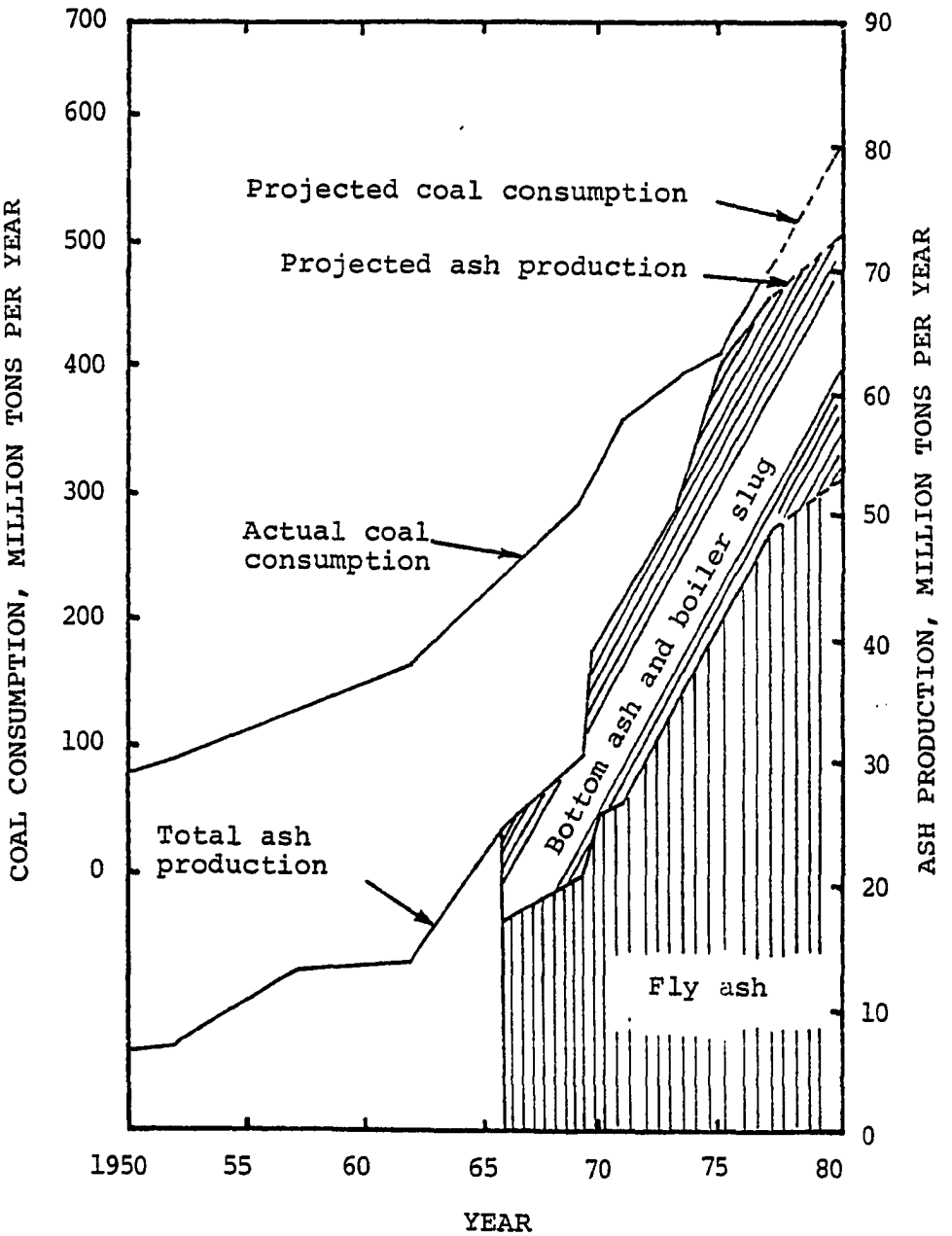

Figure 2.7: Coal consumption and ash production by United States electric utilities (after Yuan, 1979)

TABLE 2.5: TYPICAL COMPOSITION OF FLY ASH *

Principal Constituents	Amount, %
SiO_2	10-70
Al_2O_3	8-38
Fe_2O_3	2-50
CaO	0.5-30
MgO	0.3- 8
Na_2O	0.1- 8
K_2O	0.1- 3
TiO_2	0.4-3.5
SO_3	0.1-30

* (Diamond, 1981)

of iron, calcium, magnesium and sulphur. Table 2.5 gives typical ranges of values for the chemical composition of fly ash (Diamond, 1981).

Silt size particles that range from grey to tan to reddish brown are dominant constituents of fly ash. Data from various investigators (Chang et al., 1977; Page, Elsewi, and Strangham, 1979; Townsend and Hogdson, 1973) indicate that in general that fly ash has a silt-loam texture. A survey of fly ash produced in 21 states (Furr et al., 1977) revealed 60 percent of the samples as having a "floury consistency" and 40 percent as having a "fine granular texture". Depending on the type of removal system approximately 65 percent to 90 percent of the fly ash is finer than 0.010 mm (EPRI, 1979). The fine texture of fly ash reflects the variable but generally low hydraulic conductivity ranging from 9 cm/day of water through compacted fly ash to 70 cm/day through uncompacted fly ash (Dvorak, Lewis et al., 1978), low bulk density and specific gravity that ranges from 2.1 to 2.6 (EPRI, 1979). By and large, the physical and chemical properties of the fly ashes produced in the eastern and western part of the United States are the same. The two significant differences are that western United States fly ash contains higher amounts of free lime and lesser amounts of sulphur oxide than eastern fly ash. Thus, western fly ashes show higher self hardening characteristics than

eastern fly ashes as a result of the higher calcium oxide content.

Scanning electron and light microscopes have been used in the investigations of fly ash morphology. Thin walled hollow spherical particles referred to as "cenospheres" are observed and are estimated to account for 20 percent by volume of total fly ash (Rask, 1968). Cenospheres packed with smaller spheres are reported by Fisher, Chang and Brummer (1976) and suggested that the filled spheres be called "plerospheres". Paulson and Ramsden (1970) describe the presence of (i) black irregularly shaped particles; (ii) angular, transparent and opaque fragments; and (iii) glassy spheres and globules ranging in color from black to yellow to red.

Fly Ash Mineralogy. The mineralogy of fly ash has been studied by X-ray powder diffraction by several investigators. Natusch et al. (1977) state that alpha-quartz, mullite, hematite, and magnetite are present in fly ashes, however, amorphous material predominates in the fly ash matrix. They also found small amounts of gypsum in a few western ashes. Fly ash from eastern coals often displays higher percentages of amorphous material than does fly ash derived from western coals (Fisher, Chang, and Brummer, 1976). Data on the mineralogical variation of fly ashes from the United Kingdom, United States, and Japan are presented in Table 2.6 (Rehsi, 1974).

TABLE 2.6: VARIATIONS IN MINERALOGICAL COMPOSITION OF FLY ASHES FROM THREE COUNTRIES *

Phase Composition	United States %	United Kingdom %	Japan %
Amorphous Glass	50-90	50-90	69-84
Mullite	0-16	9-35	8-18
Magnetite	0-30	5	NA
Hematite	1- 8	5	0.5-5.3
Quartz	0- 4	1.0-6.5	5.4-11.8

NA = Not Available

* (Rehsi, 1974)

Fly Ash Stabilization. In response to the ever increasing restrictive regulations against discharge of smoke, a series of studies on the uses of fly ash have been underway. Nowadays, fly ash finds extensive use as a stabilizing agent in highway construction either alone or in combination with lime, Portland cement or other additives. Extensive work is also being done on the potential use of fly ash in concrete, brick making, water pollution control, fillers for plastics and oil drilling mud.

The characteristics of a particular fly ash depend upon the coal source, coal preparation procedures, boiler type, and the ash collection device (Sam I. Thornton et al., 1975). Thus, fly ash generally exhibits a wide range in chemical and physical properties. These properties, in turn, determine the effectiveness of the ash for use in soil stabilization. Fly ash has been mainly used as a supplement or replacement for lime and cement in soil stabilization. Laguros and Jha (1977), in their study of Oklahoma shales, have used fly ash as a main stabilizing agent, and proved effective when used in significant amounts (25 percent by weight). The addition of fly ash, a pozzolan, to nonplastic and low plasticity index soils that are nonresponsive to lime, enhances the lime-silica reaction.

The use of lime-fly ash-aggregate stabilization in

pavement components is practiced by a number of state and federal agencies (NCHRP, 1976). The characteristics of fly ash, lime and aggregates, their relative mixing proportions, curing periods and temperatures influence the overall product. Barenberg (1967), noted that below 40°F the chemical reaction for a lime-fly ash-aggregate mix virtually stops. Yang (1972), indicated the advantages of the relatively long period of time (5 years) required to achieve ultimate strength gain for lime-fly ash mixes. The unconfined compressive strength test is generally used to evaluate the quality of lime-fly ash-aggregate mixes.

The reactions that occur in lime-fly ash-water system to form cementitious materials are complex. Minnick (1967) indicates that the major cementing compounds formed in lime-fly ash mixes are probably calcium silicate hydrates and possibly etringite. An illustrative list of reactions (Minnick, 1967) may be presented as follows:

1. $RO \longrightarrow R(OH)_2$
2. $RO \longrightarrow RCO_3 + H_2O$
3. $R(OH)_2 \longrightarrow RCO_3 + H_2O$
4. $R(OH)_2 + SiO_2 \longrightarrow XRO \cdot YSiO_2 \cdot ZH_2O$
5. $R(OH)_2 + Al_2O_3 \longrightarrow XRO \cdot YAl_2O_3 \cdot ZH_2O$
6. $R(OH)_2 + Al_2O_3 + SiO_2 \longrightarrow XRO \cdot YAl_2O_3 \cdot ZSiO_2 \cdot WH_2O$
7. $R(OH)_2 + SO_3 + Al_2O_3 \longrightarrow XRO \cdot YAl_2O_3ZSO_4 \cdot WH_2O$

where

R = Ca^{++} or combinations of these ions

X,Y,Z,W = prefixes to balance equations.

Beam Strength of Compacted Specimens:

Tensile stresses can develop in earth structures, especially in multilayer pavements where the subgrade soil may be subjected to tensile stresses due to traffic loads, when the deformation moduli differ in the various layers (Ajaz and Parry, 1975). Tensile stresses can also develop and cause cracking of clay cores in earth and earth-rock dams. Little is reported in the literature on the behavior of clays either under direct or indirect (bending) tension. Three methods of bending strength analysis namely, the elastic bending theory method, the direct method, and the differential method are applicable.

The governing assumptions in the elastic bending method are that: plane sections remain plane after bending, the beam material has the same Young's modulus in tension as in compression, stress is linearly proportional to strain and no creep takes place during bending. Thus, the extreme fiber stresses in tension and in compression are given by:

$$\sigma = \frac{6M}{bd^2} \qquad (2.1)$$

where

σ = fiber stress, psi

M = bending moment in-lb

b = beam width, inches

d = beam depth, inches

In the direct method of analysis, the assumptions remain the same except that the value of deformation modulus in tension and compression may vary. Thus, the neutral axis is not necessarily at mid-height of the beam and hence extreme fiber stress values in tension and compression differ.

$$\sigma_c = \frac{3\ M}{bd^2}\left[\frac{\varepsilon_c + \varepsilon_t}{\varepsilon_c}\right] \tag{2.2}$$

$$\sigma_t = \frac{3\ M}{bd^2}\left[\frac{\varepsilon_c + \varepsilon_t}{\varepsilon_t}\right] \tag{2.3}$$

where

σ_c, σ_t = fiber stresses in compression and tension, psi

M = bending moment, in-lb

b = beam width, inches

d = beam depth, inches

ε_c, ε_t = strain in compression and tension, in/in

The differential method was advanced by Prentis (1951) for use in reinforced and prestressed concrete beams. It assumes that plane sections remain plane, but assumes no preferred relationship between stress and strain and simply represents bending stresses as a function of linear strain. The final form of Prentis' derivations are:

$$\sigma_c = \frac{1}{\varepsilon_c + \varepsilon_t} \frac{\partial}{\partial \varepsilon_c} \left[\frac{M (\varepsilon_c + \varepsilon_t)^2}{bd^2} \right] \tag{2.4}$$

$$\sigma_t = \frac{1}{\varepsilon_c + \varepsilon_t} \frac{\partial}{\partial \varepsilon_t} \left[\frac{M (\varepsilon_c + \varepsilon_t)^2}{bd^2} \right] . \tag{2.5}$$

where all the terms are as described earlier.

Ajaz and Parry (1975) have studied compacted clay beams subjected to total stress tension, compression and bending. They analyzed stress-strain relationships of clay beams from bending tests and they reported that the elastic bending method gave stress-strain curves that were different from the other two methods. The tensile stress values derived from the elastic bending method and the direct method were 1.5 and 1.4 times those by the differential method.

In a study of lime-fly ash stabilized bases and subbases, the National Cooperative Highway Research

Program (1976) evaluated beam strengths and reported that:

(i) the flexural strength of lime-fly ash-aggregate mixtures gain in strength with age as shown in Figure 2.8.

(ii) the ratio of flexural strength to compressive strength for most lime-fly ash-aggregate mixtures is between 0.18 and 0.25

(iii) the beam strengths of lime-fly ash-aggregate mixtures are approximately twice the tensile strength values evaluated under split-tensile and double-punch tests.

The modulus of elasticity values of lime-fly ash-aggregate mixtures were also found to change depending upon whether they were evaluated in compression or in flexure. Ahlberg and Barenberg (1965) indicate that flexural moduli for granular lime-fly ash-aggregate mixtures range from 1.5×10^6 to 2.5×10^6 psi. They also recommend the use of flexural moduli for pavement design calculations.

Electron Microscopy:

The study of the various levels of macro and micro structures is very important in the understanding of the engineering behavior of clay soils. Concepts of microstructure were proposed by Terzaghi (1925), Casagrande (1932), and later by Lambe (1953, 1958). Macro structure

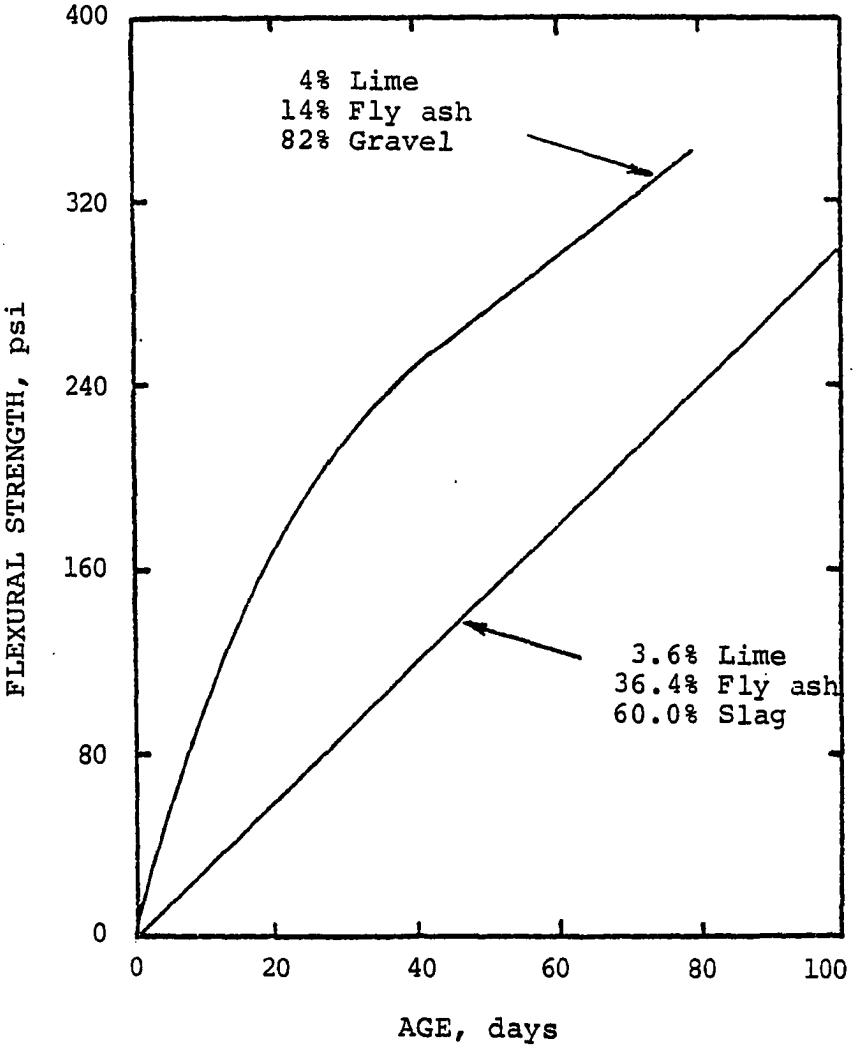

Figure 2.8: Flexural strength development of typical lime-fly ash stabilized mixtures, laboratory curing (after Ahlberg, 1969)

investigations have also been carried out by Rowe (1959), Bishop and Bjerrum (1960) and Skempton (1964). The examination of individual clay platelets requires extremely high magnifications of the order of 10,000X and upwards (Barden and Sider, 1971), and this can be effected by using an electron microscope.

There are two techniques of electron microscopy in current use. They are based on transmission and reflection. The SEM (scanning electron microscope) which uses the reflection of a beam of electrons from the surface of the object rather than the transmission through a thin section is most promising today.

Sridharan et al. (1971) used scanning electron microscopy to investigate the compressibility and strength behavior of soils. Their study stresses the fact that, even though it is apparent that such characteristics, as soil permeability and susceptibility to frost action must be intimately related to pore-size distribution as well as to void ratio, little attention has been given to the significance of the pore (void) sizes, themselves. In a study of microfabric features of soils with scanning electron micrographs, Collins (1974) states that, in addition to many other factors, the type, dominance and distribution of the microfabric features present within a soil, influence certain engineering behaviors like sensitivity, collapse and expansion. The characteristics of

the pore space component of soil microfabric such as size, shape and orientation, have been investigated by many workers, and some have classified pore space according to certain of these characteristics. Collins and McGown (1974), presented a new approach to microfabric description while maintaining most of the terminologies suggested by previous workers. Figure 2.9 is a schematic representation of particle assemblages analyzed from scanning micrographs and Figure 2.10 is a schematic representation of pore space types.

Thus far the main thrust of scanning electron microscopic studies have been qualitative, hence, few quantitative analyses are reported in the literature. McConnachie (1974) applied new techniques to analyze scanning electron micrographs in order to support his studies of the mechanism of consolidation of soils. Electron micrographs of thin slices of consolidated monomineralic kaolin were taken and different variables were measured, including length, breadth, voids, area of soil particles and packing density. Laguros and Jha (1977) also studied the void domain characteristics of raw and stabilized shales and related the voids as measured from scanning micrographs to their compressive strength values. The micrographs were on dispersed samples. In addition to void areas, they measured the largest distance between particles, i.e., "the pore-intercept". The un-

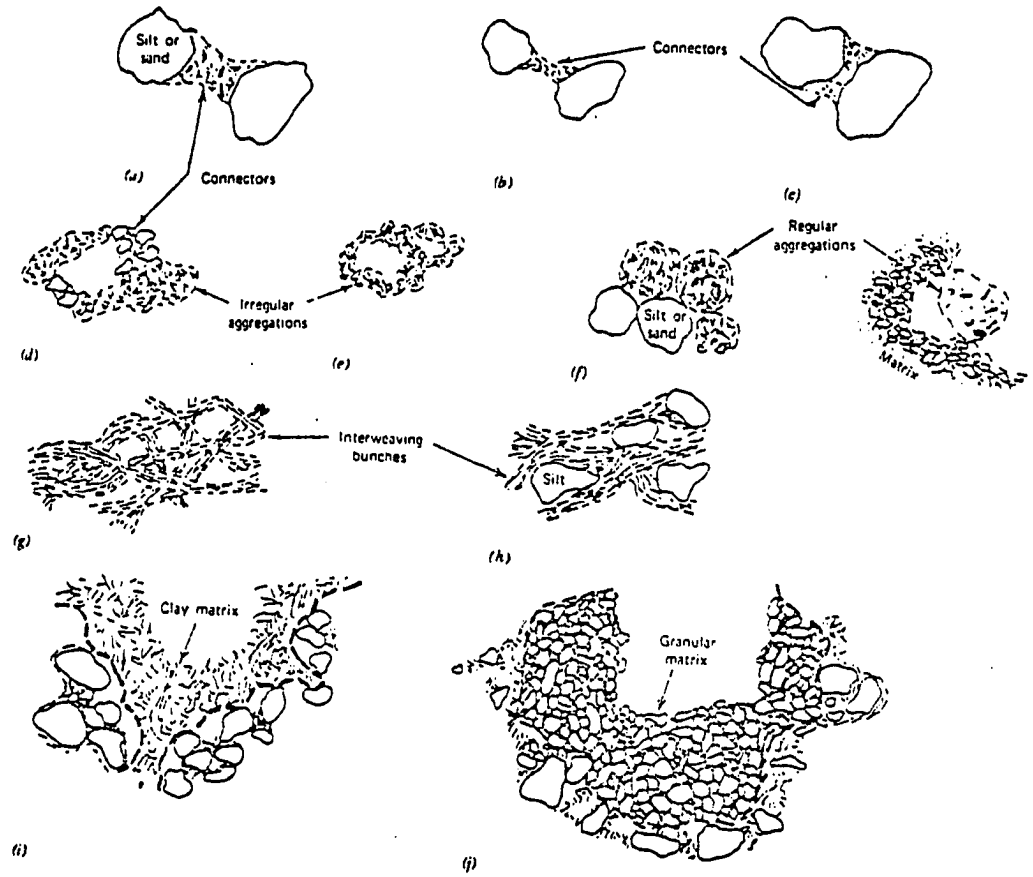

Figure 2.9: Schematic representations of particle assemblages (After Collins and McGown, 1974).

(a) Connectors. (b) Connectors. (c) Connectors. (d) Irregular aggregations by connector assemblages. (e) Irregular aggregations in a honeycomb. (f) Regular aggregation interacting with particle matrix. (g) Interweaving bunches of clay. (h) Interweaving bunches of clay with silt inclusions. (i) Clay particle matrix. (j) Granular particle matrix.

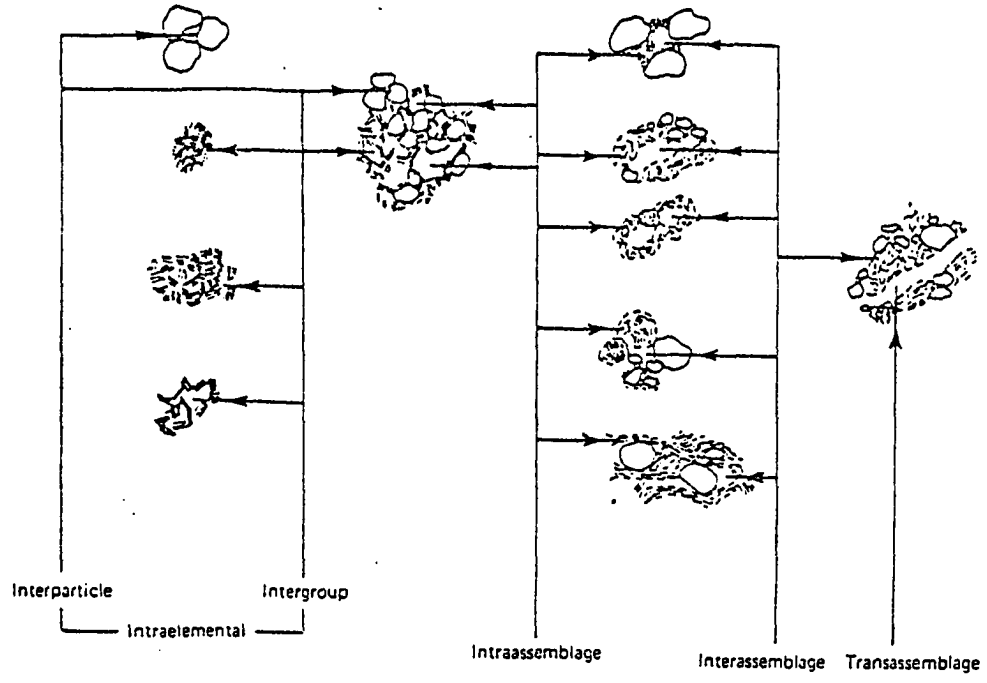

Figure 2.10: Schematic representation of pore space types (after Collins and McGown, 1974)

confined compressive strength of stabilized shales were expressed as a function of their void area and pore-intercept counterparts. Also, Rezene (1978) did some micrographic analysis of void area and pore intercept patterns of stabilized shales. A schematic representation of scanning micrographs of dispersed specimens is presented in Figure 2.11.

X-Ray Diffraction:

Both the mechanisms of lime and cement stabilizations are two stage processes. Lime-clay reactions are: (i) those which are completed rapidly (ion exchange and flocculation) and (ii) those which proceed slowly (carbonation, pozzolanic reactions and the formation of new materials). Similarly, the overall result of cement-clay interaction is the formation of: (i) primary cementitious matter that hardens into high strength "aggregate" and (ii) secondary cementitious matter that enhances the strength and stability of soil-cement by producing additional cementitious matter which increases interparticle bond strength.

X-ray diffraction and differential thermal analysis (DTA), have long been used in investigating the slowly proceeding reactions (pozzolanic reactions) of lime-clay systems, the crystalline products from primary and secondary clay-cement reactions and the changes in the crystal structure of clay minerals. Herzog and Mitchell

Total area = BxL

$$V = \frac{A}{BxL} \times 100$$

P = Longest pore (void) intercept, mm

Figure 2.11: Electron micrograph of soil mass

(1963) studied kaolinite and montmorillonite stabilized with Portland cement and pure tricalcium silicate (C_3S) and reported that X-ray diffractions of these mixes showed that: (a) calcium hydroxide was formed in hydrating clay-cement, but was rapidly used up in reactions with the clay; (b) minor alteration of kaolinite - cement X-ray pattern and marked alteration of montmorillonite-cement X-ray pattern after curing periods of twelve weeks, suggesting clay mineral structure breakdown and/or interaction with cement at particle surfaces. Eades and Grim (1962) in their study of hydrated lime reactions with pure clay minerals, reported that X-ray diffractions reveal that different rates of reactions occur with different soils. They also reported the formation of calcium silicate-hydrates and calcium carbonate from field stabilized soil-lime samples. X-ray diffraction and DTA of lime-clay slurries cured at 70°F for two years showed varying proportions of conversion of minerals and lime into pozzolanic reaction products (Glenn and Handy, 1963). According to Plaster and Noble (1970) clays, and probably other constituents of soils, suffer deterioration after cement treatment as indicated by the release of large amounts of silica and alumina and by the diminution of mineral diffraction peaks. Ho and Handy (1964) conducted experiments on lime stabilized montmorillonite slurry and reported no reaction product peak, but the in-

tensity of mineral peaks diminished with increasing lime content. Goldberg and Klein (1952) treated Wyoming bentonite with up to eight percent calcium hydroxide and reported that calcium hydroxide lines disappeared from the X-ray spectrum, and that there were no other changes in the X-ray pattern of the clay, and suggested the conversion of calcium hydroxide to calcite and some other compounds. The strength increase in lime-clay mix is partially due to the formation of new minerals such as calcium silicate hydrates which act as cementing material interlocking particles (Eades and Grim, 1960). Hilt and Davidson (1961) identified new diffraction lines for lime-montmorillonite at 8.11 Å and 7.59 Å d-spacings. Tricalcium silicate hydrates (C_3SH) or tobermorites are common lime-clay and cement-clay reaction products. Glenn and Handy (1963) hydrated tricalcium silicate for six days at room temperature. This resulted in a product they identified as tricalcium silicate hydrate. From reactions that accompanied stabilization of clay with cement, Herzog and Mitchell (1963) and Taylor (1966) identified tricalcium silicate (C_3S) and dicalcium silicate (C_2S), respectively. Other important reaction products reported by Taylor (1966) and Noble (1967) are: calcium aluminum hydrate (CAH); tricalcium aluminate hydrate (C_3AH); and tetracalcium aluminum hydrate (C_4AH_n). A summary of d-spacings for clays, lime-clay

and cement-clay reaction products are presented in Table 2.7.

TABLE 2.7: SUMMARY OF CLAYS, LIME-CLAY AND CEMENT-CLAY REACTION PRODUCTS

Crystal	d-spacings, Å					Reference
Chlorite	14.00 4.70	3.60	7.18 3.50	7.02	4.80	ASTM (1966)
Kaolinite	7.18	3.58	2.50			ASTM (1966)
Illite	9.99-10.40	3.34				Carroll (1970) Grim (1968
Montmorillonite	15.40 (variable) 2.56	3.09	4.48	3.34		Carroll (1970), Ruff & Ho (1966)
Quartz	4.26	3.34	2.46			ASTM (1966)
Lime, Portlandite ($Ca(OH)_2$)		4.90	2.63	1.93		ASTM (1966)
Calcite ($CaCO_3$)	3.04	2.29	2.10			ASTM (1966)
Lime-Kaolinite	5.09	3.04	2.80	1.80		Eades and Grim (1962)
Lime-Montmorillonite	8.11	7.94	7.59			Hilt and Davidson (1961) Glenn and Handy (1963)
CAH	8.10	7.60	3.90			Noble (1967)
C_3AH	8.30	8.07	7.70			Noble (1967)
C_4AHn	7.50	4.10	3.99	2.88		Ruff and Ho (1966)
CSH	17.30	12.60	10.00	3.08		Leonard and Davidson Glenn and Handy (1963)
C_3SH, Tobermorite	14.00 3.05 1.82	9.00 3.00	6.16 2.83	3.18 2.73		Glenn and Handy (1963) Ruff and Ho (1966) Taylor (1966)
C_2S	2.88					Taylor (1966)
C_3S	3.07	2.98	2.77			Herzog and Mitchell (1963

CHAPTER III

SELECTION OF STUDY SITE AND MATERIALS

One of the principal recommendations of the study of the amenability of Oklahoma shales to various chemical additives for stabilization, by Laguros and Jha (1977), was the field implementation of stabilization and investigation of its performance under real traffic and environmental conditions. To this effect the Oklahoma Department of Transportation in cooperation with the University of Oklahoma chose United States Highway 77 and State Highway 11, in Kay County, Oklahoma, to be the study site for field stabilization. Factors considered in the selection of this site were that the shale in the area was a "problem shale", and easy accessibility to the site for sampling and testing without hampering traffic flow.

The location plan of the study site is depicted in Figure 3.1. The study section is the east side of the four lane divided highway. It is 24 ft. wide and 3200 ft. long and it lies within a fill section of the highway. It includes four 700 ft. long sections to be stabilized with lime, cement, fly ash and also conjunc-

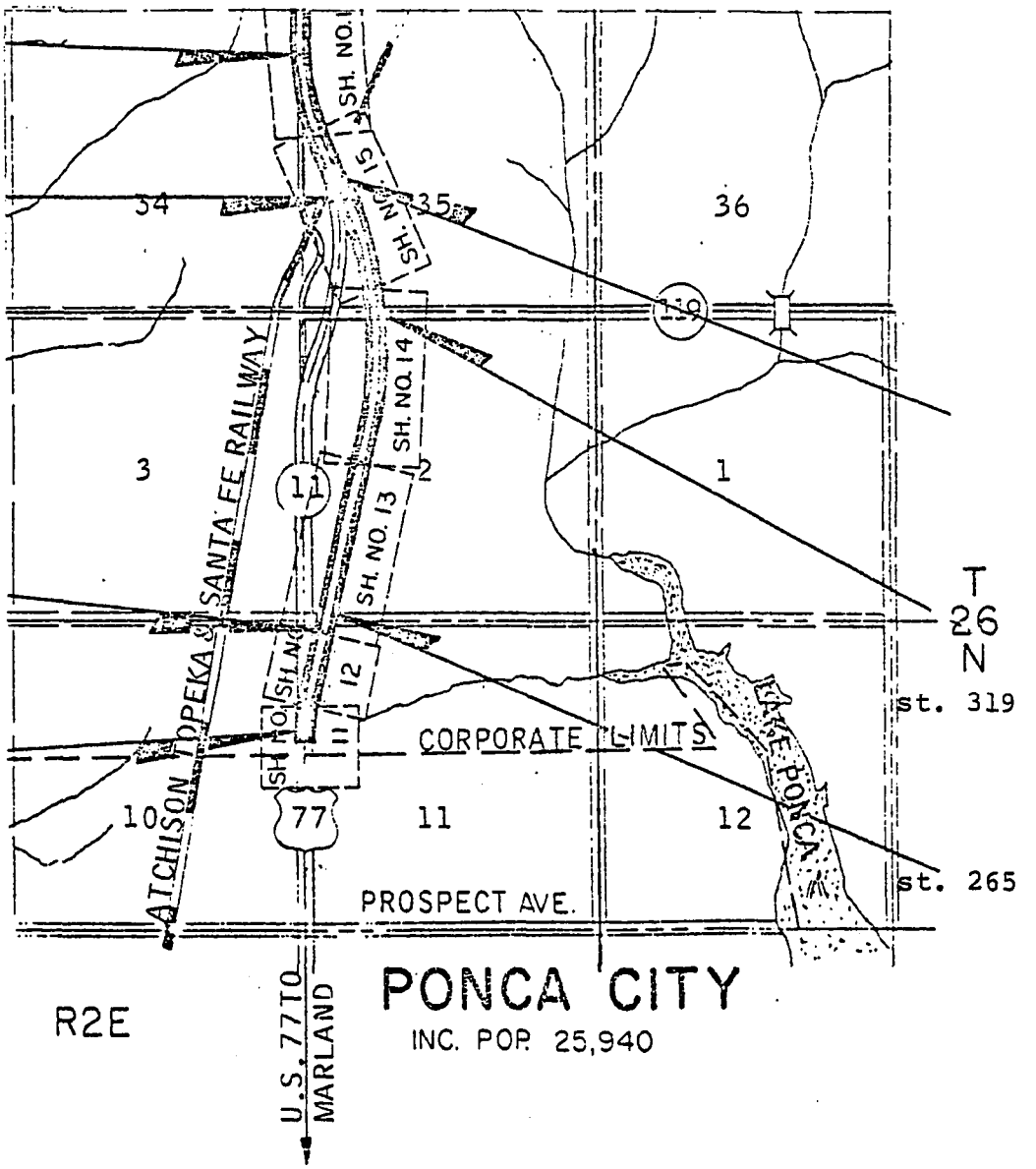

Figure 3.1: Location plan of study site

tive by using all three and a 400 ft. long control section. A total of eight samples, two from each of the four study sections (lime, cement, fly ash, conjunctive) were taken to check the variation of the subgrade material which will form the foundation of the pavement structure. Statistical sampling was carried out using the method of random tables, and the location of each sample is shown in Table 3.1.

Preliminary Testing. The shale samples obtained from the field varied in color from yellowish gray to gray and to grayish brown. Samples were air dried in the laboratory and broken to pass U.S. Standard sieve #10. To check the similarities or dissimilarities in their engineering characteristics, gradation analysis and plasticity tests were run on all samples. On the basis of these tests all eight samples fell under the A-7-6 soil group by the AASHTO classification system. As there were no significant differences among the different samples, they were all combined to form a composite sample for further studies. Table 3.2 presents the engineering characteristics and classification of each sample.

The stabilizing agents used in this study were lime, Portland cement and fly ash. The hydrated lime was obtained from Ash Grove Cement Company in Kansas City, Missouri, and the chemical analysis of the hydrated lime is presented in Table 3.3. The Portland cement type I

TABLE 3.1: SOIL SAMPLING LOCATIONS

A	B	C	Distance from Beginning of Section, ft.	Station	Offset Distance from C.L., ft.
				267+00	
01	.091	.371	291	269+91	3.1 L
02	.166	.056	531	272+32	10.7 L
03	.377	.648	1206	279+06	3.6 R
06	.397	.769	1270	279+70	6.5 R
04	.539	.972	1725	284+25	11.3 R
05	.847	.925	2710	294+10	10.2 R
08	.911	.215	2915	296+15	6.8 L
07	.946	.065	3027	297+27	10.4 L
				299+00	

TABLE 3.2: ENGINEERING PROPERTIES OF SOIL SAMPLES

Sample No. & Station	<2μ Clay, %	<5μ Clay, %	Silt %	Sand %	L.L %	P.I %	AASHTO Classification	UNIFIED Classification	USDA Classification
1. 269+91	44	52	51	5	44	26	A-7-6(26)	CL	Silty Clay
2. 272+31	41	47	55	4	48	29	A-7-6(30)	CL	Silty Clay
3. 279+06	41	47	55	4	47	29	A-7-6(30)	CL	Silty Clay
4. 279+70	44	49	51	5	48	30	A-7-6(30)	CL	Silty Clay
5. 284+25	52	66	30	18	51	30	A-7-6(25)	CH	Clay
6. 294+10	41	46	54	5	53	37	A-7-6(38)	CH	Silty Clay
7. 296+15	56	66	40	4	58	36	A-7-6(39)	CH	Clay
8. 297+27	46	54	48	6	52	32	A-7-6(33)	CH	Silty Clay

TABLE 3.3: CHEMICAL ANALYSIS OF ASH GROVE "SNOW FLAKE" HYDRATED LIME

Available calcium Hydroxide	$Ca(OH)_2$	95.25%
Equivalent to calcium oxide	CaO	72.16%
Magnesium Hydroxide	$Mg(OH)_2$	0.30%
Calcium carbonate	$CaCO_3$	1.95%
Silicon Dioxide	SiO_2	0.65%
Ferric Oxide	Fe_2O_3	0.05%
Aluminium Oxide	Al_2O_3	0.24%
Sulphur Trioxide	SO_3	0.01%
Carbon Dioxide	CO_2	0.80%
Mechanical Moisture	H_2O	0.70%
Fineness:		
Passing 400 mesh screen		99.0%
Passing 200 mesh screen		99.8%

was supplied by Martin Marietta's Western Division, Tulsa, Oklahoma. Table 3.4 shows the chemical composition of the cement used. For this study fly ash was obtained from the Muskogee Environmental Conservation Company, Muskogee, Oklahoma, and its chemical analysis is presented in Table 3.5.

TABLE 3.4: CHEMICAL COMPOSITION OF TYPE I PORTLAND CEMENT, FROM MARTIN MARIETTA'S WESTERN DIVISION, TULSA, OKLAHOMA

SiO_2	20.9%
Al_2O_3	5.2%
Fe_2O_3	2.8%
CaO	64.2%
MgO	2.0%
SO_3	3.1%
Na_2O	0.19%
K_2O	0.68%
Loss	0.9%

TABLE 3.5: MINERAL ANALYSIS OF ASH FROM MUSKOGEE ENVIRONMENTAL CONSERVATION COMPANY

Silica, SiO_2	36.23%
Aluminum Oxide, Al_2O_3	19.03%
Ferric Oxide, Fe_2O_3	9.72%
Sulphur Trioxide, SO_3	2.62%
Calcium Oxide, CaO	26.25%
Magnesium Oxide, MgO	4.94%
Available Alkalines, (Na_2O)	1.20%

CHAPTER IV

EXPERIMENTAL TESTING

In the first phase of this research, testing was limited to classifying the samples and selecting the amount of stabilizing agents to be added to the subgrade material. Subsequently the shale with the selected percentages of stabilizers was subjected to tests generally used to evaluate engineering properties of raw and stabilied highway soil materials. These tests include, grain size analysis, atterberg limits, moisture-density, unconfined compressive strength, triaxial strength, beam strength, X-ray diffraction analysis and scanning electron microscopy. These tests followed standard specifications as indicated.

Grain Size Analysis. Grain size distributions for the raw and stabilized shale were determined in accordance with ASTM Designation D422-63(72) (AASHTO Designation T-88-78). The deflocculating agent used was calgon solution. Further dispersion of clay particles was accomplished by applying a 10 psi air pressure from the Iowa dispersion jet apparatus for about 5 minutes.

Atterberg Limits. Liquid limit tests were run according

to ASTM Designation D423-66(72) (AASHTO Designation T89-76), and the plastic limit tests were conducted in accordance with ASTM Designation D424-59(71) (AASHTO Designation T-90-70).

Moisture Density Tests. The moisture density tests were run in accordance with ASTM Designation D558-57(76) (AASHTO Designation T-99-74). However, instead of the standard Proctor apparatus the Harvard Miniature apparatus was used. Specimens were compacted in three layers with a compactive effort of 25 blows per layer using a 20 lb. spring loaded press hammer. The advantage of using the Harvard miniature compaction apparatus is that about one third of the amount of soil required for standard Proctor is sufficient to run the test. Moisture density tests were run on the raw shale and shale with varying proportions of the stabilizing agents. Figures B.1 through B.3 in Appendix B show the moisture density curves.

The optimum moisture did not change when lime was added to the shale but density was reduced. Cement and fly ash stabilizations showed an increase in optimum moisture content and maximum dry density.

Unconfined Compressive Strength. Samples were compacted in the Harvard Miniature apparatus, at optimum moisture content and maximum dry density determined in accordance with ASTM Designation D2166-66(79) (AASHTO Designation

T 99-74). The samples were then extracted and immediately wrapped in saran wrap, labeled and stored in a humidifier, at 90 to 100 percent humidity. The samples were cured for 28, 90 and 180 days at 70°F and 90°F curing temperatures. At the end of the curing periods samples were removed from the humidifier unwrapped and tested for unconfined compressive strength as shown in Figure 4.1. All the compressive strength values reported in Chapter V are the average value of three specimens.

Wet-Dry Cycles. To simulate the effect of weather on the stabilized soil, the samples were subjectead to cycles of "wetting" and "drying". A wet-dry cycle in the field is defined as a dry period in a 24 hour interval, rainfall less than 0.10 inches is disregarded unless it is continuous over two 24 hour periods with a total of at least 0.10 inches.

According to the 1958 to 1968 wet-dry cycle data (Laguros, 1972), Kay County, the project area experiences about 40 wet-dry cycles per year. Generally, a period of 4 to 6 months ellapses between the construction of the stabilized subgrade and the placement of the pavement. Thus, wet-dry cycles of 5 and 15 were believed adequate. For wet-dry testing, samples were unwrapped at the end of the curing periods and placed in an oven set at 60°C to dry for 12 hours. This drying temperature was selected because it corresponds to the maximum temperatures in

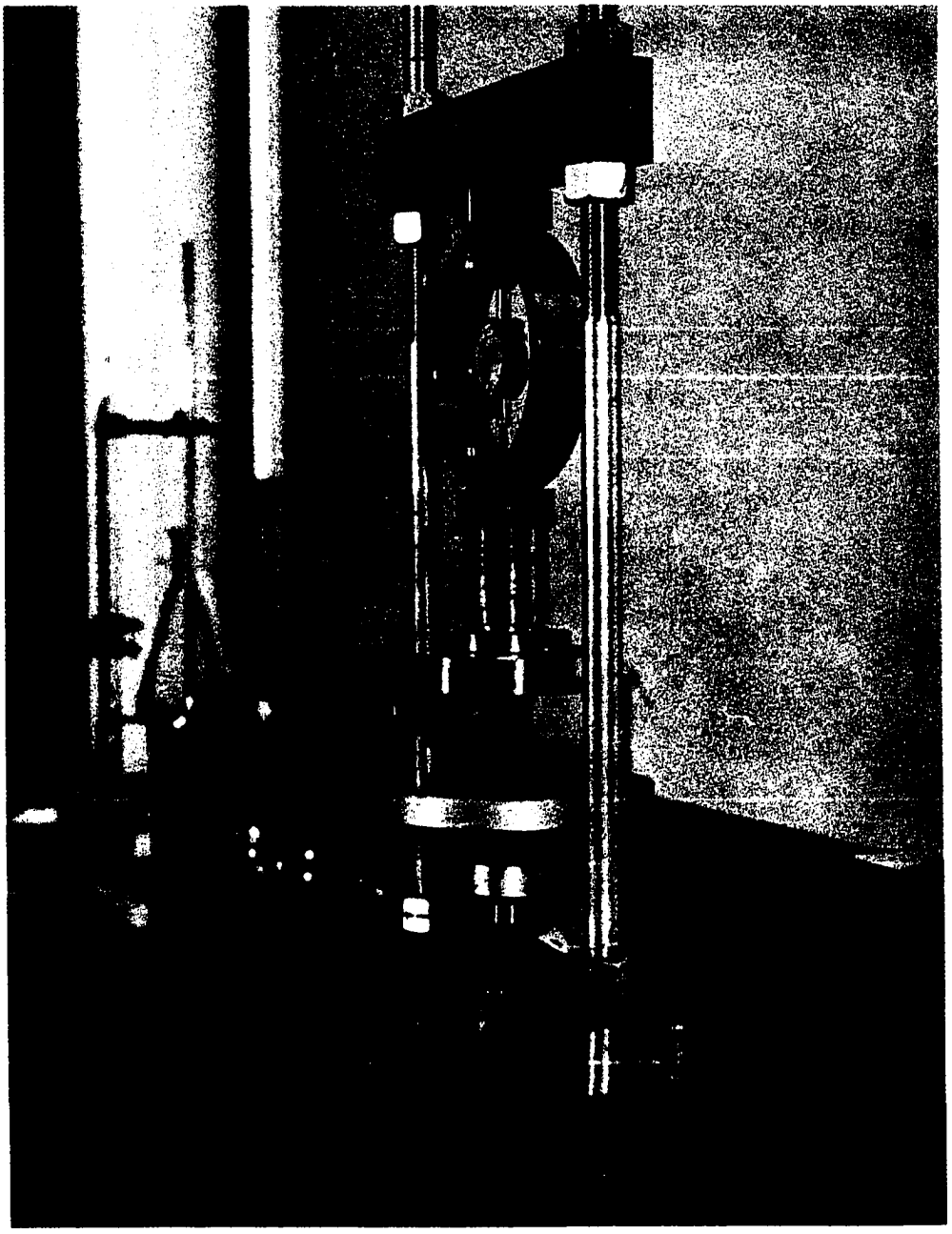

Figure 4.1: Compression strength testing device

open areas for Oklahoma. At the end of the drying period, the samples were transferred to humidifiers set at the curing temperatures (70°F and 90°F), 90 to 100 percent relative humidity and were kept there for 24 hours. This drying and wetting or humidifying, therefore, constituted one wet-dry cycle. At the end of 5 and 15 wet-dry cycles triplicate specimens were tested for each humid or wet and dry condition.

Triaxial Compressive Strength Parameters. The strength parameters of soils can be determinded by direct shear or by the triaxial compression test. The triaxial compression test is often employed to study the behavior of soils, because it duplicates better, the soil conditions prior and after construction. The general Mohr-Coulomb failure law is used in determining the parameters and is expressed by the formula:

$$\tau = c + \sigma \tan \phi \qquad (4.1)$$

where

τ = shear stress, psi

c = cohesion, psi

σ = total normal stress, psi

ϕ = angle of internal friction, degrees

Depending upon the soil-water-air interaction within the cross-sectional area normal to the load, the total normal stress, σ, includes some parameters and is generally ex-

pressed by:

$$\sigma = \bar{\bar{\sigma}} A_m + U_a A_a + U_w A_w + A - R \qquad (4.2)$$

where

$\bar{\bar{\sigma}}$ = contact stress at mineral to mineral contact points

A_m = (area of mineral to mineral contact)/-(total area)

U_a = pore air pressure

A_a = (Area of air to mineral contact)/-(total area)

U_w = pore water pressure

A_w = (area of water to mineral contact)/-(total area)

A = net attractive forces between clay platelets

R = net repulsive forces between clay platelets

In dispersed plastic clays, A and R are considered predominant, however, they cannot be measured experimentally. For other textured soils A and R are not significant and are generally disregarded. Also the mineral to mineral contact pressure $\bar{\bar{\sigma}}$ is very large, and $A_m \simeq o$ but $\bar{\bar{\sigma}} A_m$ is finite and is equal to the effective stress ($\bar{\sigma}$), and $A_a + A_w \simeq 1$.

The total normal stress for fully saturated and partially saturated soils is given by equations 4.3 and 4.4 respectively.

$$\sigma = \bar{\sigma} + U_w \tag{4.3}$$

$$\sigma = \bar{\sigma} + U_a + A_w\ (U_w - U_a) \tag{4.4}$$

In terms of the effective stress the Mohr-Coulomb equation is give by

$$\tau = \bar{c} + \bar{\sigma} \tan \bar{\phi} \tag{4.5}$$

where

$\bar{c}$ = true cohesion, psi

$\bar{\sigma}$ = effective normal stress, psi

$\bar{\phi}$ = true angle of internal friction, degrees

Both the total stress and the effective stress approach are applicable in design practice. For the purposes of this study the strength parameters were determined by the total stress method (unconsolidated-undrained) without pore water measurements. This method is appropriate for two reasons: (i) when embankments are constructed or highway slopes are cut, the soil is stressed quickly and no time elapses for the pore water to dissipate, and (ii) the thickness of bases and subbases being small, the pore water pressure build up is

not critical.

Sample Preparation and Testing. Triaxial compression testing was done in accordance with ASTM Designation D2850-70 (AASHTO Designation T-216-74). Samples for triaxial testing were prepared in the same manner as those for the unconfined compression tests and they were cured at 70°F and 90°F and at 90 to 100 percent humidity. After curing periods of 28, 90 and 180 days, specimens were prepared for testing. They were unwrapped, the diameter, height and weight of each specimen was measured and recorded.

The testing machine used was a Clockhouse triaxial machine. The set-up is shown in Figure 4.2. The machine has a loading capacity of 10,000 lb. and is capable of constant deformation of 0.00007 in/min to 0.16 in/min. The confining cell pressure was applied by a liquid mixture of glycerine and distilled water. Specimens were tested at three cell pressures, 10 ps, 20 psi and 30 psi. Typical triaxial test failure patterns are depicted in Figure 4.3.

Beam Strength. The strength ameliorations of stabilized soils are generally investigated by standard tests such as the unconfined compressive strength, the triaxial test and some durability tests. On the basis of these tests most pavements with lime, fly ash or cement treated bases or subbases are designed as flexible pavements. However,

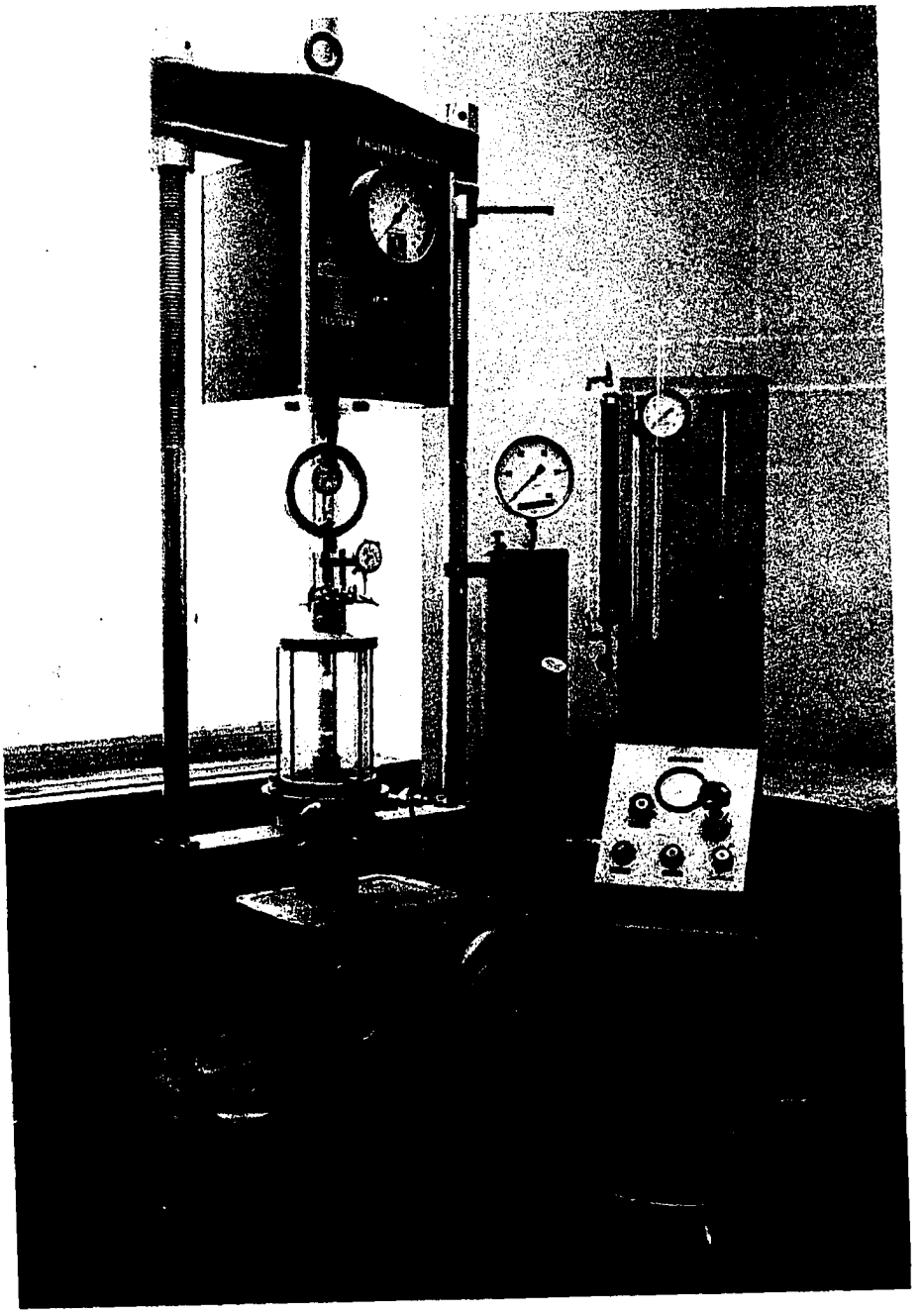

Figure 4.2 Triaxial compression test set up

Figure 4.3: Failure patterns of triaxial samples

some stabilized soils, when cured properly can develop high modules of elasticity values which may make the pavement perform as a slab or beam rather than as a flexible pavement. Thus, raw and stabilized shale beams were made to test their strength in bending. Samples were prepared in accordance with ASTM Designation D1635-63. The soil material used was that passing U.S. Standard sieve No. 4. On the basis of maximum dry density and optimum moisture content relations a precalculated amount of shale-stabilizer-water proportion was prepared to fill a steel mold 2 3/4" x 4" x 16". The shale and stabilizer were dry mixed using a Hobart mortar mixer to a uniform color, water was then added and mixing continued for a few minutes. The mix was then carefully transferred to the mold and compacted under a static load in two layers. The specimens were then extracted and wrapped in saran wrap for moisture control and left to cure in a chamber at 70°F and 90 to 100 percent relative humidity.

At the end of 28 days curing, the specimens were taken out of the humid chamber, unwrapped and prepared for testing. The testing was done in accordance with ASTM Designation C78-75; which relates to the flexural strength of concrete using simple beam third point loading. The unsupported beam length was 15 inches and the testing arrangement was as shown in Figure 4.4. Under

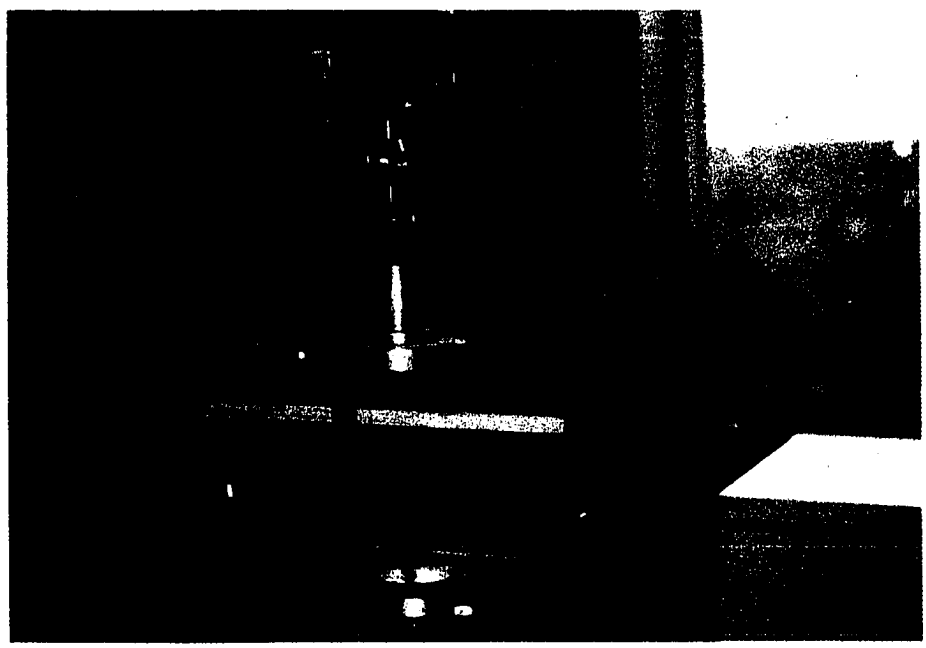

Figure 4.4: Beam loading arrangement

the bending loads all the beams failed within the middle third span where the moment is maximum. Fig 4.5 depicts the mode and location of failure of a beam.

Scanning Electron Microscopy. After unconfined compressive tests were run, portions of the failed specimens were saved in a glass jar. Thin slices were carefully prepared from the specimens without damaging the failure plane. The slices were oven dried and attached to an aluminum metal stub. They were then thinly coated with gold palladium and were dried by evaporation under a 7×10^{-5} mm mercury vacuum unit. The specimen stubs were then placed in the scanning electron microscope and four photographic exposures from the four quadrants of the stub were obtained using self-developing photographic packets (Polaroid). Magnification of photographic areas was 3000X.

X-Ray Diffraction. X-ray diffractograms were used in the analysis of the mineralogical composition of the raw and stabilized shale. Portions of the unconfined compressive specimens were collected after testing. These samples were ground with pestle and mortar to pass United States standard sieve No. 200 and were saved in closed glass containers.

Two types of X-ray diffraction equipment were used in obtaining the diffractograms, the Siemens Diffractometer Unit, and an APD-360 Phillips Automated X-ray

Figure 4.5: Mode and failure location of the beam

powder diffractometer were used in obtaining the diffractograms. Thus, two methods of specimen preparations were used: (i) the bottom of a 50 ml beaker was covered with the soil finer than sieve No. 200. Distilled water was added to a volume of 40 ml. The soil water mixture was exposed to ultrasonic vibrations for five minutes. The sample was then left to settle for 1½ to 2 hours, to allow materials coarser than 2 micron to settle. The finer material in suspension was then drawn off with an eye dropper and loaded on a 37 x 37 mm glass plate. The sample was then left to dry overnight at room temperature, (ii) grooved glass slides were packed with the shale-stabilizer powder finer than sieve No. 200.

The sedimented slides were run in the Siemens diffractometer unit and the powder slides were run in the APD-360 Phillips powder diffractometer. The rate of scanning used with the Siemens diffractometer was a 1°(2θ) per minute. Other data pertinent to this equipment include: KV = 35V, MA = 18, rate meter = $2x10^4$ cycles per second, standard deviation of 2 percent and chart speed of 1cm per minute. The rate of scan on the Phillips powder diffractometer was 2 degrees per minute. Diffractions were run to 45 degrees. The intensity of the powder diffractograms below the 20 degree (2θ) scan were attenuated to give better peaks.

CHAPTER V

PRESENTATION AND DISCUSSION OF TEST RESULTS

This chapter deals with the characterization of the stabilized shale product. However, it is considered appropriate to state briefly the processes involved in the preliminary evaluation. Basic engineering tests were used to characterize the project shale. These tests were the grain size distribution, plasticity, moisture density, unconfined compressive strength and triaxial compressive strength. In order to determine the amount of stabilizers to be used in the field for the successful stabilization of the shale, trial mixes of shale-lime (3, 5, 6 and 9 percent), shale-cement (10, 12, 14 and 18 percent), shale-fly ash (20, 25 and 30 percent) and shale-conjunctive (cement + lime + fly ash, 6 + 3 + 22 and 6 + 4 + 18) were studied. The final design mixes were then chosen and the gain in strength of the shale-stabilizer-water mixes was studied. The flexural strength characteristics of the compacted stabilized beams were investigated and correlations between axial and flexural strengths are presented. Changes in void patterns resulting from fabric changes which are due to shale-

stabilizer-water interaction were examined employing SEM and the micrographs and discussions are presented. X-ray diffraction analyses to detect any clay mineral changes or new mineral crystal formations resulting from stabilization are also included.

Grain Size Analysis. Grain size analyses were run on the raw and stabilized shale cured at 70°F for 28 days at 90 to 100 percent relative humidity. The grain size distribution curves of raw and stabilized shale are presented in Figure 5.1. The gradation curves depict that all stabilizers substantially reduced the silt-and clay-size fraction of the shale. The aggregation index (AI) as defined by Jha (1977) is calculated for the different stabilizers in order to compare the agglomeration or crowding of the clay - size fraction. This term is mathematically defined as:

$$AI = \frac{\text{percent nonclay-size material of shale and stabilizer}}{\text{percent nonclay-size material of raw shale}}$$

Cement stabilization gave the highest aggregation index followed by lime and fly ash in that order. The degree of cementation or aggregation is also found to be directly proportional to the amounts of cementing agents used. The clay, silt and sand fractions of the stabilized shale are presented in Table 5.1. The aggregation index values that correspond to the grain size distribution curves in Figure 5.1 are reported in Table 5.2.

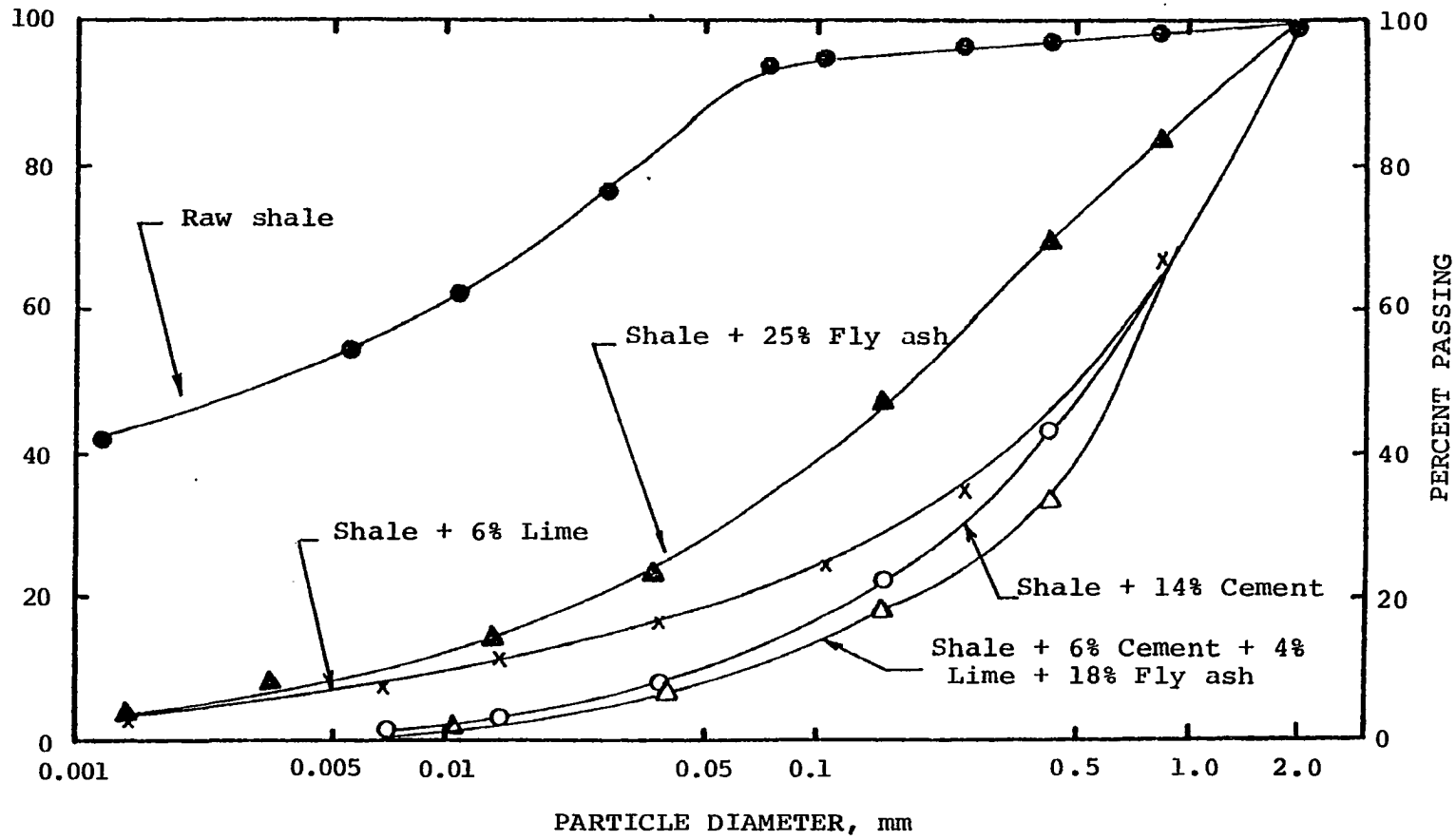

Figure 5.1: Grain size distribution curves

TABLE 5.1: ENGINEERING PROPERTIES OF RAW AND STABILIZED SHALE

Type of Mix	< 2μ Clay,%	< 5μ Clay,%	Silt %	Sand %	L.L. %	P.I. %
Raw Shale	46	53	48	6	50	31
Shale + 3% lime	9	12	19	72	41	11
+ 6% lime	4	7	18	78	43	9
+ 9% lime	2	2	11	87	47	8
Shale + 10% cement	1	2	11	88	NP	NP
+ 14% cement	1	2	13	86	NP	NP
+ 18% cement	0	0	14	86	NP	NP
Shale + 20% fly ash	8	13	32	60	37	13
+ 25% fly ash	6	10	30	64	39	12
+ 30% fly ash	6	12	36	58	38	13
Shale + Combinations						
6%C+3%L+22% FA	0	0	16	84	NP	NP
6%C+4%L+18% FA	0	0	12	88	NP	NP

TABLE 5.2: AGGREGATION INDEX OF RAW AND STABILIZED SHALE CURED AT 70°F FOR 28 DAYS, 90 to 100 PERCENT RELATIVE HUMIDITY

Type of Mix	Aggregation Index
Raw Shale	1.00
Shale + 25 percent fly ash	1.74
Shale + 6 percent lime	1.78
Shale + 14 percent cement	1.83
Shale + conjunctive (6%C + 4%L + 18%FA)	1.85

In terms of the aggregation index, the effectiveness of adding 14 percent cement (AI = 1.83) to the shale is equivalent to the conjunctive addition of 6 percent cement, 4 percent lime and 18 percent fly ash (AI = 1.85). Similarly and, as evidenced from Table 5.2, 25 percent fly ash is comparable to 6 percent lime. The gradation curves for all shale-lime, shale-fly ash, shale-cement and shale-conjunctive mixes are included in Figures B.1 through B.4, Appendix B.

Atterberg Limits. As reported in Chapter III, the shale was very clayey and had high plasticity. All stabilizers lowered the plasticity index of the shale significantly. Cement and conjunctive stabilization rendered the soil nonplastic. This is in agreement with the gradation results, because these two cases gave maximum reduction of the clay-size fraction which also infers higher aggregation. Lime stabilization reduced the plasticity index from 31 percent to 10 percent while fly ash stabilization lowered it to 12 percent. The gradation and plasticity data of the stabilized shale, cured for 28 days at 70°F and 90 to 100 percent relative humidity are included in Table 5.1.

Moisture-Density Relations. The moisture-density test results on samples compacted immediately after mixing are reported in Table 5.3. Admixtures changed both the optimum moisture and maximum dry density but not substan-

TABLE 5.3: MOISTURE DENSITY RESULTS

Type of Mix	Optimum Moisture Content, %	Maximum Dry Density, pcf
Raw Shale	18.5	101.0
Shale + 3% lime	18.4	99.5
+ 6% lime	19.3	97:3
+ 9% lime	21.3	94.8
Shale + 10% cement	18.5	101.5
+ 14% cement	19.0	103.0
+ 18% cement	18.0	102.5
Shale + 20% fly ash	18.8	104.5
+ 25% fly ash	19.0	104.3
+ 30% fly ash	18.0	105.0

tially. The addition of cement and fly ash produced little change in the optimum moisture content of the shale but increased the maximum dry density from 101 pcf to 103 and 104.3 pcf, respectively, on the other hand, the addition of lime lowered the maximum dry density to 97.3 pcf and increased the optimum moisture content. Fly ash caused the highest increase of maximum dry density. The moisture-density curves for the raw and stabilized shale are included in Figures C.1 to C.7 in Appendix C.

Dry and Immersed Strengths. The unconfined compressive strength test results are presented in Tables D.1 through D.5 of Appendix D. The purpose of the immersed strength evaluations was to establish a measure of the durability or permanence of the strength gain resulting from stabilization. Table D.1 presents the strength levels attained by the various amounts for different stabilizers used. In general, the higher the amount of the stabilizer added, the higher the strength gain. However, the rate of strength increase is reduced at higher soil-stabilizer proportions. For instance, the addition of 3, 6 and 9 percent lime gave strengths of 137, 193 and 200 psi, respectively.

The suitability and amount of stabilizer required to impart an acceptable degree of amelioration to the shale was based on the 28 day immersed strength and the plasticity index of the shale-stabilizer mixes. In cement

stabilized soils, the Portland Cement Association recommends a strength of 250 psi for light traffic and 400 psi for heavy traffic conditions. However, there are no such stringent guidelines on the strength levels of lime and fly ash stabilized soils. The general practice in the determination of amount of lime for adequate stabilization is the use of McDowell's charts (1966) and a minimum of unconfined compressive value of 50 psi for subgrade or subbase and 100 psi for base materials. Hence, the Portland Cement Association, and McDowell's plasticity index and strength criteria were used to select the amount of cement, lime and fly ash, respectively. The following stabilizer proportions, therefore, proved adequate and were selected to be adopted as final design proportions:

(i) 6 percent lime

(ii) 25 percent fly ash

(iii) 14 percent cement

(iv) conjunctive use of 8 percent cement, 4 percent lime and 18 percent fly ash

The effects of curing at slightly higher temperature, i.e., 90°F upon the unconfined compressive strengths of the selected proportions were evaluated and the values are reported in Tables D.2 through D.5 of Appendix D.

Lime Stabilization. Addition of lime to the shale resulted in strength gains, but in all cases, the values

fell below those for the cement and fly ash stabilized shale. Both the 70°F and 90°F cured specimens gained strength with aging. At the end of 180 days, the dry strength of the specimens cured at 70°F was 210 psi, a value almost twofold the strength at 28 days (107.6 psi). Higher curing temperature (90°F) resulted in higher strengths than those cured at 70°F; also, the rate of strength gain with aging was higher when curing took place at higher temperature. Immersion of specimens in water for 24 hours, reduced the strength. Specimens curved at 70°F lost about 36 percent of their strength while those cured at 90°F, lost about 33 percent of their strength. Thus, the 90-day dry strength of the 70°F and 90°F cured specimens (129.3 and 187.7 psi, respectively) was reduced by approximately 20 percent upon soaking in water. This seems to suggest that the adverse effect of immersing specimens in water for 24 hours is less with longer curing periods. Figure 5.2 presents the relationship of strength and curing time of lime stabilized shale.

Fly Ash Stabilization. Fly ash stabilization of the shale resulted in higher dry and immersed strengths than lime did. The 28-day dry strength values for the 70°F and 90°F curing conditions were 193.8 and 208 psi, respectively, and after 180 days of curing the corresponding values were 257 and 409.9 psi. Also, with tempera-

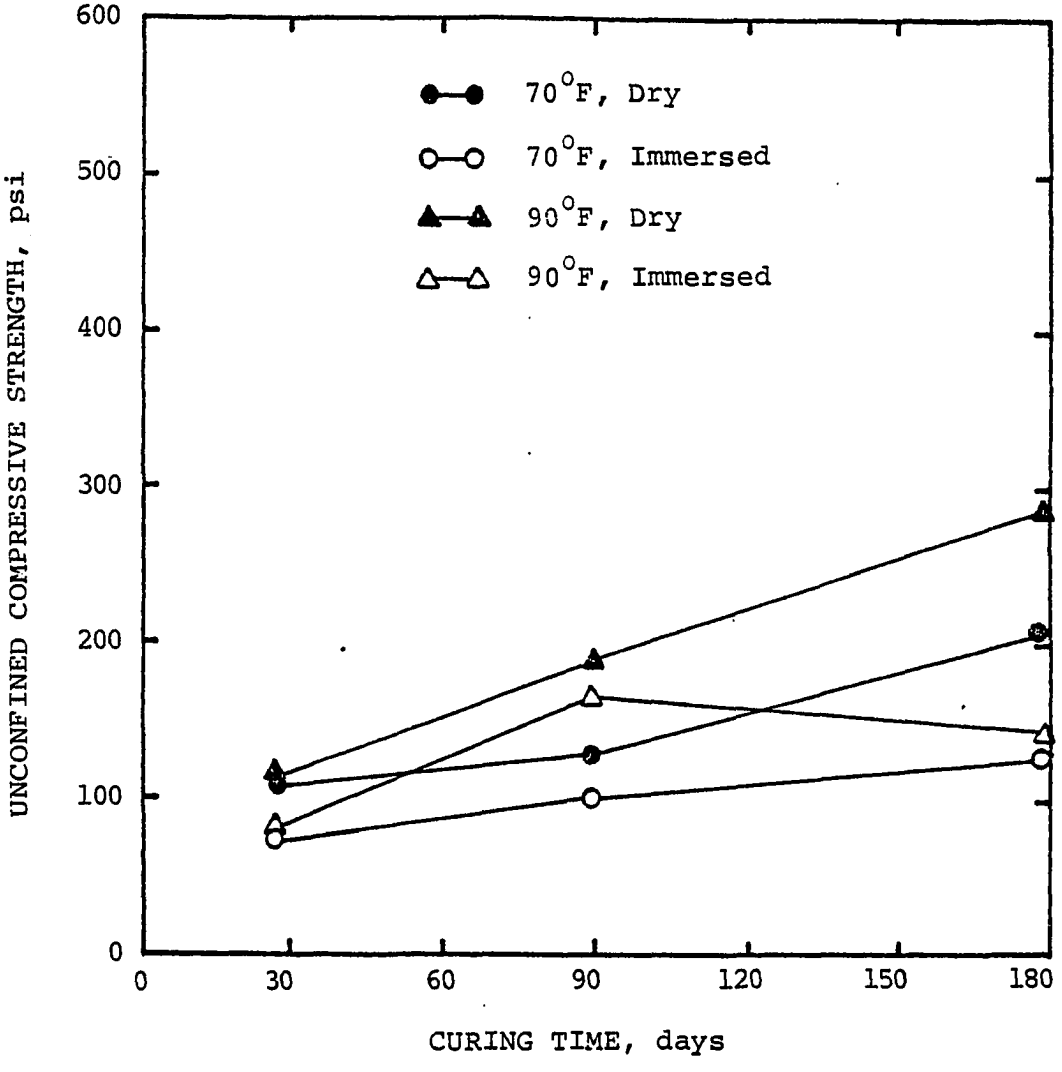

Figure 5.2: Dry and immersed strength of 6 percent lime stabilized shale, cured at 70°F and 90°F, 90 to 100 percent relative humidity

ture kept constant at 70°F the strength increase from 28 to 180 days was lower (257-193.8 = 63.2 psi) than at 90°F (409.9-208 = 201.9 psi). Thus, the rate of strength increase of fly ash stabilized shale was higher for higher curing temperature. Immersion in water for 24 hours reduced the strength of the specimens. The average strength loss for specimens cured at 70°F was 38 percent, and for those cured at 90°F it was 28 percent. Fly ash stabilized shale, therefore, seems to be less adversely affected by soaking in water when cured at higher temperatures. Figure 5.3 presents the dry and immersed strength levels of the fly ash stabilized shale.

Cement Stabilization. The unconfined compressive strength values of cement stabilized shale were much higher than the lime and fly ash stabilized shale strength values. In fact, the 28-day dry strength of cement stabilized shale, cured at 70°F was 580 psi which is higher than the 180-day, 90°F cured dry strength of lime stabilized shale (289 psi) and of the fly ash stabilized shale (409.9 psi). As presented in Table D.4, cement stabilization increased strength values with higher curing temperature and longer curing periods. All specimens experienced loss in strength upon soaking in water for 24 hours. However, those cured at 70°F showed slightly higher strength loss (33 percent) than those cured at 90°F (30 percent). The immersed strengths of cement sta-

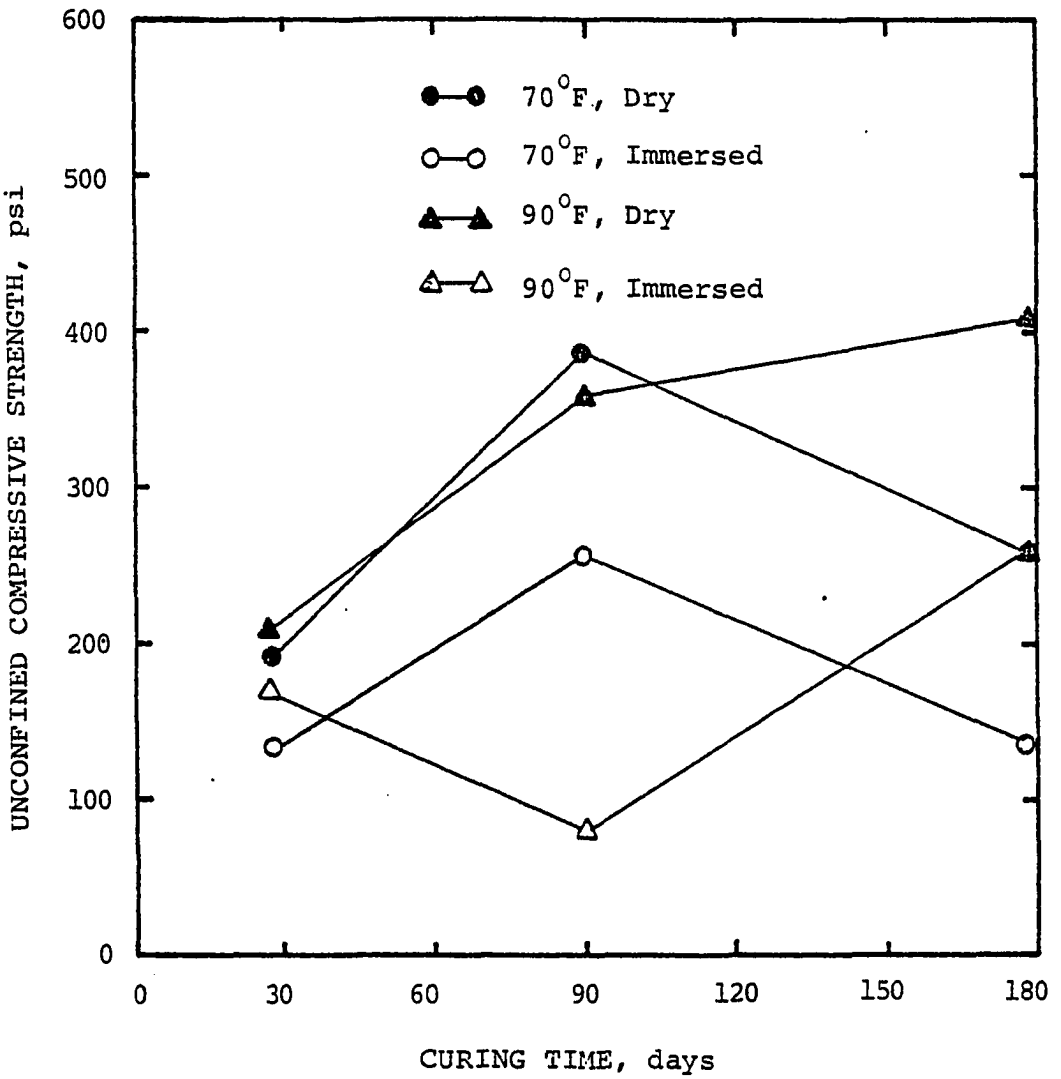

Figure 5.3: Dry and immersed strength of 25 percent fly ash stabilized shale, cured at 70°F and 90°F, 90 to 100 percent relative humidity

bilized shale were substantially higher than the immersed strengths of lime and fly ash stabilized shale. Figure 5.4 shows the dry and immersed strengths of cement stabilized shale.

Conjunctive Stabilization. Conjunctive use of cement, lime and fly ash resulted in very high dry and immersed strength values. The 28-day strength of the 70°F and 90°F cured specimens were lower than their cement stabilized counterparts. With prolonged curing, however, the 90 and 180-day conjunctive stabilization gives higher strengths (749.4 and 817.6 psi) than cement stabilization (630 and 761.2 psi). As with the other stabilizers, higher curing temperature led to the development of higher strength. Conjunctively stabilized specimens were more durable than their cement, lime and fly ash counterparts. Specimens lost only 13 to 16 percent of their strength as a result of immersion in water for 24 hours. Figure 5.5 depicts the dry and immersed strengths of conjunctively stabilized shale.

In examining the strength values obtained, it is possible to make a few general remarks, covering all stabilized forms of shale, about the dependence of strength on temperature and time. As discussed in the previous sections, the unconfined compressive strength values of the shale-stabilizer mixes increased when cured for longer periods and at higher temperature. On the basis of

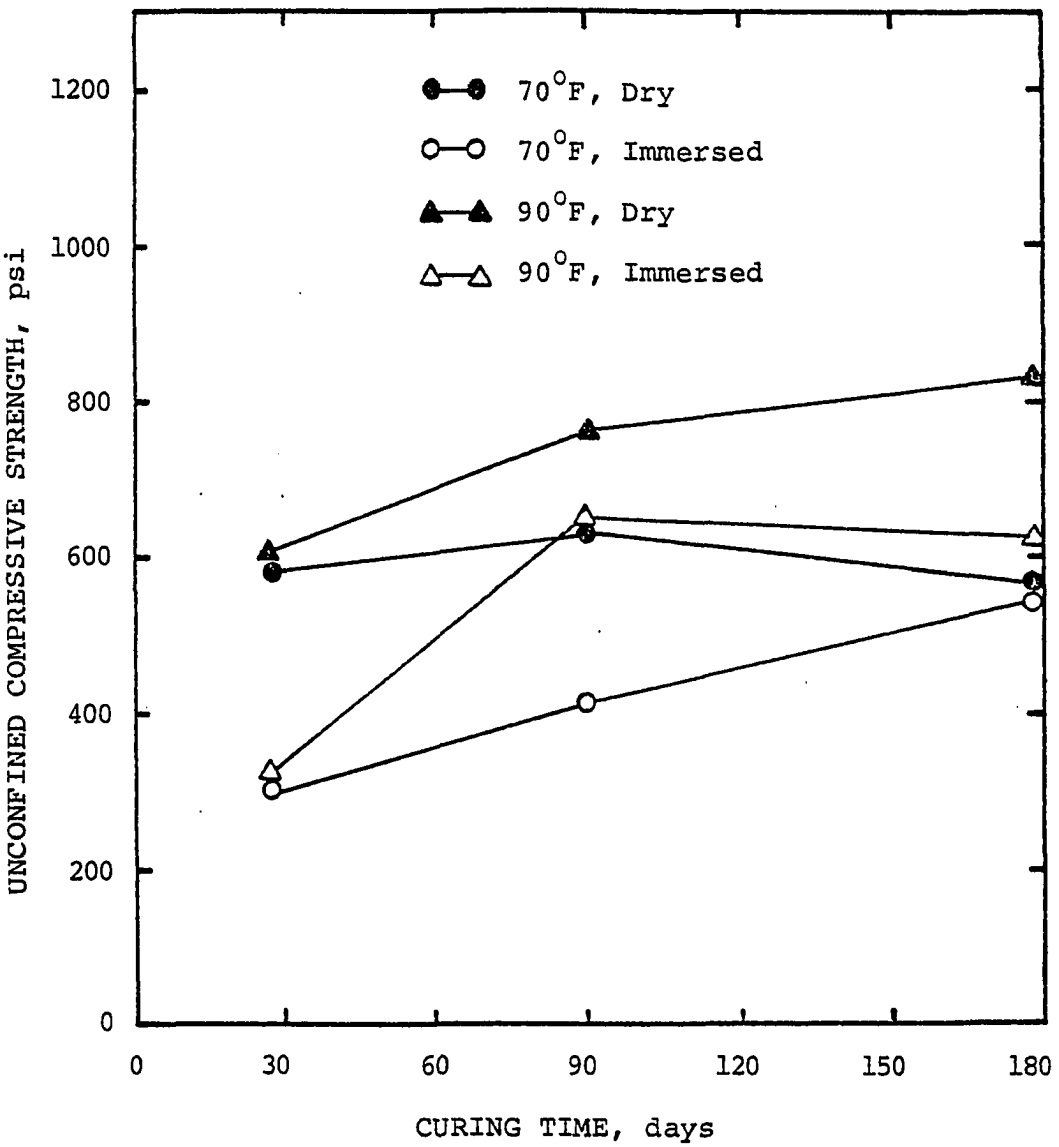

Figure 5.4: Dry and immersed strength of 14 percent cement stabilized shale, cured at 70°F and 90°F, 90 to 100 percent relative humidity

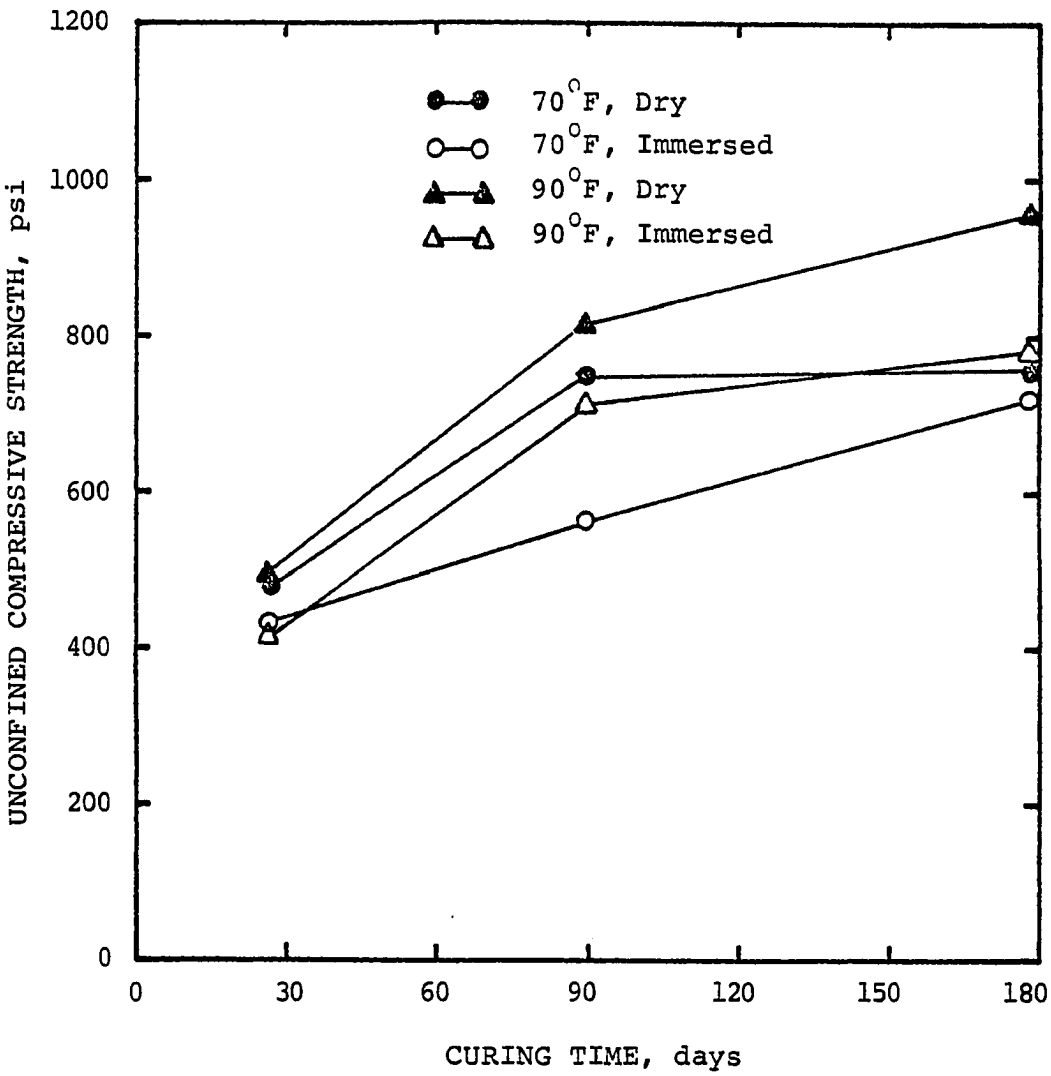

Figure 5.5: Dry and immersed strength of conjunctively (8% cement + 4% lime + 18% fly ash) stabilized shale, cured at 70°F and 90°F, 90 to 100 percent relative humidity

dry strength values Equations 5.1 through 5.4 below were developed to predict the strength levels for the shale-lime, shale-fly ash, shale-cement and shale-conjunctive mixes, respectively.

$$U.C. = 2.44X_1 + 0.91X_2 - 112.45 \quad (5.1)$$

$$U.C. = 2.33X_1 + 0.78X_2 + 38.55 \quad (5.2)$$

$$U.C. = 5.52X_1 + 0.99X_2 + 140.08 \quad (5.3)$$

$$U.C. = 4.75X_1 + 2.34X_2 + 95.65 \quad (5.4)$$

where

U.C. = unconfined compressive strength, psi

X_1 = curing temperature, degrees Fahrenheit

X_2 = curing time, days

In order to investigate the strength responses of the stabilized shale to the influence of curing temperature and curing period, a term called the degree-day was generated by multiplying the number of curing days by the curing temperature and plotted versus the unconfined compressive strength. The advantage of using the degree-day parameter is that it presents the combined effect of curing temperature and curing time. However, it is essential to understand its limitations. For example, a 490 degree-day can be attained by curing a specimen at 70°F for 7 days, or at 490°F for 1 day or at 10°F for 49

days, but these curing conditions can not be expected to result in similar strength levels. And it appears that the notion of degree-day can be applicable within reasonable ranges of temperature 40 to 120°F and time, 3 to 360 days.

Figure 5.6 shows the graphs of the strength versus curing condition for the shale-stabilizer mixes. In all cases the increase in strength was higher for lower degree-days and flatten out for higher degree-day temperatures. A fact worth noting also is the rate of strength increase for the cement and fly ash stabilized shale. Up to about 2400 degree-days (i.e. 28 day curing), cement stabilized shale exhibits higher strength than the conjunctively stabilized shale. However, at higher degree-days, the conjunctively stabilized shale is stronger. One possible explanation may be that the fly ash in the conjunctive stabilization was slow in reacting with the shale initially. Hence, the strength gain was retarded but over longer curing periods, i.e., higher degree-day temperatures, the reaction proceeded normally and higher strength was attained.

"Wet-Dry" Cycles. Following curing, the specimens were subjected to a number of "wetting" and "drying" cycles. The unconfined compressive strength values were then determined at the end of 5 and 15 cycles. The strength data of all shale-stabilizer, curing temperature and

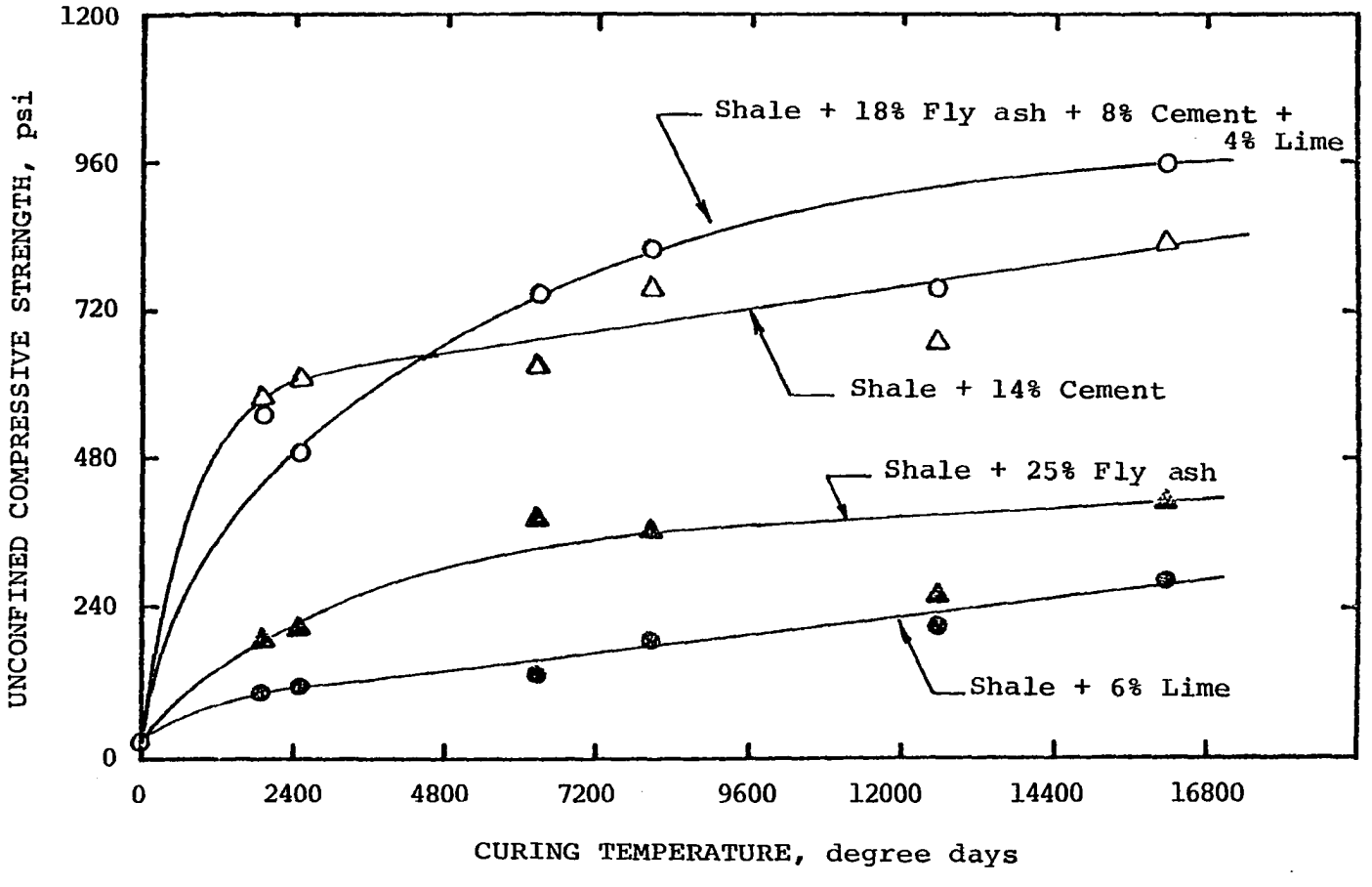

Figure 5.6: Unconfined compressive strength levels of stabilized shale

curing time combinations are presented in Tables 5.4 through 5.7. This process of cyclic wetting and drying substantially raised the unconfined compressive strengths. At the end of 5 cycles of "wetting" and "drying", the "dry" strengths of shale-lime mixes cured at 70°F and 90°F for 180-days were 364 and 387 psi, respectively. For the corresponding conditions shale-fly ash gave 356 and 571 psi, shale-cement 1363 and 1441 psi, and shale-conjunctive 1126 and 1457 psi, respectively.

Triaxial Compressive Strength Test. As presented in Chapter IV, the strength parameters, cohesion (c) and angle of internal friction (ϕ) of the raw and stabilized shale were determined under the triaxial compressive testing. To arrive at the cohesion and at the angle of internal friction values the K_f line was plotted using the p and q values instead of using the conventional Mohr circle. The advantages in using the p-q diagram are (i) it is easier to fit a straight line (K_f) between a number of data points than to draw a tangent line through closely packed circles, (ii) for small lateral stresses and high normal stresses, it is easier to scale the cohesion intercept. A typical p-q diagram is shown in Figure 5.7. The raw shale manifested a cohesion of 11.9 psi and an angle of internal friction of 32.9 degrees. Lime stabilization increased both the cohesion and the angle of internal friction. The former varied from 9 to 32.6 psi

TABLE 5.4: UNCONFINED COMPRESSIVE STRENGTH (psi) OF 6 PERCENT LIME STABILIZED SHALE SUBJECTED TO "WET" AND "DRY" CYCLES

Curing Time,	70°F				90°F			
Days	5 Cycles		15 Cycles		5 Cycles		15 Cycles	
	"Wet"	"Dry"	"Wet"	"Dry"	"Wet"	"Dry"	"Wet"	"Dry"
28	165	214	230	299	139	348	177	324
90	244	332	134	296	206	428	236	267
180	288	364	191	358	249	387	208	319

TABLE 5.5: UNCONFINED COMPRESSIVE STRENGTH (psi) OF 25 PERCENT FLY ASH STABILIZED SHALE SUBJECTED TO "WET" AND "DRY" CYCLES

Curing Time,	70°F				90°F			
Days	5 Cycles		15 Cycles		5 Cycles		15 Cycles	
	"Wet"	"Dry"	"Wet"	"Dry"	"Wet"	"Dry"	"Wet"	"Dry"
28	446	738	387	556	229	382	238	413
90	371	469	290	451	228	588	200	377
180	223	356	211	351	316	571	222	486

TABLE 5.6: UNCONFINED COMPRESSIVE STRENGTH (psi) OF 14 PERCENT CEMENT STABILIZED SHALE SUBJECTED TO "WET" AND "DRY" CYCLES

Curing Time,	70°F				90°F			
Days	5 Cycles		15 Cycles		5 Cycles		15 Cycles	
	"Wet"	"Dry"	"Wet"	"Dry"	"Wet"	"Dry"	"Wet"	"Dry"
28	405	626	566	604	432	627	352	489
90	618	989	570	735	484	1013	536	1008
180	618	1363	479	732	704	1441	1017	1097

TABLE 5.7: UNCONFINED COMPRESSIVE STRENGTH OF CONJUNCTIVELY STABILIZED SHALE SUBJECTED TO "WET" AND "DRY" CYCLES

Curing Time, Days	70°F				90°F			
	5 Cycles		15 Cycles		5 Cycles		15 Cycles	
	"Wet"	"Dry"	"Wet"	"Dry"	"Wet"	"Dry"	"Wet"	"Dry"
28	352	621	314	436	718	888	630	774
90	427	758	557	649	734	1005	677	975
180	707	1126	526	855	1248	1457	539	960

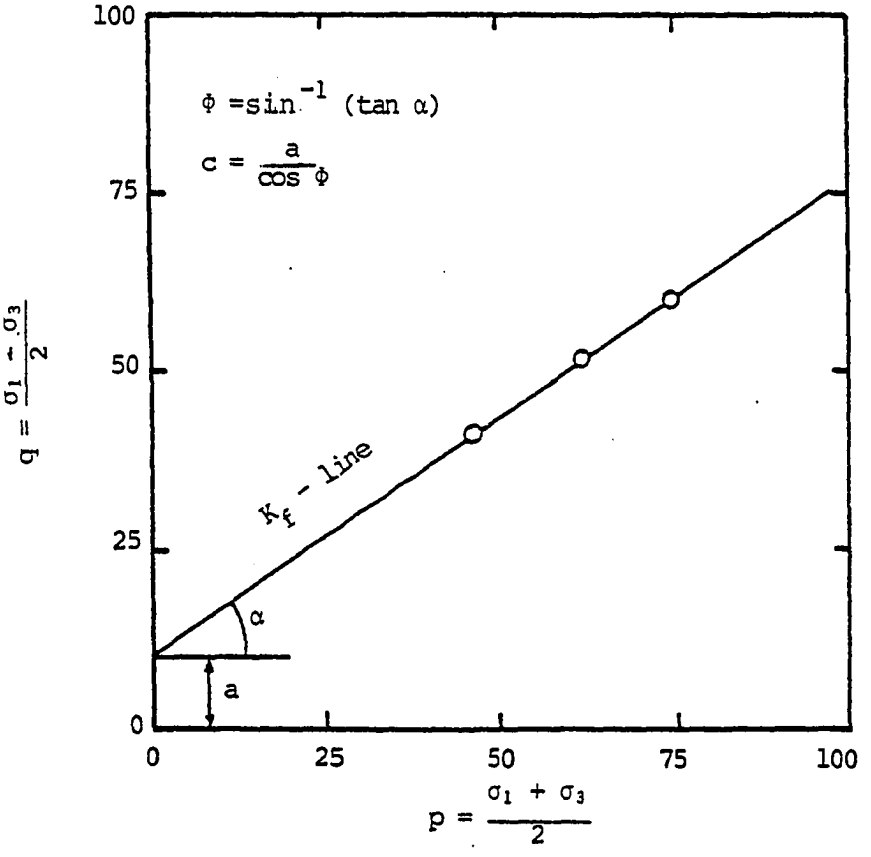

Figure 5.7: Illustrative p - q diagram

and the latter ranged from 50.4 to 62.2 degrees. In many cases, immersing the specimens in water for 24 hours reduced cohesion. The 90°F curing resulted in higher angles of internal friction and lower cohesion than the 70°F curing.

Addition of fly ash (25 percent) contributed to the attainment of higher cohesion and angle of internal friction. The average cohesion for specimens tested dry was 19.1 psi and for immersed specimens it was 18.5 psi. The average angle of internal friction was also lower for the immersed specimens (55.6°) than the dry tested specimens (58.3°). The average cohesion and angle of internal friction of the shale-fly ash were higher than those of the shale-lime.

Cement (14 percent) imparted higher cohesion and angle of internal friction than either lime or fly ash. The dry tested specimens for 28 and 90 days gave an average cohesion of 22 psi and average angle of internal friction of 57.6°, while the immersed specimens gave an average cohesion of 28.4 psi and angle of internal friction of 58.6°. The cement stabilized shale, thus, under went an increase in cohesion and angle of internal friction upon immersion. After 180 days curing, the specimens reached strength levels above the capacity of the triaxial equipment. Conjunctive stabilization resulted in very high triaxial compressive strength values. The

dry specimens were so strong that they did not fail within the maximum load capacity of the triaxial proving ring. The test had to be stopped before failure. However, the 28 and 90 day cured specimens, immersed in water for 24 hours, failed within the proving ring load capacity and resulted in higher cohesion and higher angle of internal friction than the other shale-stabilizer counterparts. The triaxial test results for all stabilizers, curing temperatures and curing periods are reported in Tables 5.8 through 5.11.

TABLE 5.8: STRENGTH PARAMETERS OF 6 PERCENT

LIME STABILIZED SHALE

Curing time, days	70°F				90°F			
	Dry		Immersed		Dry		Immersed	
	Cohesion, C (psi)	Angle of Internal Friction, ϕ (degrees)	Cohesion, C (psi)	Angle of Internal Friction, ϕ (degrees)	Cohesion, C (psi)	Angle of Internal Friction, ϕ (degrees)	Cohesion, C (psi)	Angle of Internal Friction, ϕ (degrees)
28	9	56.4	14	41.4	16.6	53	10.1	42
90	19.2	58.7	32.6	52.2	17.2	60.4	10.8	62.2
180	25.1	50.4	16.5	50.4	14.5	56.4	5.9	59.7

TABLE 5.9: STRENGTH PARAMETERS OF 25 PERCENT FLY ASH STABILIZED SHALE

Curing time, days	70°F				90°F			
	Dry		Immersed		Dry		Immersed	
	Cohesion, C (psi)	Angle of Internal Friction, ϕ (degrees)	Cohesion, C (psi)	Angle of Internal Friction, ϕ (degrees)	Cohesion, C (psi)	Angle of Internal Friction, ϕ (degrees)	Cohesion, C (psi)	Angle of Internal Friction, ϕ (degrees)
28	16.8	55.5	27.5	43.4			12.5	66.4
90	9.0	63.7	15.9	50.9	28.5	57	17.6	63
180	20.5	54.1	14	60	20.7	61.1	23.4	50.1

TABLE 5.10: STRENGTH PARAMETERS OF 14 PERCENT CEMENT STABILIZED SHALE

Curing time, days	70°F				90°F			
	Dry		Immersed		Dry		Immersed	
	Cohesion, C (psi)	Angle of Internal Friction, ϕ (degrees)	Cohesion, C (psi)	Angle of Internal Friction, ϕ (degrees)	Cohesion, C (psi)	Angle of Internal Friction, ϕ (degrees)	Cohesion, C (psi)	Angle of Internal Friction, ϕ (degrees)
28			32.7	50.1	22.2	47.5	13.6	54.1
90	20.7	61.1	40.7	62.2	23.0	64.2	26.5	67.8
180	ND	ND	ND	ND	ND	ND	ND	ND

ND = Not Determined

TABLE 5.11: STRENGTH PARAMETERS OF CONJUNCTIVELY STABILIZED SHALE *

Curing time, days	70°F				90°F			
	Dry		Immersed		Dry		Immersed	
	Cohesion, C (psi)	Angle of Internal Friction, ϕ (degrees)	Cohesion, C (psi)	Angle of Internal Friction, ϕ (degrees)	Cohesion, C (psi)	Angle of Internal Friction, ϕ (degrees)	Cohesion, C (psi)	Angle of Internal Friction, ϕ (degrees)
28	ND	ND	31.1	67.3	ND	ND	25.3	64.2
90	ND	ND	29.8	68.3	ND	ND	29.1	69.9
180	ND	ND	ND	ND	ND	ND	ND	ND

ND = Not Determined

* (8 Percent cement + 4 percent lime + 18 percent flyash)

Beam Action:

The load and deflection parameters were measured for the various shale-stabilizer beams at the end of the curing period. The results presented and discussed in this chapter are, therefore, load-deflection patterns, modulus of rupture and modulus of elasticity. Compressive and flexural strength and modulus of elasticity values from axial and flexural tests are also correlated.

Load Deflection. Four beams were tested for each shale-stabilizer mix. The data points of the load-deflection curves of the four specimens fell very close to each other; thus, the average was plotted. Figures E.1 through E.4 in Appendix E present the load versus deflection curves. These Figures suggest that shale-stabilizer mixes containing large amounts of stabilizer require high loads to undergo the same deflection as those containing lower amounts of stabilizer. The slope of the load deflection curves in all cases, increased at lower loads and was constant at higher loads.

Modulus of Rupture. The maximum load required to fail each beam in bending was used to calculate the maximum moment within the middle third span. The elastic bending method was adopted to calculate the modulus of rupture (flexural stress) from the following relationship:

$$MR = \frac{PL}{bd^2} \qquad (5.5)$$

where

L = span length, inches

MR = modulus of rupture, psi

P = load, pounds

b = beam width, inches

d = beam depth, inches

The modulus of rupture values for all the various stabilizers used are reported in Table 5.12. Four specimens per mix were tested and the values are averages of four beams. The 28-day unconfined compressive strength counterparts are also included in Table 5.12.

The higher the amounts of stabilizers used, the higher the flexural strengths were. As in the uniaxial compressive strength results, lime stabilized shale resulted in the least flexural strength (37 psi) while conjunctively stabilized (143 psi) and cement stabilized (101.4 psi) beams showed high flexural strengths. Figure 5.8 presents the 28-day flexural strength levels of beams versus amount of stabilizer used. The ratios of the flexural to the compressive strengths of the stabilized shale cover a narrow range. The ratio for lime stabilized shale ranges from 0.18 to 0.25, for fly ash from 0.17 to 0.25 and for cement from 0.17 to 0.23. A linear

TABLE 5.12: UNCONFINED COMPRESSIVE AND MODULUS OF RUPTURE VALUES OF STABILIZED SHALE, CURED FOR 28 DAYS AT 70°F, 90 to 100 PERCENT RELATIVE HUMIDITY

Type of Mix	Dry U.C. Strength, (psi)	Modulus of Rupture, (psi)
Shale + 3% lime	85.0	19.6
+ 6% lime	107.6	27.0
+ 9% lime	204.0	36.5
Shale + 15% fly ash	160.0	26.7
+ 20% fly ash	177.8	41.1
+ 25% fly ash	193.8	47.7
Shale + 10% cement	313.0	73.2
+ 14% cement	515.0	93.7
+ 18% cement	580.0	101.4
Shale + 18% fly ash + 8% cement + 4% lime	476.6	142.7

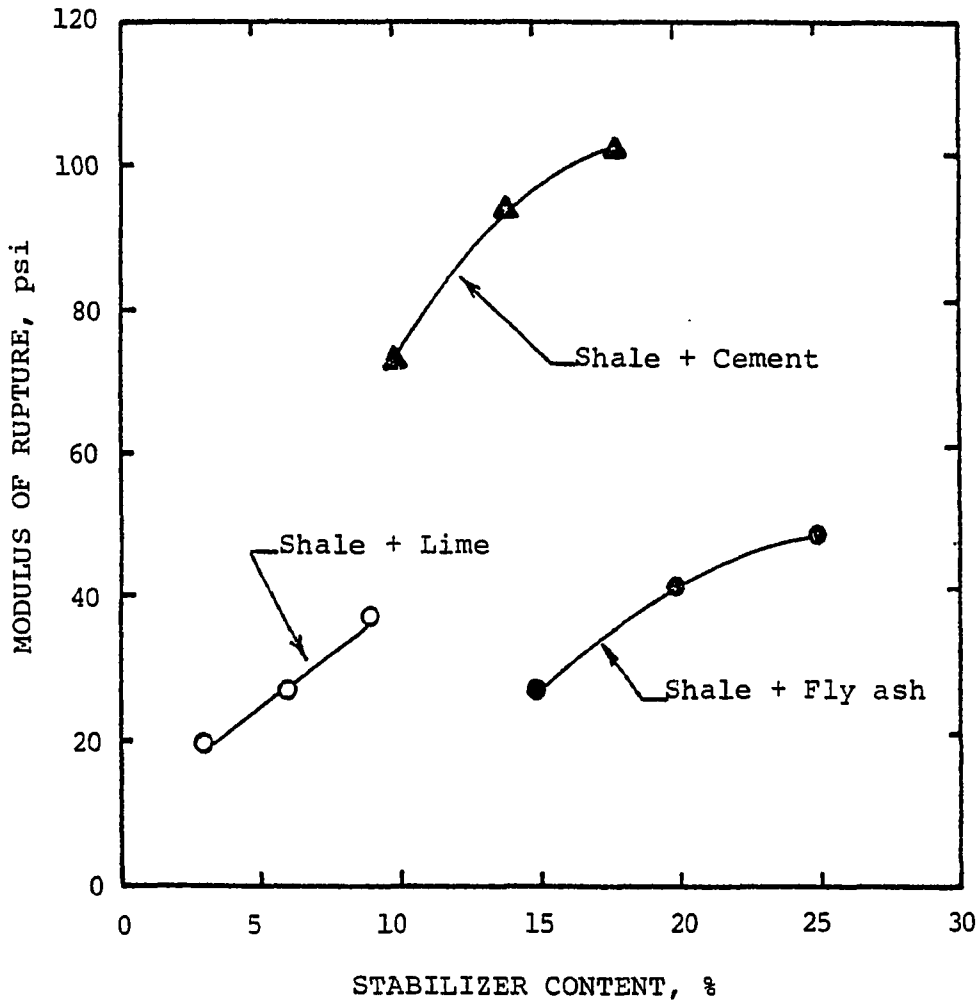

Figure 5.8: Effect of stabilization on modulus of rupture of shale

regression (R=0.98) between the modulus of rupture and the unconfined compressive strength values of the stabilized shale resulted in Equation 5.6.

$$MR = 8.37 + 0.168\sigma_c \tag{5.6}$$

where

MR = modulus of rupture, psi

σ_c = unconfined compressive strength, psi

Modulus of Elasticity. The flexural modulus of elasticity values of the stabilized shale beams were calculated from the following relationship:

$$EI = \frac{5PL^3}{324Y} \tag{5.7}$$

where

E = modulus of elasticity, psi

I = moment of inertia, in^4

P = load, pounds

L = span length, inches

Y = deflection, inches

These values ranged from 3×10^3 to 6×10^3 psi. The modulus of elasticity values in compression were also calculated within the initial elastic region of the stress-strain curves. These values varied from 1.4×10^4 to 5.5×10^4 psi. Both the flexural and compressive modulus of elasticity values are reported in Table 5.13.

TABLE 5.13: MODULUS OF ELASTICITY VALUES OF STABILIZED SHALE CURED FOR 28 DAYS AT 70°F, 90 TO 100 PERCENT RELATIVE HUMIDITY

Type of Mix	Flexural Modulus of Elasticity, (psi)	Compressional Modulus of Elasticity, (psi)
Shale + 3% lime	2782	13636
+ 6% lime	4178	17708
+ 9% lime	4616	21495
Shale + 15% fly ash	3551	18182
+ 20% fly ash	4197	25974
+ 25% fly ash	3877	22989
Shale + 10% cement	4632	36765
+ 14% cement	5504	54545
+ 18% cement	5073	42857
Shale + 18% fly ash + 8% cement + 4% lime	5839	48889

Equation 5.8 was derived to express the flexural modulus of elasticity in terms of the compressive modulus of elasticity.

$$E_f = 2697.8 + 0.057\ E_c \qquad (5.8)$$

where

E_f = flexural modulus of elasticity, psi

E_c = compressive modulus of elasticity, psi

Application of Beam Strength Results:

The principal objective in the design of pavements is to reduce subgrade stress and pavement deflections by either incorporating more rigid upper layers and/or by increasing the thicknesses of existing layers. These features tend to minimize pavement distress associated with subgrade shear and densification due to applied loads. However, an important fact that must be realized is that even though the stiffer layers reduce the risk associated with a subgrade mode of distress, the presence of a stiff layer brings about an increase in the tensile stress magnitude at the bottom of the layer as well as an increase in the horizontal shearing stress (Yoder, 1975). Hence, a design analysis is required to ensure that both the flexural and the shearing resistance of the stiff layer are higher than the high stress conditions that exist.

An example of the application of this design analysis employing the modulus of rupture values for the assumed field conditions is presented below:

Problem Statement. A pavement structure with an eight inch stabilized base and a four inch bituminous surface is to carry medium volume traffic, and the design vehicle properties are, contact radius a = 6 inches and contact pressure p = 100 psi. The structural properties of the pavement materials are given below. Investigate the adequacy of the pavement using the stress method.

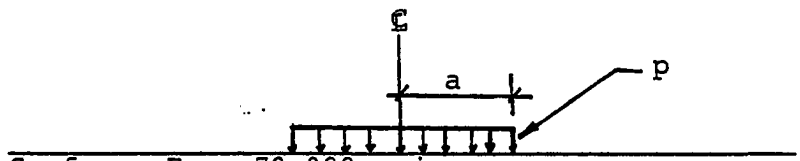

Surface, E_1 = 70,000 psi

h_1 = 4"

Stabilized base, E_2 = 18,000 psi (Table 5.13)

σ_t = 27 psi (Table 5.12)

h_2 = 8"

Subgrade, E_3 = 10,000 psi

h_3 = ∞

Solution. From Yoder's charts (1975), pp. 74-75

(i) $A = \frac{a}{h_2} = \frac{6"}{8"} = 0.75$

$K_2 = \frac{E_2}{E_3} = \frac{18,000}{10,000} \cong 2$

The tensile to vertical stress ratio when $A = 0.75$ and $K_2 = 2$ is 0.2

therefore, tensile stress, $\sigma_t = 0.2P =$ $0.2 \times 100 = 20$ psi

(ii) $K_1 = \frac{E_1}{E_2} = \frac{70,000}{18,000} \cong 4$

depth $= h_1 = 4"$

The horizontal shear stress to vertical stress, when $K_1 = 4$ and $h = 4"$ is 0.17

therefore, horizontal shear stress,

$\tau_{rz} = 0.17 \times 100 = 17$ psi

The flexural strength of the stabilized base (27 psi) is higher than the flexural stress and the horizontal shear stress induced, hence, the pavement is adequate.

Scanning Electron Microscopy:

The results of the electron microscopic studies of the raw and stabilized shale and some typical micrographs are presented in this section. Fly ash powder was also scanned under the electron microscope. In almost all cases the degree of magnification of the scans was 3000X.

It is important to note that the general remarks and observations presented herein are from micrographs of a very small area of samples and should not be extrapolated to form a basis for statistical inferences.

Raw Shale. The micrographs of raw shale present massive, blocky arrangement of groups of particles. As seen in Figure 5.9 and 5.10, the particles appear loosely packed. No single grains can be identified; however, the edges of colonies of particles are distinct as they are separated by open spaces. These open spaces or voids are interconnected by very narrow constrictions while in other cases they are not connected. The projected void areas in each micrograph were measured and were found to constitute about 14 percent of the total projected area.

Fly Ash Powder. Rounded spherical particles were prevalent in the micrographs of shale specimens containing fly ash. In addition, scans of fly ash powder alone (Figure 5.11) were taken and confirmed the existence of spherical particles. The spheres vary in size and, as reported by Diamond (1981), they may be full, partially full or empty. These states are bound to affect the density and strength of mixes containing fly ash.

Shale-Lime Mixes. The micrographs of lime stabilized shale show regular and irregular aggregations of particles (Figures 5.12 and 5.13). Silt size granular matrices are also visible. The open spaces or voids of shale-

3000X (a)

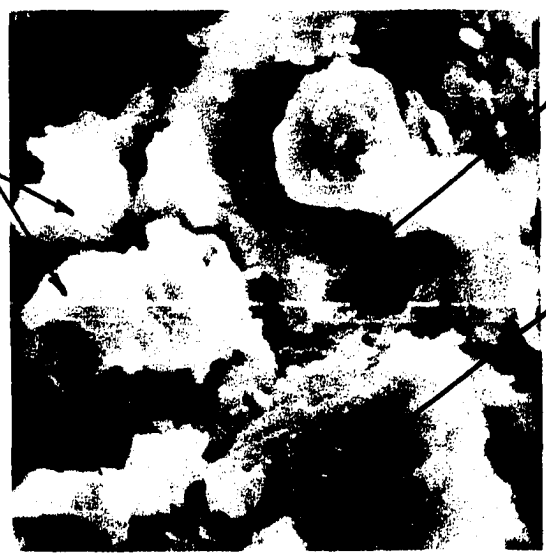

3000X (b)

Figure 5.9: Micrographs of raw shale
(a) general (b) details identified

3000X (a)

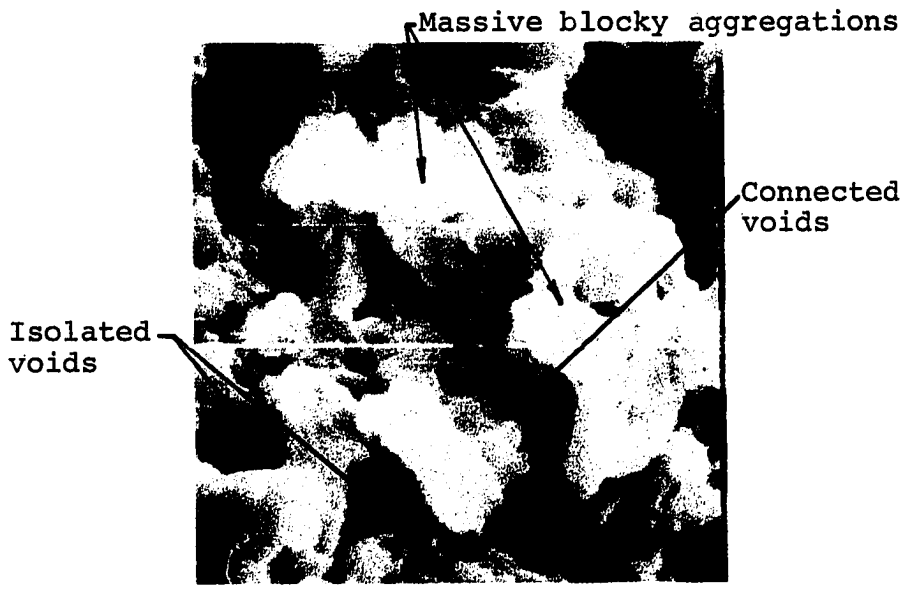

3000X (b)

Figure 5.10: Micrographs of raw shale
(a) general (b) details identified

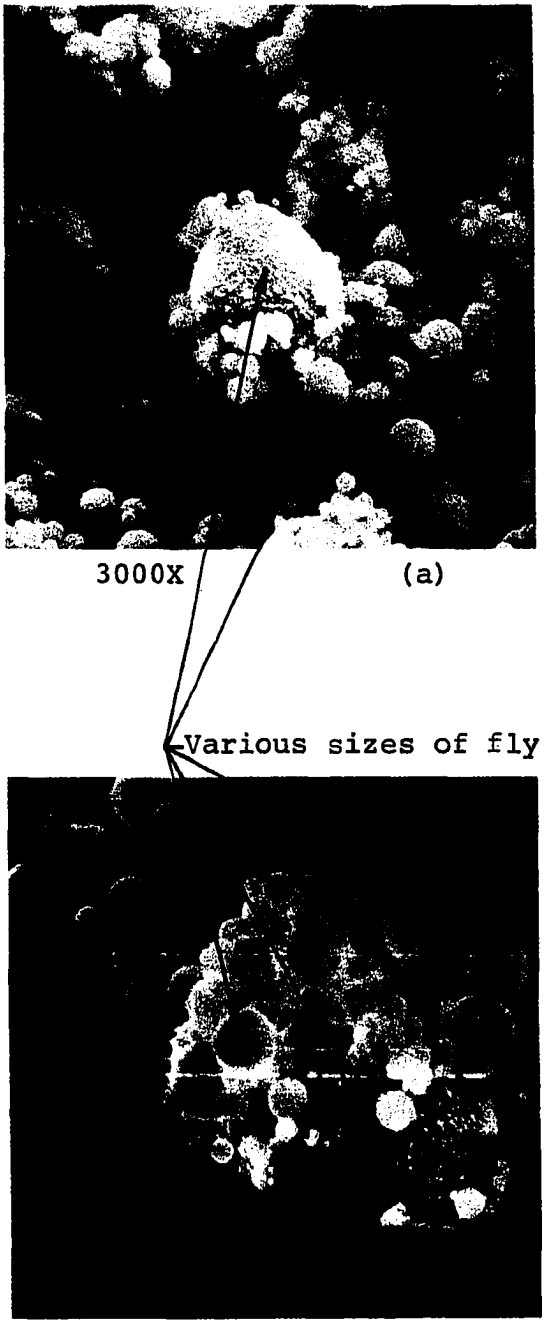

Figure 5.11: Micrographs of fly ash powder (a) and (b) details identified

3000X (a)

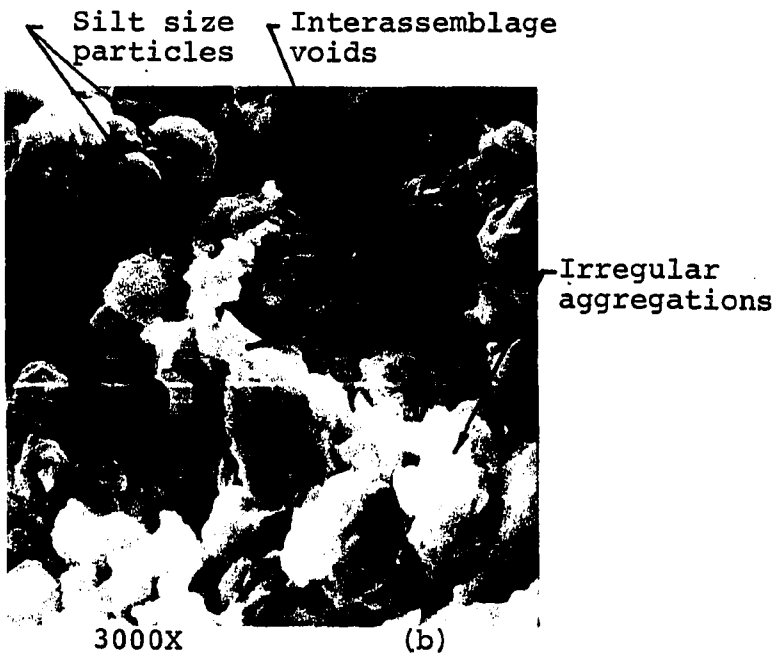

3000X (b)

Figure 5.12: Micrographs of lime stabilized shale (6%, 70°F, 90 days) (a) general (b) details identified

3000X (a)

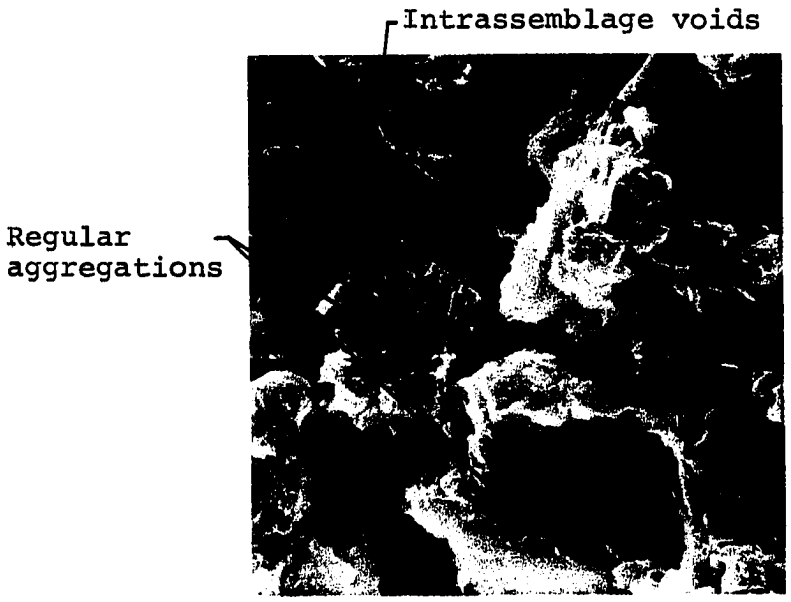

3000X (b)

Figure 5.13: Micrographs of lime stabilized shale (6%, 70°F, 90 days) (a) general (b) details identified

-lime micrographs are much smaller than the voids in the raw shale micrographs. The voids are located within an assemblage or colony of particles or between groups of colonies or assemblages of particles. The influences of curing temperature and time upon the lime-stabilizer micrographs do not show any single consistent pattern in so far as void reduction is concerned. As depicted in Table 5.14, the area of voids of the lime stabilized shale, as measured from the projected areas of micrographs, range from 2 to 5 percent.

Shale-Fly Ash Mixes. The micrographs of fly ash stabilized shale seem to contain substantial information. As depicted in Figures 5.14, 5.15, and 5.16, spherical fly ash particles are abundant in all micrographs. The coarse fly ash particles are either covered and/or interconnected by irregular aggregations of fine fly ash and soil particles. Broken fly ash particles are also observed, some are split into halves and look like a crater. These are the empty or partially filled particles referred to as cenospheres. However, others have the top shell peeled off and are solid inside, these are referred to as plerospheres.

All specimens cured at 90°F and at 70°F for 180 days show spiny tube like crystals on top of the aggregations of particles. These hydration products are the tobermorite (C_3SH) crystals. In general, the voids measured

TABLE 5.14: VOID AREAS FROM MICROGRAPHS OF RAW AND STABILIZED SHALE

Type of Mix	Area of Voids as Percent of Total Area					
	70°F			90°F		
	28	90	180	28	90	180
Raw Shale	14					
Shale + lime	2.2	3.7	2	2.3	5.0	4.5
Shale + fly ash	2.1	1.8	0.6	2.0	1.7	1.8
Shale + cement	1.4	1.5	-	1.9	1.3	-
Shale + conjunctive	1.1	0.7	1.1	1.5	-	1.1

3000X (a)

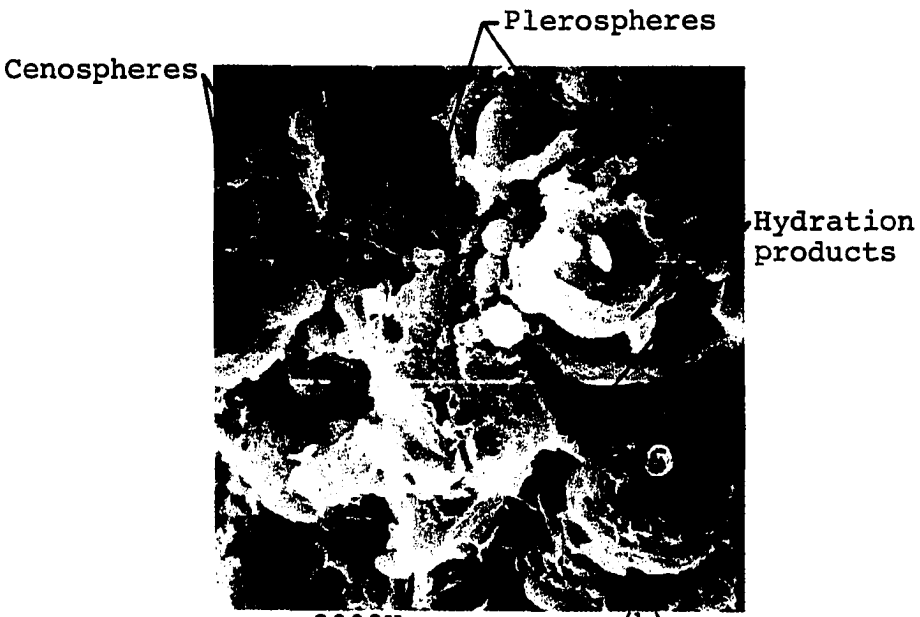

3000X (b)

Figure 5.14: Micrograph of fly ash stabilized shale (25%, 70°F, 180 days) (a) general (b) details identified

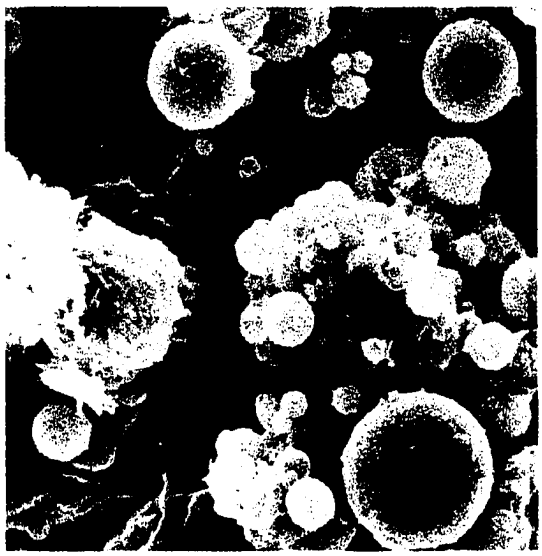

3000X (a)

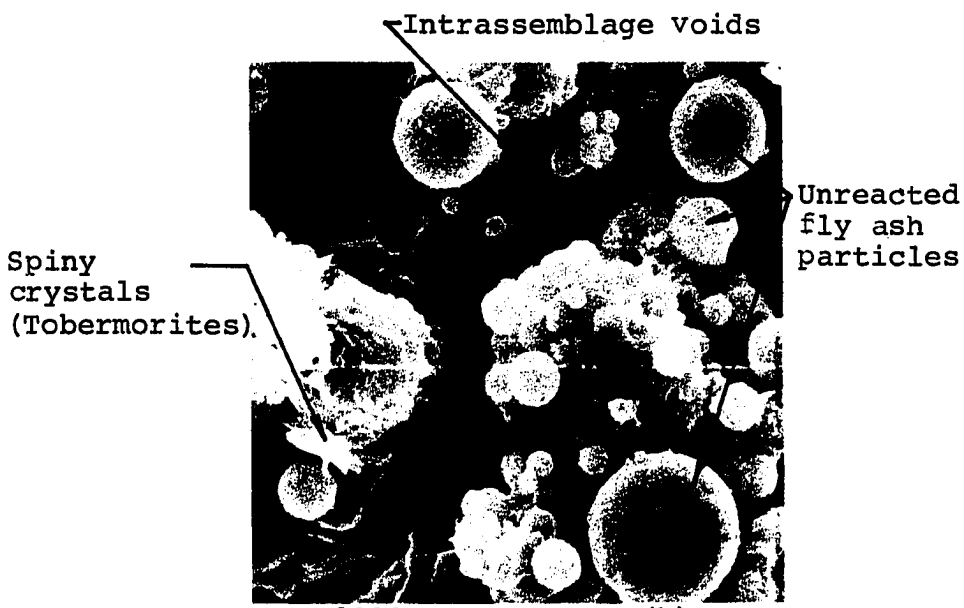

3000X (b)

Figure 5.15: Micrographs of fly ash stabilized shale (25%, 70°F, 180 days) (a) general (b) details identified

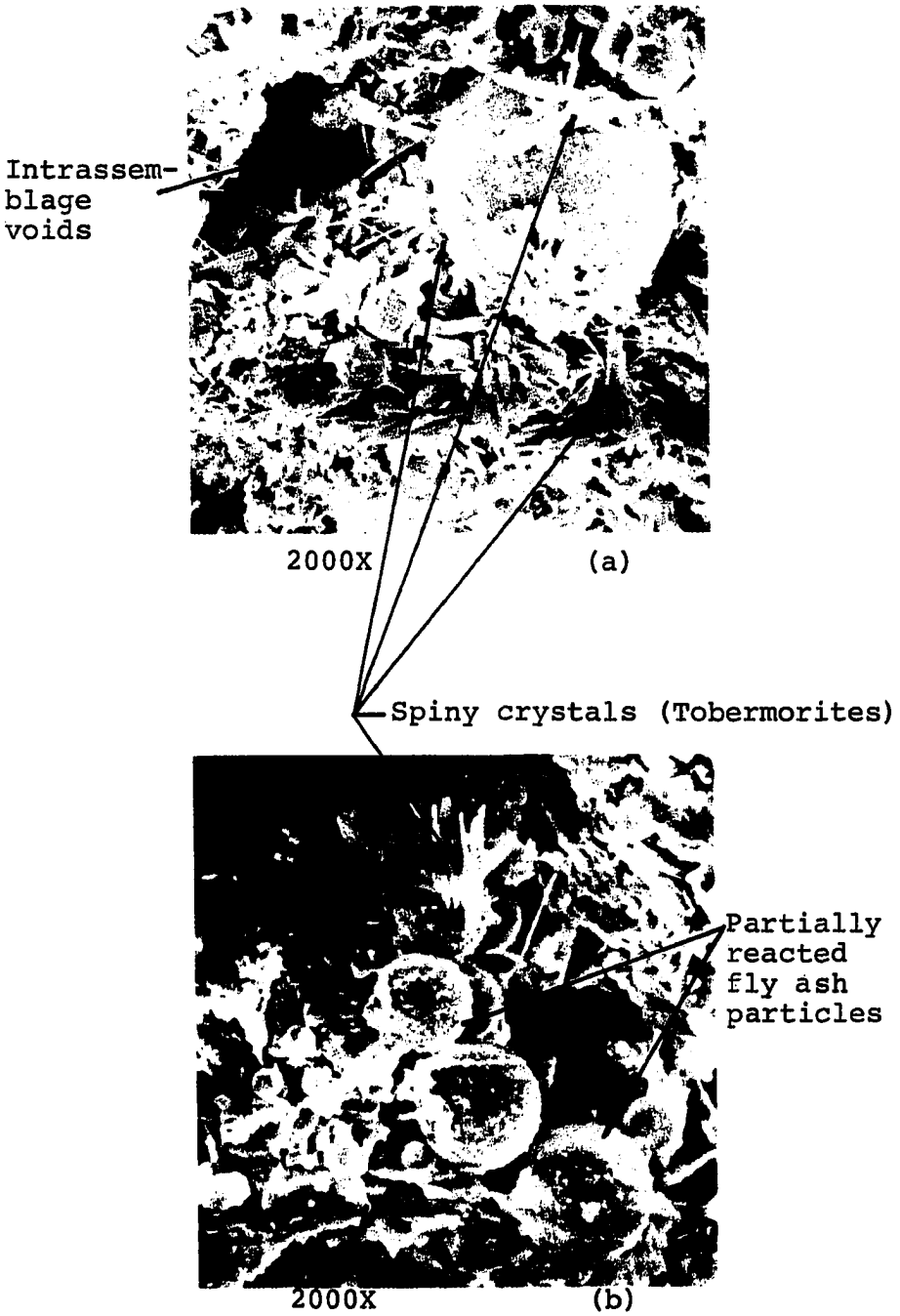

Figure 5.16: Micrographs of fly ash stabilized shale (25%, 90°F, 28 days) (a) and (b) details identified

from the projected micrograph areas (Table 5.14) were reduced as a result of fly ash stabilization. However, the micrographs do not present a void reduction that can be traced to variations in curing temperature and time. The void arrangements were similar to those of lime stabilized specimens and they were of the interassemblage type.

Shale-Cement Mixes. The micrographs of cement stabilized shale show regular aggregations of silt size particles. A gray cementitions reaction product (alumina and silica gel) covers the aggregations. No spiny crystals are visible in the shale-cement mixes. As evidenced by Figure 5.17, shale-cement micrographs show a predominance of densely packed aggregations of particles. The void areas of cement stabilized shale, reported in Table 5.14, range from 1.3 to 1.9 percent and are smaller than the voids of lime and fly ash stabilized shale.

Shale-Conjunctive Mixes. Micrographs of conjunctively stabilized shale show combinations of cement and fly ash stabilized shale features. The particles show high degree of aggregation and fly ash particles by in large are covered by hydration products. As can be observed in Figure 5.18 the open areas or voids are very small. The spiny crystals (tobermorite) that were detected in the micrographs of fly ash stabilized specimens are also observed in this instance, and also broken and solid fly

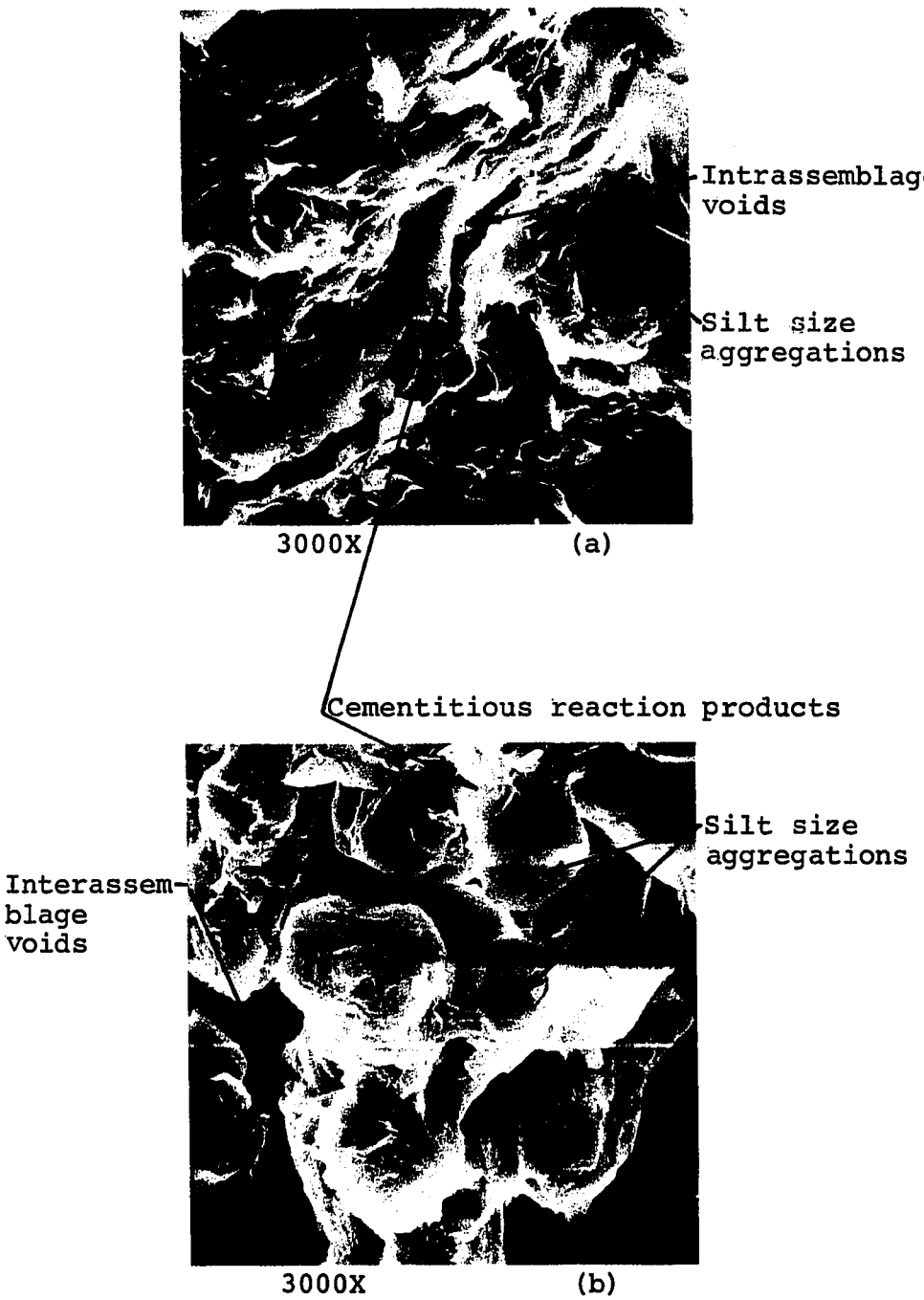

Figure 5.17: Micrographs of cement stabilized shale
(a) 14%, 70°F, 90 days
(b) 14%, 90°F, 90 days

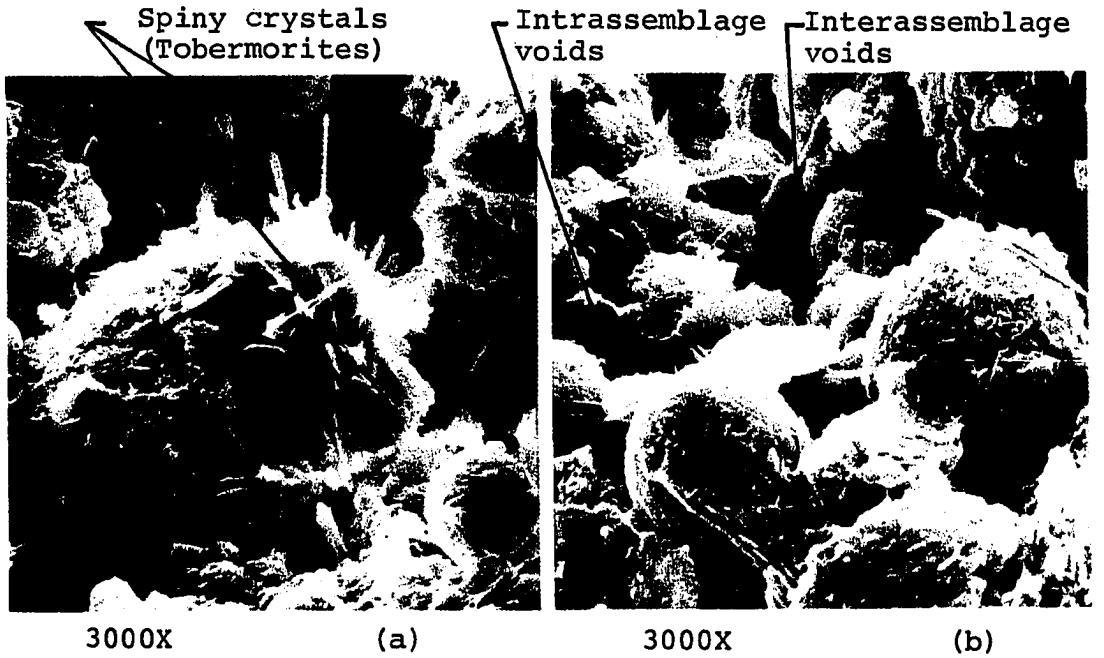

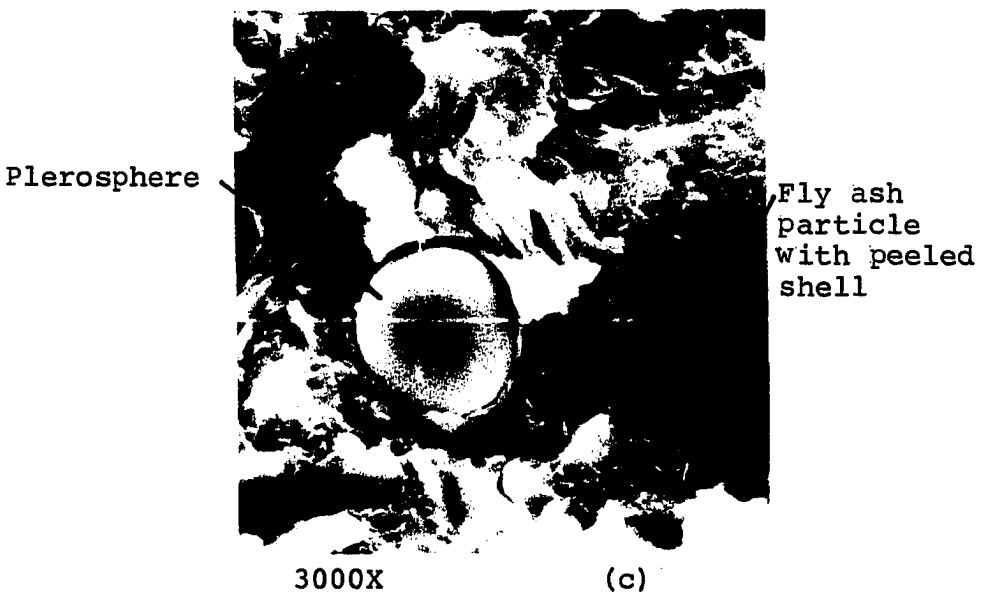

Figure 5.18: Micrographs of conjunctively stablized shale (a) 70°F, 28 days; (b) 70°F, 90 days; (c) 90°F, 180 days

ash particles are prevalent.

The electron micrographs of the raw and stabilized shale, in addition to the texture, microfabric, and possibly reaction products, manifested the size of the voids of projected areas. As discussed in the previous sections, all forms of stabilizers reduced the void area of the raw shale from 14 to less than 5 percent. Inasmuch as a densely packed particulate mix manifests higher resistance to shear deformations than its loosely packed counterpart, it may be safely advanced that the stabilized forms of shale can sustain greater loads than the raw shale. However, a dependable mathematical relationship between compressive strength and voids has not been established thus far. Figure 5.19 is a scatter plot of void areas and strengths of raw and stabilized shale. The narrow band of scatter point shows that as the void area decreases strength increases.

X-Ray Diffraction:

The mineralogical composition of the raw shale was analyzed using the sedimented slides in the Siemens diffractometer unit and the powder slides in the Phillips Automated Powder Diffractometer. The results of both diffractions are discussed in this section. The raw shale diffractions are used as a reference to investigate, the response of the clay minerals to the chemical stabilizers and the formation of new crystals.

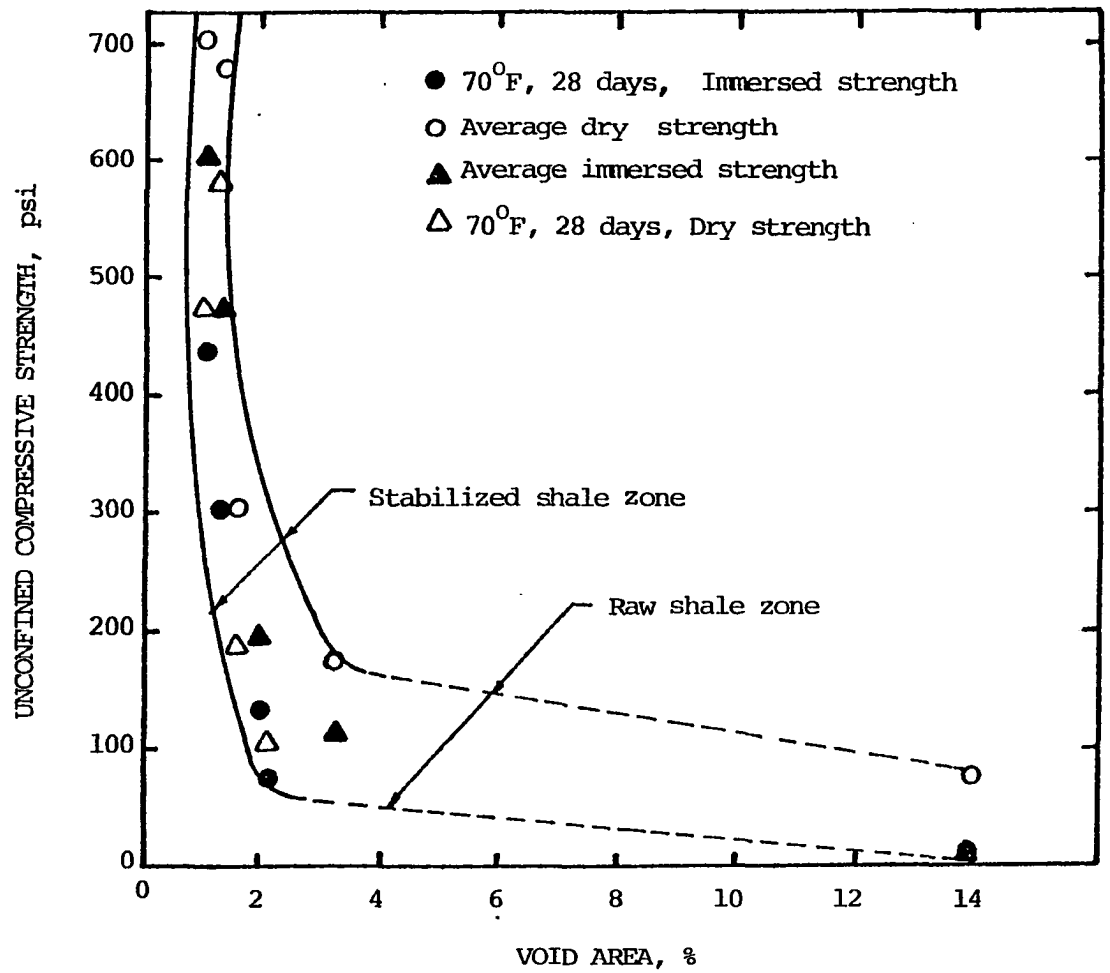

Figure 5.19: Unconfined compressive strength response to void area.

For the X-ray analysis of shale-stabilizer interaction, the following samples were diffracted: (i) shale-lime specimens cured at 70°F and 90°F for 28 and 90 days, (ii) shale-fly ash specimens cured at 70°F and 90°F for 28 and 90 days, (iii) shale-cement specimens cured at 70°F and 90°F for 28 and 90 days, and (iv) shale-conjunctive specimens cured at 70°F and 90°F for 28 and 90 days. The X-ray diffractograms are included in Figures F.1 to F.16, Appendix F. The d-spacings (Å) of the crystals, the peak heights normalized to the highest peak of quartz, energy counts and base width of crystal peaks are listed in Tables F.1 through F.16, Appendix F.

Raw Shale. As depicted in Figure F.1 of Appendix F, the major clay mineral in the shale is the mixed layer type, with traces of illite and kaolinite. By measuring the peak areas (Laguros, 1962), the relative clay mineral proportions are: mixed layer, 84 percent; illite 12 percent and kaolinite 4 percent.

Clay Mineral Responses. Close examination of the X-ray diffractograms of the stabilized shale may help establish some trends of clay mineral responses to the chemical stabilizers. As reported in Table 5.15, the kaolinite peak is absent in almost all the stabilized shale diffractograms, possibly due to the masking effect of shale-stabilizer reaction products. The mixed layer and the illite peaks though, are present in all stabilized shale

TABLE 5.15: CLAY MINERAL PEAKS OF RAW AND STABILIZED SHALE, CURED AT 70°F, 28 DAYS, 90 TO 100 PERCENT RELATIVE HUMIDITY

Clay Mineral Peak	Raw Shale	Shale + Lime	Shale + Fly Ash	Shale + Cement	Shale + Conjunctive
Mixed Layer	X	X	X	X	X
Kaolinite	X	-	X	-	-
Illite	X	X	X	X	X

X = presence of mineral peak

\- = absence of mineral peak

diffractograms, but their crystal peaks are substantially reduced. Hence, the following discussion pertains to the responses of these two minerals, i.e, the mixed layer and illite.

Mixed Layer. For each shale-stabilizer mix, the crystal base width and the peak height were read from the Automated Phillips peak algorithm. The area under the mixed layer crystal peak is calculated from a triangle of the base width and height equal to one half of the peak energy count (as the counts were done in the ascending and descending directions). As is shown in Table 5.16, the peak heights and, consequently the area under the peak (AUP), of the stabilized shale decreased. The average peak area reduction due to lime stabilization is 12 percent, and fly ash and cement stabilizations reduced it by 17 and 20 percent, respectively. The maximum peak area reduction (52 percent) is achieved when the shale was stabilized conjunctively. The relevance of the peak area reductions to strength attained can be observed in Figure 5.20. The more the shale-stabilizer interaction advance, i.e., the higher the strength levels attained. However, the strength reaches a maximum value when the crystals lose about 20 percent of their crystallinity as measured by peak area.

Illite. The areas under the illite crystals are calculated in the same manner as those of the mixed layer.

TABLE 5.16: MIXED LAYER CRYSTAL RESPONSE TO STABILIZATION

Type of Mix	Peak Base Width	Peak Height	Area Under Peak
Raw Shale	0.32	42	6.6
Shale + 6% lime			
70°F, 90 days	0.31	37	5.7
90°F, 28 days	0.32	39	6.3
90°F, 90 days	0.31	36	5.5
Shale + 25% fly ash			
70°F, 28 days	0.31	35	5.3
70°F, 90 days	0.42	31	6.4
90°F, 28 days	0.25	35	4.4
90°F, 90 days	0.39	31	5.9
Shale + 14% cement			
70°F, 28 days	0.36	34	6.0
70°F, 90 days	0.31	34	5.3
90°F, 28 days	0.27	29	3.9
90°F, 90 days	0.37	33	6.1
Shale + Conjunctives			
70°F, 28 days	0.42	17	3.6
70°F, 90 days	0.19	15	1.4
90°F, 28 days	0.42	16	3.3
90°F, 90 days	0.43	21	4.4

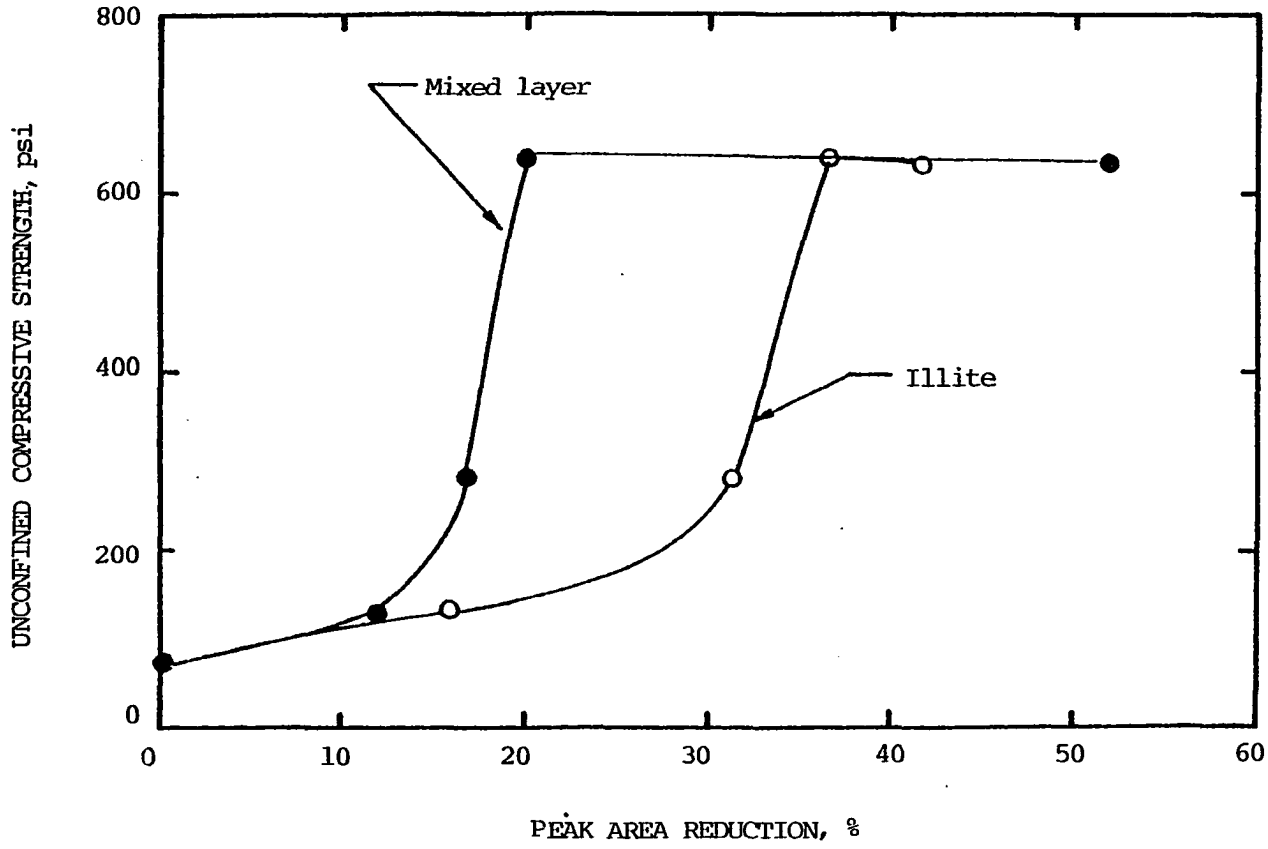

Figure 5.20: Strength response to peak area reduction.

layer. Table 5.17 presents the data and the results are close to those of the mixed layer. Cement stabilization is most effective in reducing the peak areas of illite followed by conjunctive, fly ash and lime in that order. As shown in Figure 5.20, the maximum strength occurs at 35 percent peak area reduction.

Reaction Products:

Diffractograms of the stabilized shale were examined for possible new crystals. The diffractograms from the Siemens and the Automated Phillips diffractometer unit did not provide identifiable new crystals peaks. Therefore, the search for new crystals was supplemented by the Automated Phillips diffractogram algorithm data. The data on the identified crystals is reported in Tables F.1 through F.16, Appendix F. The reaction products of the stabilized shale are reported in Tables 5.18 through 5.20.

Shale-Lime Reaction Products. Lime stabilization resulted in the formation of new crystals at various basal spacings. Calcium aluminum silicate ($Ca_2Al_2SiO_2$) peak was present at 3.86Å d-spacing. Two forms of calcium aluminum silicate hydrate (CASH) are formed at d-spacings of 3.12Å ($CaAlSiO_2H_2O$) and 2.99Å, 2.93Å, 2.84Å ($CaAl_2Si_7O_{18}6H_2O$).

In some cases, crystalline peaks that were formed after 28-days curing were absent in the 90-day diffracto-

TABLE 5.17: ILLITE LAYER CRYSTAL RESPONSE TO STABILIZATION

Type of Mix	Peak Base Width	Peak Height	Area Under Peak
Raw Shale	0.31	12	1.9
Shale + 6% lime			
70°F, 90 days	0.36	9	1.6
90°F, 28 days	0.4	6	1.2
90°F, 90 days	0.39	7	1.4
Shale + 25% fly ash			
70°F, 28 days	0.30	9	1.4
70°F, 90 days	0.38	5	1.0
90°F, 28 days	0.34	9	1.5
90°F, 90 days	-	-	
Shale + 14% cement			
70%F, 28 days	0.31	6	0.9
70°F, 90 days	0.34	7	1.2
90°F, 28 days	0.42	5	1.1
90°F, 90 days	0.31	7	1.1
Shale + Conjunctives			
70°F, 28 days	0.31	7	1.1
70°F, 90 days	0.33	9	1.6
90°F, 28 days	0.30	7	1.0
90°F, 90 days	0.37	6	1.1

grams. It is unlikely that the crystals would be destroyed due to further curing. Possibly the masking of the crystals may be more with more reaction products forming or that the degree of reproducibility of X-ray diffractions may not be high.

Shale-Fly Ash Reaction Products. Fly ash stabilization resulted in more new crystal formations than lime did. Table 5.18 presents the new crystals indentified and the extent of crystallization as measured by the area under each crystal peak. Tetracalcium aluminum silicate hydrate (C_4ASH) was identified at 5.62Å d-spacing, calcium aluminum silicate (CAS) at 3.86Å, calcium silicate hydrate (CSH) at 2.77Å and tricalcium silicate (C_3S) at 2.69Å.

No consistent pattern seems to be present for the AUP with respect to curing time and temperatures. However, on the basis of the sizes of AUP, the degree of crystallization was in the following order: tricalcium silicate was highest followed by calcium silicate hydrate, calcium aluminum silicate, tetracalcium aluminum silicate hydrate.

Shale-Cement Reaction Products. The new crystals formed in the cement stabilized shale were mostly hydrated forms of calcium aluminum and calcium silicate. Calcium aluminum silicate (3.86Å), calcium silicate hydrate (2.77Å) and calcium aluminum silicate hydrate (2.60Å) were pre-

TABLE 5.18: SIZES OF NEWLY FORMED CRYSTAL PEAKS OF SHALE-FLY ASH MIXES

Curing Condition	AUP			
	C_4ASH, (5.62A°)	CAS, (3.86Å)	CSH, (2.77Å)	C_3S (2.69Å)
70°F, 28 days	1.32	1.73	1.85	3.42
90°F, 28 days	-	2.23	0.73	3.19
70°F, 90 days	0.75	2.67	-	3.78
90°F, 90 days	1.75	1.63	3.78	3.05

sent in all shale-cement diffractions. In addition, tetracalcium aluminum hydrate (4.21Å) and tetracalcium aluminum silicate hydrate (5.58Å) were present in the 70°F-28 day and 90°F-90 day cured specimens, respectively. As reported in Table 5.19, the extent of crystallization of the newly formed crystals, manifested by the AUP is significant. However, as with the shale-fly ash reaction products, it seems difficult to relate crystallinity to curing time.

Shale-Conjunctive Reaction Products. The diffractions of the conjunctively stabilized shale contained all the newly formed crystals identified in the shale-fly ash and shale-cement diffractions. Crystals common to all curing conditions were tetracalcium aluminum silicate hydrate (5.59Å), calcium aluminum silicate (3.86Å), calcium silicate hydrate (2.77Å), tricalcium silicate (2.69Å) and calcium silicate (2.56Å). As evidenced by the peak areas in Table 5.20, the degree of crystallinity of the hydrated and unhydrated forms of calcium silicate were higher than the calcium aluminum silicate groups. The latter are believed to form slowly as the shale-stabilizer reactions advance.

TABLE 5.19: SIZES OF NEWLY FORMED CRYSTAL PEAKS OF SHALE-CEMENT MIXES

Curing Condition,	AUP		
	CAS, (3.86Å)	CSH, (2.77Å)	CASH, (2.60Å)
70°F, 28 days	1.89	5.58	5.61
90°F, 28 days	2.04	2.25	4.44
70°F, 90 days	2.30	3.60	3.63
90°F, 90 days	1.23	3.97	1.89

TABLE 5.20: SIZES OF NEWLY FORMED CRYSTAL PEAKS OF SHALE-CONJUNCTIVE MIXES

Curing Condition,	AUP				
	C_4ASH, (5.59Å)	CAS, (3.86Å)	CSH, (2.77Å)	C_3S, (2.69Å)	CS, (2.56Å)
70°F, 28 days	0.60	1.65	5.47	2.18	6.25
90°F, 28 days	-	2.08	2.90	2.36	4.75
70°F, 90 days	0.94	1.84	2.59	1.32	4.81
90°F, 90 days	0.64	1.48	2.54	2.88	5.2

CHAPTER VI

CONCLUSIONS AND RECOMMENDATIONS

This study addressed the response of the Wellington shale of Kay County (north of Ponca City) to lime, cement and fly ash stabilization. On the basis of the data of the various engineering and physical test evaluations, the following conclusions are drawn:

1. The addition of 6 percent lime, 14 percent cement, 25 percent fly ash to the shale and the conjunctive use of 8 percent cement plus 4 percent lime and 18 percent fly ash with the shale result in adequate strength attainment and favorable plasticity characteristics.
2. The use of lime (6%), cement (14%), fly ash (25%), and conjunctives (8% cement + 4% lime + 18% fly ash) reduced the less than 2-micron fraction of the shale to below 6 percent.
3. In terms of the degree of aggregations of the clay-size fraction, cement (14%) and conjunctive (8% cement + 4% lime + 18% fly ash) stabilizations are equivalent and lime (6%) and fly ash (25%) stabilizations are comparable.

The former gave an AI of 1.83 and 1.85, respectively, and the latter an AI of 1.78 and 1.74, respectively.

4. Cement and conjunctives rendered the shale nonplastic while lime and fly ash stabilizations lowered the plasticity index to 10 and 12 percent, respectively.
5. Lime stabilization lowered the maximum dry density and increased the optimum moisture content of the shale while cement and fly ash stabilizations increased the maximum dry density and produced little change in the optimum moisture content.
6. All forms of stabilization resulted in a substantial increase in unconfined compressive strength. Strengths were higher when specimens were cured at higher temperatures and for longer curing periods. The rate of strength gain was higher when cured at higher temperatures.
7. Conjunctive stabilization attained the highest unconfined compressive strength values followed by cement, fly ash, and lime, in that order.
8. The permanence of strength as measured by unconfined compressive test after immersion in water for 24 hours was highest in conjunctively

stabilized specimens and least in lime stabilized specimens. Cement and fly ash stabilizations were intermediate.

9. Subjecting stabilized specimens to cyclic "wetting" and "drying" increased their unconfined compressive strengths.
10. All stabilizers raised the cohesion of the shale and its angle of internal friction.
11. The flexural strengths of stabilized beams were in direct proportion to the amount of stabilizers used. Conjunctive stabilization (8% cement + 4% lime + 18% fly ash) resulted in the highest flexural strengths followed by cement (14%), fly ash (25%), and lime (6%).
12. The ratio of flexural strength to unconfined compressive strength for lime (6%) stabilization ranged from 0.18 to 0.25, for fly ash (25%) from 0.17 to 0.25, and for cement (14%) from 0.17 to 0.23.
13. For all stabilized beams the modulus of rupture (flexural strength) can be estimated from the unconfined compressive strengths by the expression:

$$MR = 8.37 + 0.168\sigma_c$$

14. The flexural modulus of elasticity of stabilized beams can be determined from the

modulus of elasticity in compression by the equation:

$$E_f = 2697.8 + 0.057E_c$$

15. Micrographs of stabilized shales reveal a dense packing of particles thereby reducing the open spaces or voids as measured from projected surfaces and the unconfined compressive strength values increase as a result of void area reduction.

16. Cement (14%) and conjunctive (8% cement + 4% lime + 18% fly ash) stabilizations show higher dense packing than fly ash (25%) and lime (6%) stabilizations.

17. Diffractograms reveal that all stabilizers reduced the peaks of the mixed layer and the illite crystals. Lime (6%) reduced the mixed layer by 12 percent and the illite peak by 16 percent. Fly ash (25%), cement (14%), and conjunctive (8% cement + 4% lime + 18% fly ash) stabilizations reduced the mixed layer peak and the illite peak by 17 and 31 percent; 20 and 35 percent; and 51 and 41 percent, respectively.

18. New crystal peaks were identifiable from diffractograms of stabilized shale. Thus, lime (6%) stabilization produced calcium aluminum silicate hydrate; fly ash (25%) stabilization

produced tetracalcium aluminum silicate hydrate, calcium aluminum silicate and tricalcium silicate; and cement (14%) stabilization produced hydrated forms of calcium aluminum and calcium silicate.

Based on the conclusions formulated above, the following recommendations appear to be in order:

1. The modulus of rupture and modulus of elasticity values in bending are more realistic criteria in analyzing the stability of pavements. However, beam tests use excessive material and are time consuming to run. Therefore, the relationships established between flexural and unconfined compressive strength can be utilized but more extensive tests covering a wide range of stabilized soils will help in introducing greater refinement in the established relationships.
2. SEM is a very useful and significant tool in making qualitative observations regarding the particle arrangements, pore space or void area characteristics, and identification of some reaction products. The limitation has been that the micrographed area is so small that it may or may not constitute a fair representation of the specimen. This may be overcome by

micrographing the whole cross sectional area of a specimen piece by piece and investigating the possibility of feeding the micrographs into a scanner that scales and sums up the dark areas (voids) and the gray areas (soil mass). Such results could then be used to make some quantitative estimates with some statistical significance.

In addition, some of the recommendations made at the conclusion of earlier studies (Jha, 1977) are still pertinent and valid and therefore, they are presented herein:

3. Field implementation is expected to yield observations that, in all likelihood, will deviate from laboratory behavior. The deviations will accrue, for example, when No. 4 material is used instead of No. 10 or when delayed compaction in the field assumes dimensions different than those in the laboratory. The assessment of these deviations is essential for purposes of formulating design procedures and specifications.
4. Laboratory studies are performed under well controlled conditions. Differences in stabilization effectiveness may also result, primarily in terms of strength and durability,

from less strict requirements employed in the field. Accordingly, a program of assessing the degree of field quality control and assurance should be initiated so that such statistical parameters as variability tolerances could be evaluated and service related to the performance of stabilized shale pavements.

5. Associated with field implementation there should be improvised a program leading to the development of a pavement design. Accordingly, the design should have the elements of a time continuous method wherein changing properties of the stabilized material below the highway pavement could be taken into account. Starting from the time of opening the highway to traffic, samples from the highway construction projects should be obtained at periodic intervals to study the effects of weathering and traffic stresses on the durability and other predictive characteristics of the stabilized shale materials. The data obtained from the present study could then be correlated with and/or modified according to the field data.

REFERENCES

Adams, J. I. (1958), "Fly Ash - Lime Stabilization for Road-Base Construction", Ontario Hydro Research News.

Ahlberg, H. L. and Barenberg, E. J. (1965), "Pozzolanic Pavements", Engineering Experiment Station Bulletin, No. 473, University of Illinois.

Ahlberg, H. L. and McVinnie, W. W. (1962), "Fatigue Behavior of a Lime-Fly Ash-Aggregate Mixture", Highway Research Board Bulletin, No. 335, pp. 1-10.

Ajaz, A. and Pary, R.H.G. (1975), "Stress - Strain Behavior of Two Compacted Clays in Tension and Compression", Geotechnique, Vol. 25, No. 3, pp. 495-512.

Anday, M.C. (1963), "Accelerated Curing for Lime Stabilized Soils", Highway Research Board Bulletin, No. 29, pp. 13-26.

Andres, R. J., Jibala, R., and Barenberg, E. J. (1976), "Some Factors Affecting the Durability of Lime - Fly Ash-Aggregate Mixtures", Transportation Research Record, No. 560, pp. 1-10.

Asuri, S. Altschaeffi, A.G. and Diamond, S.(1971), "Pore Size Distribution Study", Journal of the Soil Mechanics and Foundation Division, American Society of Civil Engineers, Vol. 97, No. SM-5, pp. 771-787.

Bacon, L. D. (1976), "Fly Ash for Construction of Highway Embankments", Proceedings: Fourth International Ash Utilization Symposium, St. Louis.

Barden, L. and Sides, G. (1971), "Sample Disturbance in the Investigation of Clay Structure", Geotechnique Institution of Civil Engineers, London, Vol. 21, No. 3, pp. 211-222.

Barenberg, E.J. (1965), "Behavior of Pozzolanic Pavements Under Load", Highway Research Record, No. 112, pp. 1-24.

Barenberg, E.J. (1967, "Evaluating Stabilized Materials", Report to National Cooperative Highway Research Program, Highway Research Board, Enginering Experiment Station, University of Illinois.

Barenberg, E. J. (1970), "Evaluation of Remolded Field Samples of Lime-Cement-Fly Ash-Aggregate Mixtures", Highway Research Record, No. 315, pp. 112-121.

Barenberg, E. J., "Lime-Fly Ash-Aggregate Mixtures in Pavement Construction", Process and Technica Data, National Ash Association.

Barenberg, E.J. (1973), "Utilization of Ash in Stabilized Base Construction", Third International Ash Utilization Symposium, Pittsburgh, PA.

Biswas, B. (1972), "Study of Accelerated Curing and Other Factors Influencing Soil Stabilization", Ph.D. Thesis, Texas A & M University, College Station, TX.

Blocker, W.V. (1973), et al., "Marketing Power Plant Aggregates as a Road Base Materials", Third International Ash Utilization Symposium, Pitsburgh, PA.

Bracket, C.E. (1973), "Production and Utilization of Ash in the United States", Third International Ash Utilization Symposium, Pittsburgh, PA.

Brennan, P.J., "The Stabilization of a Fine-Grained Soil Using Low Percentages of Portland Cement and Fly Ash", Highway Research Board, Special Report S-2.

Buer, H.M. (1954), "The Stabilization of a Fine-Grained Soil Using Lime and Fly Ash", Delaware Enginering Experiment Station Report, No. S-1.

Capp, J. P. and Gillmore (1973), O.W., "Soil-Making Potential of Power Plant Fly Ash in Mined-Land Reclamation", Third International Ash Utilization Symposium, Pittsburgh, PA.

Chang, A.C. (1977), et al., "Physical Properties of Fly Ash Amended Soils", Journal of Environmental Quality, Vol. 6, No. 3, pp. 267-270.

Chu, T. Y., Davidson, D. T. , Goecker, W. and Moh, F. C., (1955) "Soil Stabilization with Lime-Fly Ash Mixtures: Preliminary Studies with Silt and Clayey Soils", Highway Research Board Bulletin, No. 108, pp. 102-112.

Collins, K. and McGown, A. (1974), "The Form and Function of Microfabric Features in a Variety of Natural Soils", Geotechnique, Institution of Civil Engineering, London, Vol. 24, No. 2, pp. 223-254.

Cominsky, R.J. and Cumberledge, G. (1970), "Characteristics and Performance of Aggregate-Lime-Pozzolan Mixture", Pennsylvania Department of Transportation Research Report, Bureau of Materials, Testing and Research.

Cumberledge, G., Hoffman, G. L. and Bhajandas (1976), "Curing and Tensile Strength Characteristics of Aggregate-Lime-Pozzolan", Highway Research Record, No. 560, pp. 21-29.

David, F.N. (1967), "Reactions and Strength Development in Portland Cement-Clay Mixtures", Highway Research Board Record, No. 198, pp. 39-56.

Davidson, D.T. and Hilt, G.H. (1960), "Lime Fixation in Clayey Soils", Highway Research Board Bulletin, No. 262, pp. 20-30.

Davidson, D.T. and Hilt, G.H. (1961), "Isolation and Investigation of a Lime-Montmorillonite Crystalline Reaction Product", Highway Research Board Bulletin, No. 304, pp. 51-64.

Davidson, D.T.(1959), et al., "Activation of The Lime-Fly Ash Reaction by Trace Chemical", Highway Research Board Bulletin, No. 231, pp. 67-81.

Davidson, D.T. (1958), et al., "Reactivity of Four Types of Fly Ash with Lime", Highway Research Board Bulletin, No. 193, pp. 24-31.

Davidson, D. T. , et al., "Use of Fly Ash with Portland Cement for Stabilization of Soils", Highway Research Board Bulletin, No. 198, pp. 1-12.

Davidson, D.T., Mateos, M., and Barnes, H.F. (1960), "Improvement of Lime Stabilization of Montmorillonitic Clay Soils with Chemical Additives", Highway Research Board Bulletin, No. 262, pp. 33-50.

Dawson, R.F. (1956), "Special Factors in Lime Stabilization", Highway Research Board Bulletin, No. 129.

Dempsey, B. J. and Thompson, M.R.(1968), "Durability Properties of Lime Soil Mixtures", Highway Research Record, No. 235, pp. 61-75.

Depsey, B. J. and Thompson, M. R. (1972), "Effects of Freeze-Thaw Parameters on the Durability of Stabilized Materials", Highway Research Record, No. 379, pp.10-18.

Depuy, G.W. (1965), "Petrographic Investigations of Rock Durability and Comparison of Various Test Procedures", Journal of American Association of Engineering Geology, Vol. 2, pp. 31-46.

Diamond, S. (1981), "The Characterization of Fly Ashes", Materials Research Society, Symposium N, Annual Meeting, pp. 12-23.

Diamond, S. (1970), "Pore Size Distribution in Clays", Clays and Clay Minerals, Journal of the Clay Mineral Society, London, Vol. 18, No. 1, pp. 7-23.

Diamond, S., White, J.L. and Doleh, W.L. (1963), "Transformation of Clay Minerals by Calcium Hydroxide Attack", Clay and Clay Minerals, 12th National Conference, Atlanta, GA.

DiGioia, A. M. and Nuzzo, W. L. (1972), "Fly Ash as a Structural Fill", Journal of Power Division, American Society of Civil Engineers, Vol. 98, pp. 77-92.

Dobie, T. R. (1975), et al., "A Laboratory Evaluation of Lignite Fly Ash as a Stabilization Additive for Soils and Aggregates", Twin City Testing and Engineering Laboratory, Inc., Laboratory No. 0-5373.

Dorathy, C. (1970), "Clay Minerals; A Guide To Their X-ray Identification", The Geological Society of America, Boulder, Colorado.

Drake, J. A. and Haliburton, T. A. (1972), "Accelerated Curing of Salt and Lime Treated Cohesive Soils", Highway Research Record, No. 381, pp. 10-19.

Dvorak, A. J., Lewis, B. G. (1978), et al., "Impacts of Coal Fired Power Plants on Fish, Wildlife, and Their Habitats", Division of Environmental Impact Studies, Argone National Laboratory FWS/OBS-78/29, pp 1-240.

Dyer, M. R. and O'Flaherty, C. A. (1972), "Lime-Fly Ash Stabilization of Soil: Development of the Technology, Parts 1 and 2", Highway Design and Construction, Vol. 40, No. 1754, Oct., No. 1755, Nov.

Eades, J. L. (1958), "Base and Subgrade Stabilization Experiments", Virginia Council of Highway Investigation and Research, Virginia Department of Highways and the University of Virginia, Progress Report, No. 2.

Eades, J. L. and Grim, R. E. (1966), "A Quick Test To Determine Lime Requirements for Lime Stabilization", Highway Research Record, No. 139, pp. 61-72.

Eades, J. L. and Grim, R.E.(1960), "Reaction of Hydrated Lime with Pure Clay Minerals in Soil Stabilization", Highway Research Board Bulletin, No. 262, pp. 51-63.

Eades, J. L., Nichols, F. P. Jr. and Grim, R. E. (1962), "Formation of New Minerals with Lime Stabilization as Proven by Field Experiments in Virginia", Highway Research Board Bulletin, No. 335, pp. 31-39.

Electric Power Research Institute (EPRI), "Coal Ash Disposal Manual", FP-1257, Research Project 1404-1, pp. 1-347.

Entatiev, D. (1973), "Engineering Properties of Compacted Fly Ash-Discussion", Journal of The Soil Mechanics and Foundations Division, American Society of Civil Engineers, Vol. 99.

Faber, J. H. (1979), "United States Overview of Ash Production and Utilization", 5th International Ash Utilization Symposium METC/SP-79/10, pp. 24-28.

Faber, J. H. and DiGioia, A. M. Jr. (1976), "Use of Fly Ash in Embankment Construction", Transportation Research Board, Annual Meeting, January, pp. 1-31.

Fairweather, V. I. (1975), "Fly Ash Pavements, Runways To Take Off", Civil Engineering, American Society of Civil Engineers, pp. 57-58.

Fang, J. H. and Bloss, F. D. (1966), "X-Ray Diffraction Tables", Southern Illinois University Press.

Federal Highway Administration, "Use of Fly Ash in Portland Concrete and Stabilized Base Construction", January, 1974.

Fisher, G. L., Chang, D. P. Y. and Brummer, M. (1976), "Fly Ash Collected from Electrostatic Precipitators", Science, Volume 5, pp. 553-554.

Glenn, R. G. and Handy, R. L. (1963), "Lime-Clay Mineral Reaction Products", Highway Research Board Record, No. 29, pp. 70-82.

Goecker, W. L. (1956), et al., "Stabilization of Fine and Coarse-Grained Soils with Lime Fly Ash Admixtures", Highway Research Board Bulletin, No. 129.

Goldberg, I. and Klein, A. (1952), "Some Effects of Treating Expansive Clays with Calcium Hydroxide", Proceedings of the American Society for Testing Materials, 50th Annual Meeting.

Gray, D. H. and Lin, Y. K. (1972), "Engineering Properties of Compacted Fly Ash", Journal of Soil Mechanics and Foundations Division, American Society of Civil Engineers, Volume 98,No. SM4, pp. 361-380.

Greenwell, H. F. and Pizzella, J. R. (1976), "Lime Fly Ash Soil Stabilization", Proceedings: Fourth International Ash Utilization Symposium, St Louis.

Grim, R. E. (1968), Clay Mineralogy, McGraw-Hill Company Second Edition.

Handy, R. L. (1960), et al., "Chemical Treatments for Surface Hardening of Soil-Cement and Soil-Lime-Fly Ash", Highway Research Board Bulletin, No. 241, pp. 49-66.

Hardymon, J. F. (1958), "A Study of Lime and Fly Ash with Regard to Soil Stabilization", Highway Research Laboratory, Kentucky Department of Highways, pp. 49-66.

Helm, R. B., et al. (1976), "Environmental Aspects of Compacted Mixtures of Fly Ash and Wastewater Sludge", Proceedings: Fourth International Ash Utilization Symposium, St. Louis.

Herrin, M. and Mitchell, M. (1961), "Lime Soil Mixes", Highway Research Board Bulletin, No. 304, pp. 99-138.

Herzog, A. and Mitchell, J. K. (1963), "Reactions Accompanying Stabilization of Clay with Cement", Highway Research Board Record, No. 36, pp. 146-171.

Hoffman, G. (1974), "Curing and Tensile Strength Characteristics of Aggregate-Lime-Pozzolan", Pennsylvania Department of Transportation Research Report, Bureau of Materials, Testing and Research.

Hollon, G. W. and Dannor, E. (1959), "Effect of Number of Test Specimens on Test Results on Slag-Lime- Fly Ash Mixtures", Highway Research Board Bulletin, No. 231, pp. 82-91.

Hollon, G. W. and Marks, B.A. (1963), "A Correlation of Published Data on Lime-Pozzolan-Aggregate Mixtures for Highway Base Course Construction", Highway Research Abstracts, Vol. 33, No. 2.

Holman, F. L. (1967), "Lime and Lime-Fly Ash Soil Stabilization", Alabama Highway Research, Alabama Highway Department, Report No. 36.

Hoover, J. M., et al. (1958), "Durability of Soil-Lime-Fly Ash Mixes Compacted Above Standard Proctor Density", Highway Research Board Bulletin, No. 193, pp. 1-11.

Hoover, J. M., et al (1962), "Soil Stabilization Field Trials, Primary Highway 117, Jasper County, Iowa", Highway Research Board Bulletin, No. 357, pp. 41-68.

Huang, R. J. W. and Roderick, G. L. (1969), "Cement Content of Soil Cement by X-ray Fluorescence", Highway Research Record, No. 263, pp. 60-68.

Ingles, O. G. and Metcalf, J. B. (1973), "Soil Stabilization, Principles and Practice", John Wiley, New York.

Jones, C. C. and Amos, D. F. (1976), "Physical Changes in Virginia Soils Resulting from the Additions of High Rates of Fly Ash", Proceedings: Fourth International Ash Utilization Symposium, St. Louis, March.

Joshi, R. C., et al. (1976), "Performance Record of Fly Ash as a Construction Material", Proceedings: Fourth International Ash Utilization Symposium, St. Louis.

Katti, R. K., Davidson D. T. and Sheeler, J. B. (1973), "Soil Stabilization, Principles and Practice", John Wiley, New York.

Kinder, D. L. (1976), "Fly Ash Utilization: A Land Development Concept", Proceedings: Fourth International Ash Utilization Symposium, St. Louis.

Kumar, S. (1974), "A Study of the Effects of Simulated Weathering and Repeated Loads on Four Lime Stabilized Oklahoma Shales", a Ph.D. Dissertation, University of Oklahoma, Norman, Oklahoma, Unpublished.

Laguros, J. G. (1965), "Lime Stabilized Soil Properties and the Beam Action Hypothesis", Highway Research Board Record, No. 92, pp. 12-20.

Laguros, J. G. (1972), "Predictability of Physical Changes of Clay Forming Materials in Oklahoma", Report No., ODOH 68-03-2, OURI 1677, University of Oklahoma, School of Civil Engineering and Environmental Science, Norman, Oklahoma.

Laguros, J. G. and Jha, K. (1977), "Stabilization of Oklahoma Shales", Report No. ODOT 73-04-2 ORA 158-602, University of Oklahoma, School of Civil Engineering and Environmental Science, Norman, Oklahoma.

Laguros, J. G, Kumar, S. and Annamalai, M. (1974), "A Comparative Study of Simulated and Natural Weathering of Some Oklahoma Shales", Clays and Clay Minerals, Journal of the Clay Mineral Society, London, Vol. 22, pp. 111-115.

Lamb, D. W., "Ash Disposal in Dams, Mounds, Structural Fills and Retaining Walls", Third International Ash Utilization Symposium, Pittsburgh, PA.

Lamb, D. W., et al., "Fly Ash as Construction Material For Water Retaining Structures", Proceedings: Fourth International Ash Utilization Symposium, St. Louis.

Lambe, T. W.(1958), "The Structure of Compacted Clay", Journal of Soil Mechanics and Foundation Divison, Proceedings of American Society of Civil Engineers, Vol. 83, No. SM-2, pp. 1-34.

Leonard, G. S. (1964), "Quantitative Interpretation of Mineralogical Composition from X-Ray and Chemical Data for the Pierre Shale, USGS Professional Paper 391, Analytical Methods in Geochemical Investigations of the Pierre Shale, pp. C1-C31.

Leonard, R. J. and Davidson, D. T. (1959), "Pozzolanic Reactivity Study of Fly Ash", Highway Research Board Bulletin, No. 231, pp. 1-14.

MacConnache, I. (1974), "Fabric Changes in Consolidated Kaolin", Geotechnique, Institution of Civil Engineers, London, Vol. 24, No. 2, pp. 207-222.

MacMurdo, F. D. and Barenberg, E. J. (1973), "Determination of Realistic Cut Off Dates for Late - Season Construction with Lime-Fly Ash and Lime-Cement-Fly Ash Mixtures", Highway Research Record, No. 442, pp. 92-101.

McDowell, C. (1959), "Stabilization of Soils with Lime-Fly Ash and Other Lime Reactive Materials", Highway Research Board Bulletin, No. 231, pp. 60-66.

Marks, B. D. and Haliburton, T. A. (1972), "Accelleration of Lime-Clay Reactions with Salt", Soil Mechanics and Foundation Division, American Society of Civil Engineers, Vol. 98, No. SM-4, pp. 327-340.

Mateos, M. (1964), "Heat Curing of Sand-Lime-Fly Ash Mixtures", Highway Research Abstract, Vol. 34.

Mateos, M. (1964), "Stabilization of Soils with Fly Ash Alone", Highway Research Record, No. 52, pp. 59-65.

Mateos, M. and Davidson, D. T. (1963), "Compaction Characteristics of Soil-Lime-Fly Ash Mixtures", Highway Research Record, No. 29, pp. 27-41.

Mateos, M. and Davidson, D. T. (1961), "Further Evaluation of Promising Chemical Additives for Accelerating the Hardening of Soil-Lime-Fly Ash Mixtures", Highway Research Board Bulletin, No. 304, pp. 32-50.

Mateos, M. and Davidson, D. T. (1962), "Lime and Fly Ash Proportions in Soil-Lime and Fly Ash Mixtures and Some Aspects of Soil - Lime Stabilization", Highway Research Board Bulletin, No. 335. pp. 40-64.

Mateos, M. and Davidson, D. T. (1962), "Steam Curing and X-Ray Studies of Fly Ashes", Proceedings, American Society for Testing and Materials, Vol. 62, pp. 1003-1018.

McDowell, C. (1959), "Stabilization of Soils with Lime-Fly Ash and Other Lime Reactive Materials", Highway Research Board Bulletin, No. 231, pp. 60-66.

Metcalf, J. B. (1963), "The Effect of High Curing Temperature on the Unconfined Compressive Strength of a Heavy Clay Stabilized with Lime and with Cement", Fourth

Australia- New Zealand Conference on Soil Mechanics and Foundations, pp. 126-130.

Meyers, J. F., et al. (1976), "Guide or he Design and Construction of Cement Stabilized Fly Ash Pavements", Proceedings: Fourth International Ash Utilization Symposium, St. Louis.

Miller, R. H. and Couturier, R. R. (1961), " An Evaluation of Gravels for Use in Lime- Fly Ash- Aggregate Composition", Highway Research Board Bulletin, No. 304, pp. 139-147.

Miller, R. H. and McNichol, W. J., "Structural Properties of Lime-Fly Ash-Aggregate Compostions", Highway Research Board Bulletin, No. 193, pp. 12-23.

Minnick, L. J. (1967), "Reaction of Hydrated Lime with Pulverized Coal Fly Ash", Proceedings: Fly Ash Utilization Symposium, U. S. Bureau of Mines Information, Circular No. 8348.

Minnick, L. J., et al. (1970), "Prediction of Fly Ash Performance", Proceedings: Second Ash Utilization Symposium, Bureau of Mines Information Circular No. 8488, U.S. Department of Interior.

Minnick, L. J. and Meyers, W. F. (1953), "Properties of Lime-Fly Ash-Soil Composition Employed in Road Construction", Highway Research Board Bulletin, No. 69, pp. 1-28.

Minnick, L. J. and Miller, R. H.(1952), "Lime-Fly Ash Compositions in Highway Constructions", Highway Research Board Bulletin, No. 30.

Minnick, L. J. and Williams, R. (1956), "Field Evaluation of Lime-Fly Ash Soil Compositions for Roads", Highway Research Board Bulletin, No. 129.

Moh, Z. C. (1965), "Reactions of Soil Minerals with Cement and Chemicals", Highway Research Record, No. 56, pp. 39-61.

Moreland and Mitchell, H. (1961), "Lime-Soil Mixtures", Highway Research Board Bulletin, No. 304, pp. 99-138.

Morgenstern, N. R. and Eigenbrod, K. D. (1974), "Classification of Argillaceous Soils and Rocks", Journal of Geotechnical Engineering Division, American Society of Civil Engineers, New York, Vol. 100, No. GT10, pp.

1137-1156.

Moulton, L. K. (1973), "Bottom Ash and Boiler Slag", Third International Ash Utilization Symposium, Pittsburgh, PA.

Moulton, L. K. et al. (1973), "Utilization of Ash from Coal Burning Power Plants in Highway Construction", Highway Research Record, No. 430, pp. 26-39.

Natusch, D. F. S. (1977), et al., "Characterization of Trace Elements in Fly Ash", Institute For Environmental Studies, University of Illinois, IES Research Report No. 3, pp. 1-34.

O'Flaherty, C.A. (1962), et al., "Fly Ash and Sodium Carbonate as Additives to Soil-Cement Mixtures", Highway Research Board Bulletin, No. 353, pp. 108-123.

Olsen, H. W. (1962),"Hydraulic Flow Through Saturated Clays", Clay and Clay Minerals, Journal of the Clay Mineral Society, London, Vol. 9, No. 2, pp. 131-145.

Paquette, R. J. and McGee, J. D., "Evaluation of Strength Properties of Several Soils Treated with Admixtures", Highway Research Board Bulletin, No. 282, pp. 1-12.

Paulson, C. A. J. and Ramsden, A. R. (1970), "Some Microscopic Features of Fly Ash Particles and Their Significance in Relation to Electrostatic Precipitation", Atmospheric Environment, Vol. 4, pp. 175-180.

Pettijohn, F. J. (1967), "Sedimentary Rocks", Harper Brothers, New York.

Pinto, S., Davidson, D. T. and Laguros, J. G., (1962) "Effects of Lime on Cement Stabilization of Montmorillonite Soils", Highway Research Board Bulletin, No. 353, pp. 64-83.

"Power Plant Ash Disposal a Growing Problem", Chemical and Engineering News, Nov. 1978.

Prentis, H. M. (1951), "The Distribution of Concrete Stress in Reinforced and Prestressed Concrete Beam When Tested to Destruction by a Pure Bending Moment", Mag. Concrete Research 2, No. 5, pp. 73-77.

Page, A. L. (1979), et al., "Physical and Chemical Properties of Fly Ash from Coal-Fired Power Plants with

Reference to Environmental Impacts", Residue Reviews, Vol. 71, pp. 83-120.

Quentin, L. R. and Marshall, R. T. (1976), "Effect of Lime Treatment on the Resilient Behavior of Fine Grained Soils", Transportation Research Record, No. 560, pp. 11-20.

Ranganatham, B. V. and Pandian, N. S. (1971), "Strength-Gain in Thermally Cured Lime Stabilized Clays", Proceedings, Fourth Conference on Soil Mechanics.

Raymond, S. and Smith, P. H. (1964), "The Use of Stabilized Fly Ash in Road Construction", Civil Engineering and Public Works Review, London, Vol. 59.

Rehsi, S. S. (1974), "Studies on Indian Fly Ashes and Their Use in Structural Concrete", United States Bureau of Mines Information Circular 8640, pp. 231-245.

Remus, M. D. and Davidson, D. T.(1961), "Relations of Strength to Composition and Density of Lime-Treated Clay Soils", Highway Research Board Bulletin, No. 304, pp. 65-75.

Robnett, O. L. and Thompson, M. R. (1969), "Soil Stabilization Literature Reviews", Civil Engineering Studies, Highway Engineering Series, No. 34, University of Illinois, Urbana, Illinois.

Roger, W. P. and David, F. N. (1970), "Reactions and Strength Development in Portland Cement Soil Mixtures", Highway Research Record, No. 315, pp. 46-63.

Rosen, W. J. and Marks, B. D. (1974), "Cold Weather Lime Stabilization", Transportation Research Record, No. 501, pp. 35-41.

Ruff, C. G. and H0, C. (1966), "Time-Temperature-Strength-Reaction Product Relationships in Lime-Bentonite Water Mixtures", Highway Research Record, No. 139, pp. 42-60.

Savage, F. M. , "Establishing a Market for Lime-Fly Ash Base", United States Bureau of Mines Information Circular, No. 8488.

Seals, R. K.(1972), et al., "Bottom Ash: An Engineering Material", Journal of Soil Mechanics and Foundations Divison, American Society of Civil Engineers, Vol. 98, No. SM-4, pp. 311-326.

Seed, H. B. and Chen, C. K. (1959), "Structure and Strength Property of Compacted Clays", Journal of Soil Mechanics and Foundations Divison, American Society of Civil Engineers, Vol. 85, No. SM-5, pp. 87-109.

Sloane, R. L. (1965), "Early Reaction Determination in Two Hydroxide-Kaolinite System by Electron Microscopy and Diffraction", Clays and Clay Minerals, Journal of the Clay Minerals Society, London, Proceedings of the 13th Conference, pp. 331-339.

Sutherland, H. B. (1970), "Factors Affecting the Frost Susceptibility Characteristics of Pulverized Fuel Ash", Canadian Geotechnical Journal, Vol. 7, No. 1.

Sutherland, H. B. (1968), et al., "Engineering and Related Properties of Pulverized Fuel Ash", Journal of the Institution of Highway Engineers, Vol. 15, No. 6.

Thompson, M. R. and Depsey, B. J. (1970), "Quantitative Characterization of Cyclic Freezing and Thawing in Stabilized Pavement Materials", Highway Research Record, No. 304, pp. 38-44.

Thornton, S. I. and Parker, D. G. (1975), "Fly Ash as Fill and Base Material in Arkansas Highways", pp. 1-81.

Townsend, D. L. and Klym, T. W. (1966), "Durability of Lime-Stabilized Soils", Highway Research Record, No. 139, pp. 25-41.

Transportation Research Board (1976), "Lime-Fly Ash-Stabilized Bases and Subbases", National Cooperative Highway Research Program Synthesis of Highway Practice, No. 37, NCHRP.

Trollope, D. M. and Chan, C. K. (1960), "Soil Structure and the Step Strain Phenomenon", Journal of Soil Mechanics and Foundations Division, American Society of Civil Engineers, Vol. 86, No. SM-2, pp. 1-40.

Underwood, L. B. (1967), "Classification and Indentification of Shales", Journal of Soil Mechanics and Foundations Division, American Society of Civil Engineers, Vol. 93, No. SM-G, pp. 97-116.

Uppal, H. L. and Dhawan, D. K. (1968), "A Resume on the Use of Fly Ash in Soil Stabilization", Road Research Papers, Central Road Research Institute, India, No. 95.

Viskochil, R. K., Handy, R. L. and Davidson, D. T.

(1957), "Effect of Density on Strength of Lime-Fly Ash Stabilized Soil", Highway Research Board Bulletin, No. 183, pp. 5-15.

Wang, J. W. (1962), et al., "Comparisons of Various Types of Commercial Limes for Soil Stabilization, "Highway Research Board Bulletin, No. 335, pp. 65-79.

Wang, J. W. H. and Handy, R. L.(1966), "Role of Magnesium Oxide in Soil-Lime Stabilization", Highway Research Board Special Report, No. 90, pp. 475-492.

Whitehurst, E. A. (1955), "Stabilization of Tennessee Gravel and Chert Bases", Highway Research Board Bulletin, No. 108.

Word, J. E. and Green, W. B. (1961), "Current Interpretation of Stability Measurements on Two Experimental Projects in Maryland", Highway Research Board Bulletin, No. 282, pp. 105-134.

Yang, N. C. (1970), "New Paving Concept for Newark Airport", Civil Engineering Magazine, American Society of Civil Engineers.

Yuan, P. C. (1979), "Chlorination of Fly Ash and Bentonite With A Gas Mixture of Silicon Tetrachloride and Chlorine", Master's Thesis, South Dakota School of Mines and Technology.

APPENDIX A

UNCONFINED COMPRESSIVE STRENGTH RESPONSES OF CEMENT STABILIZED SOILS

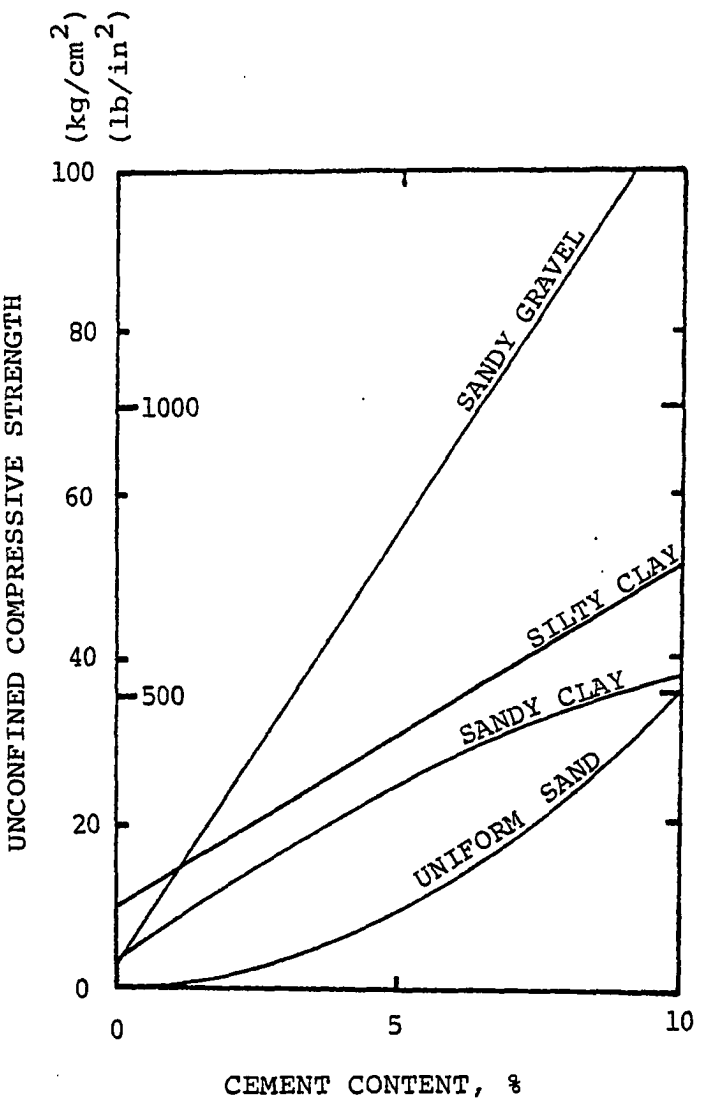

Figure A.1: Effect of cement content on strength for various soils stabilized with ordinary Portland cement and cured for seven days at 25°C, constant moisture content (after Metcalf, 1953)

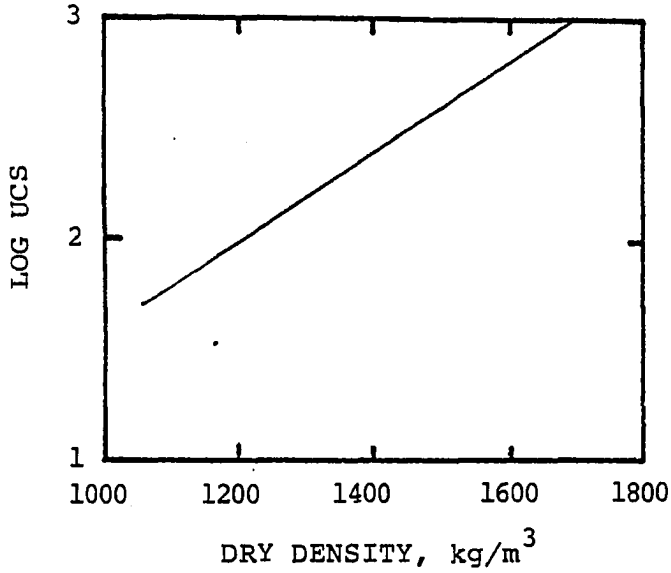

Figure A.2: Effect of density on strength of a clay stabilized with 10% cement (after Metcalf, 1959)

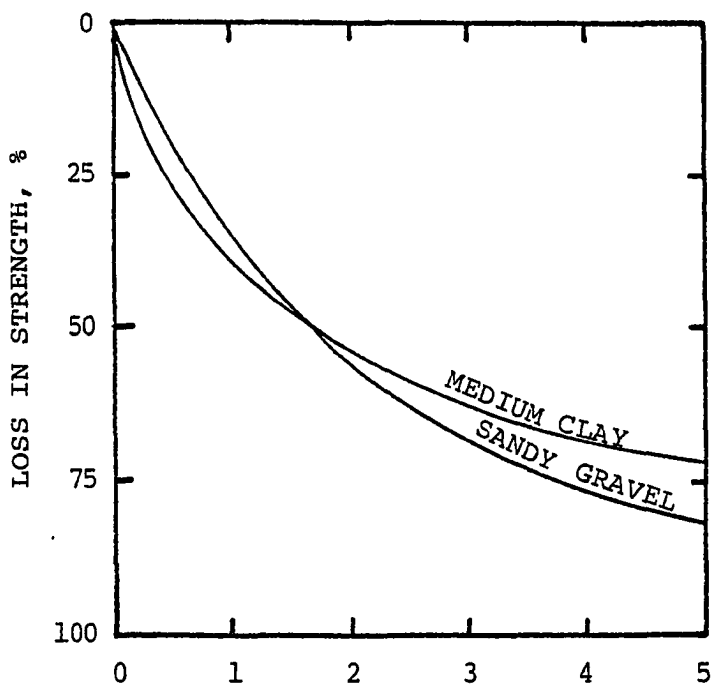

Figure A.3: Loss in strength due to delay in compaction for two soils stabilized with 10% cement; standard compaction (after West, 1953)

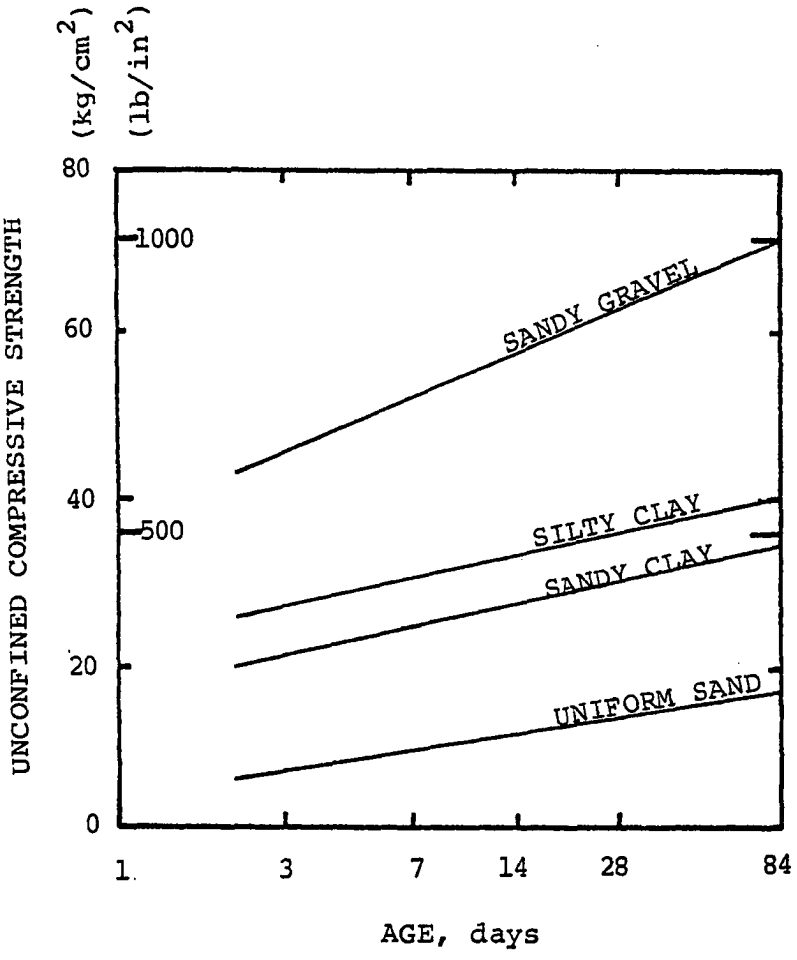

Figure A.4: Effect of age on strength of various soils stabilized with 5% cement (after Metcalf, 1973)

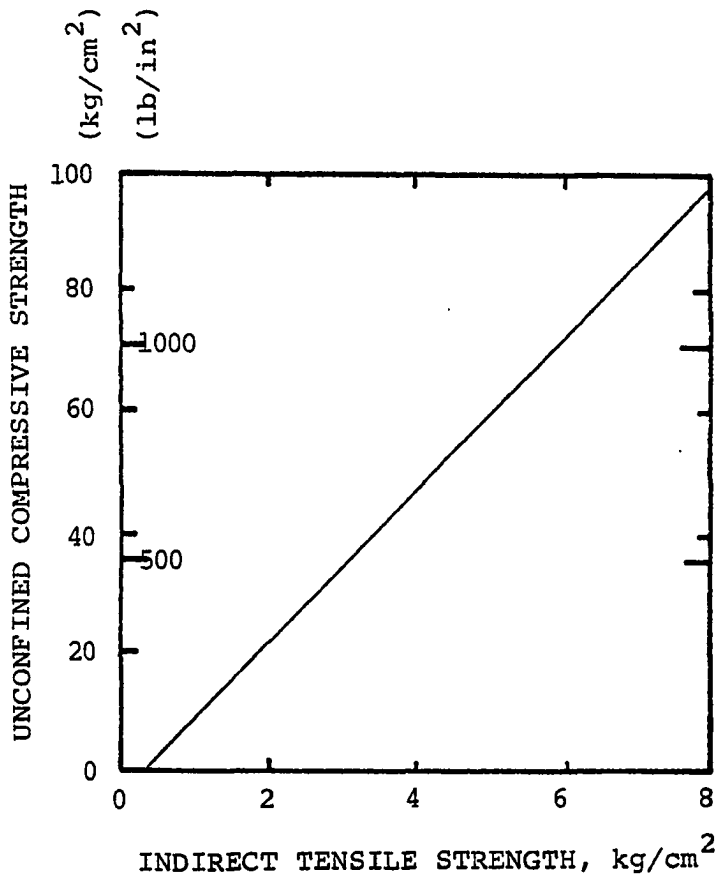

Figure A.5: Relation between compressive and tensile strength for cement stabilized soils (after Ingles and Metcalf, 1973)

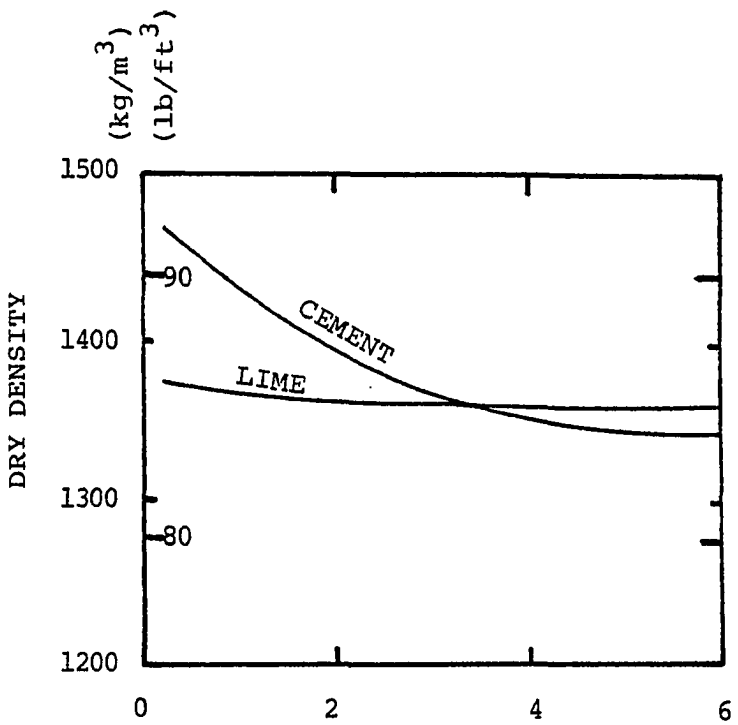

Figure A.6: Effect of delay on the compacted density of a heavy clay, stabilizer content 10 percent (after Dumbleton, 1962)

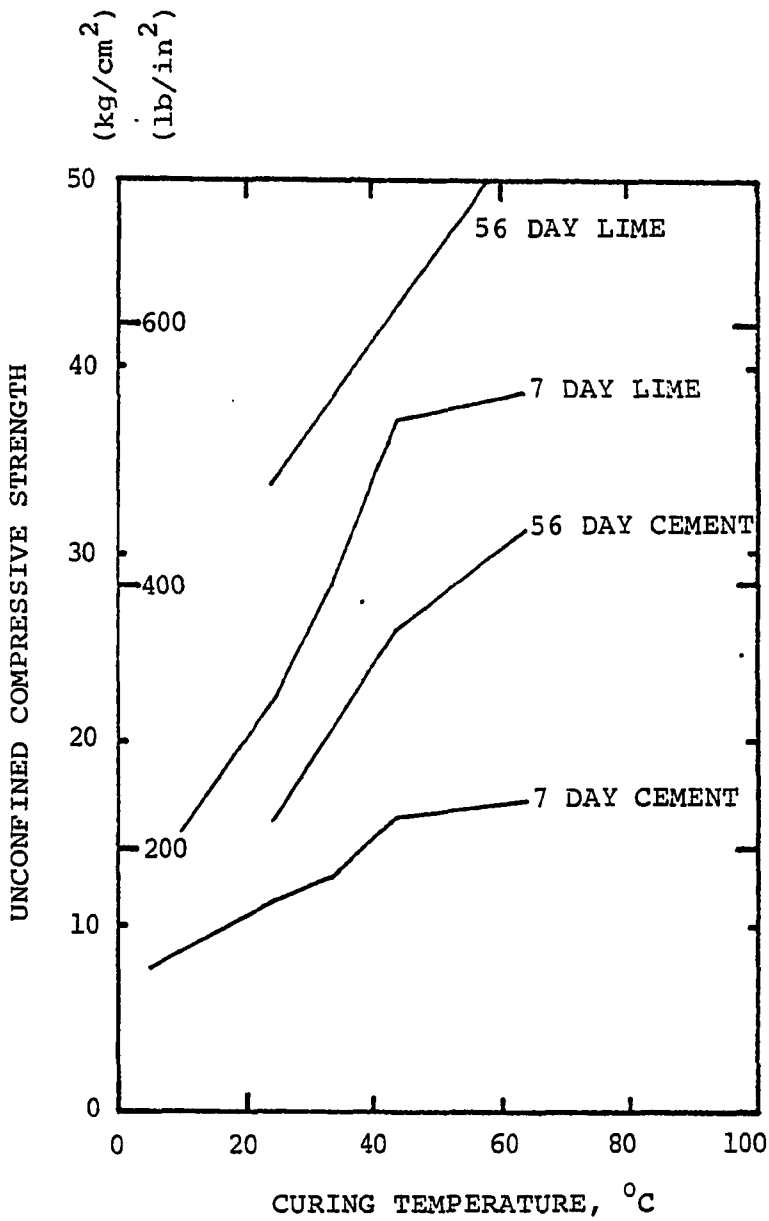

Figure A.7: Effect of curing temperature on strength of stabilized heavy clay (after Ingles and Metcalf, 1973)

APPENDIX B

GRAIN SIZE CURVES OF STABILIZED SHALE

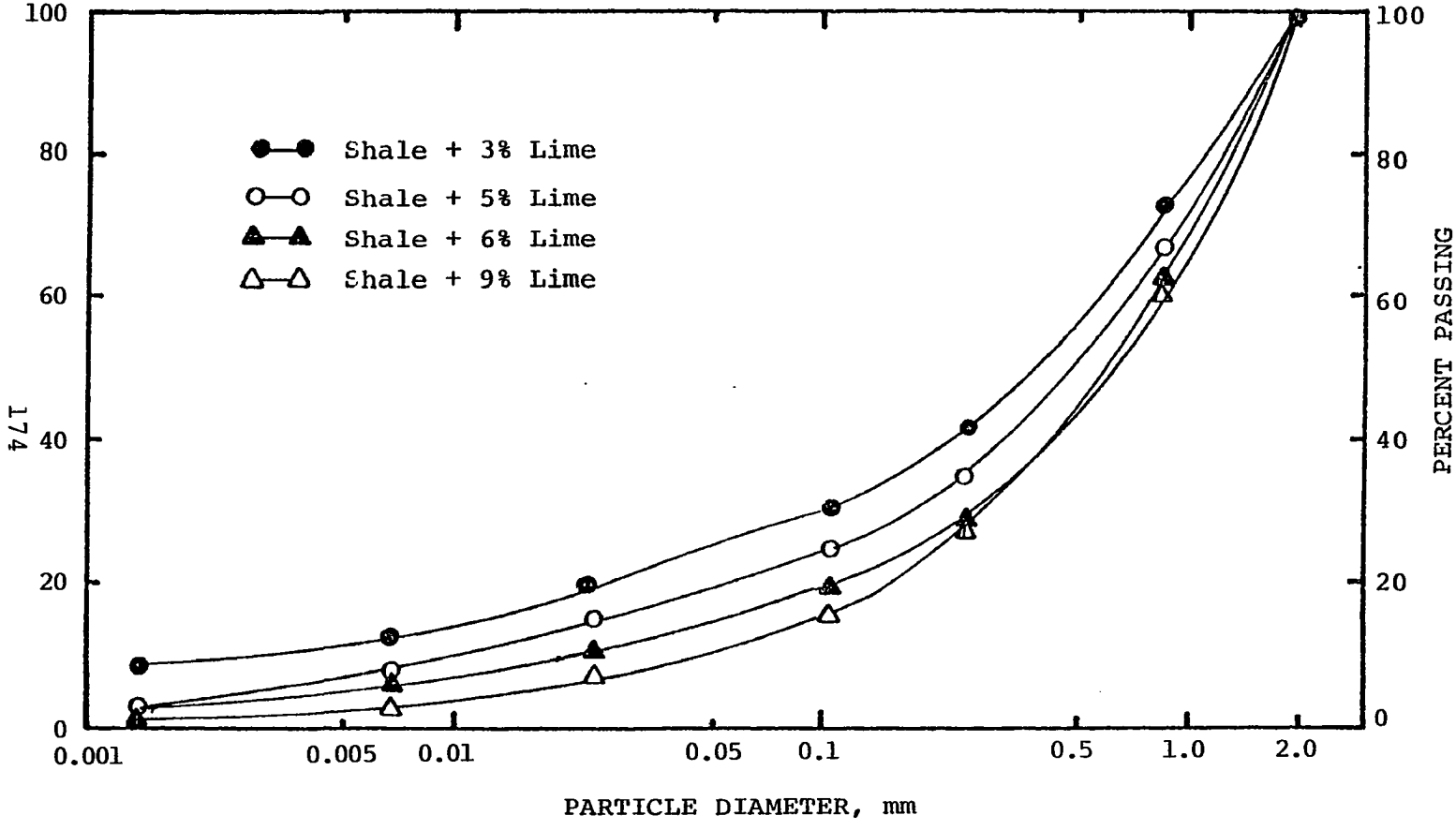

Figure B.1: Gradation curves of lime stabilized shale

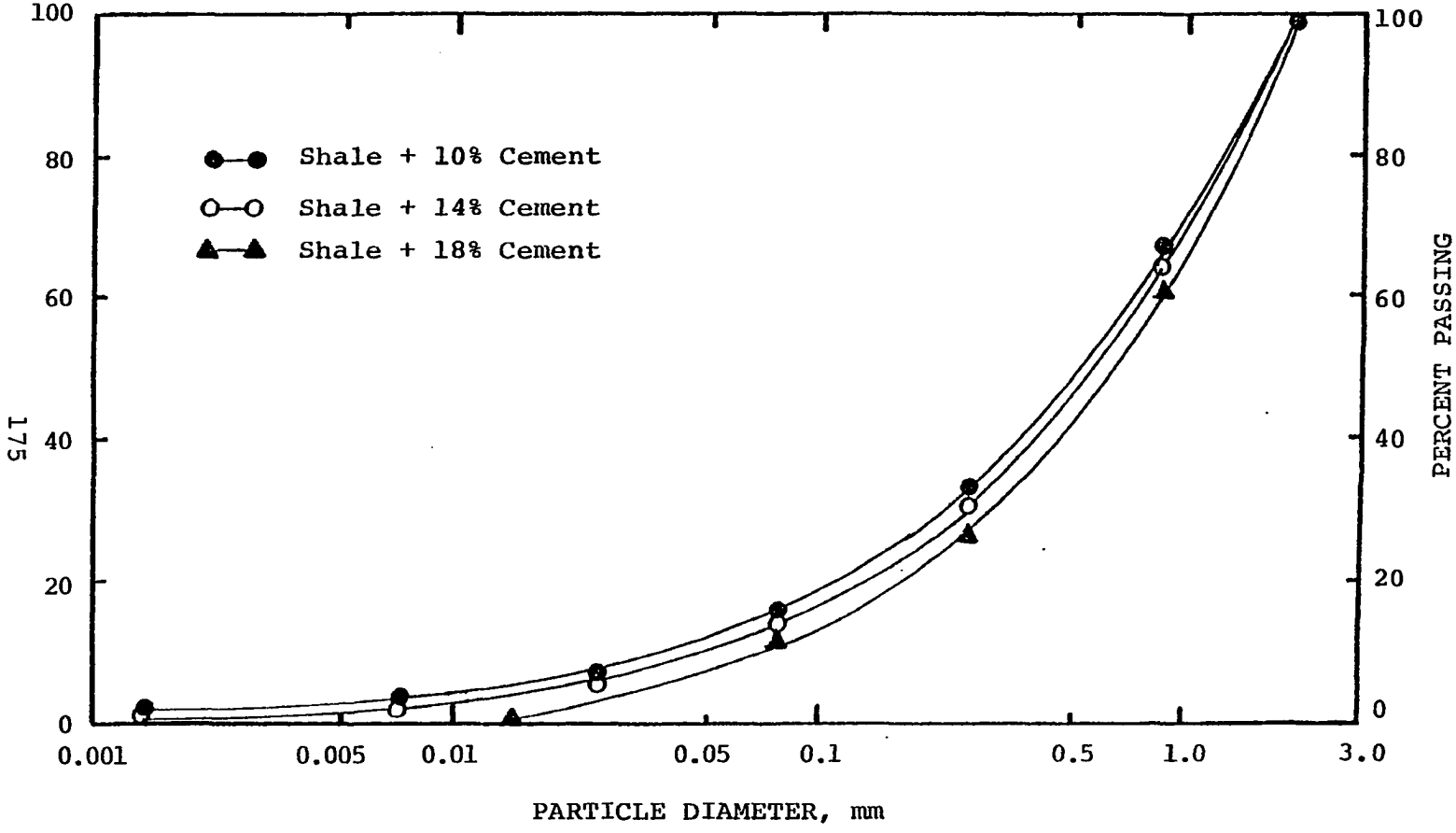

Figure B.2: Gradation curves of cement stabilized shale

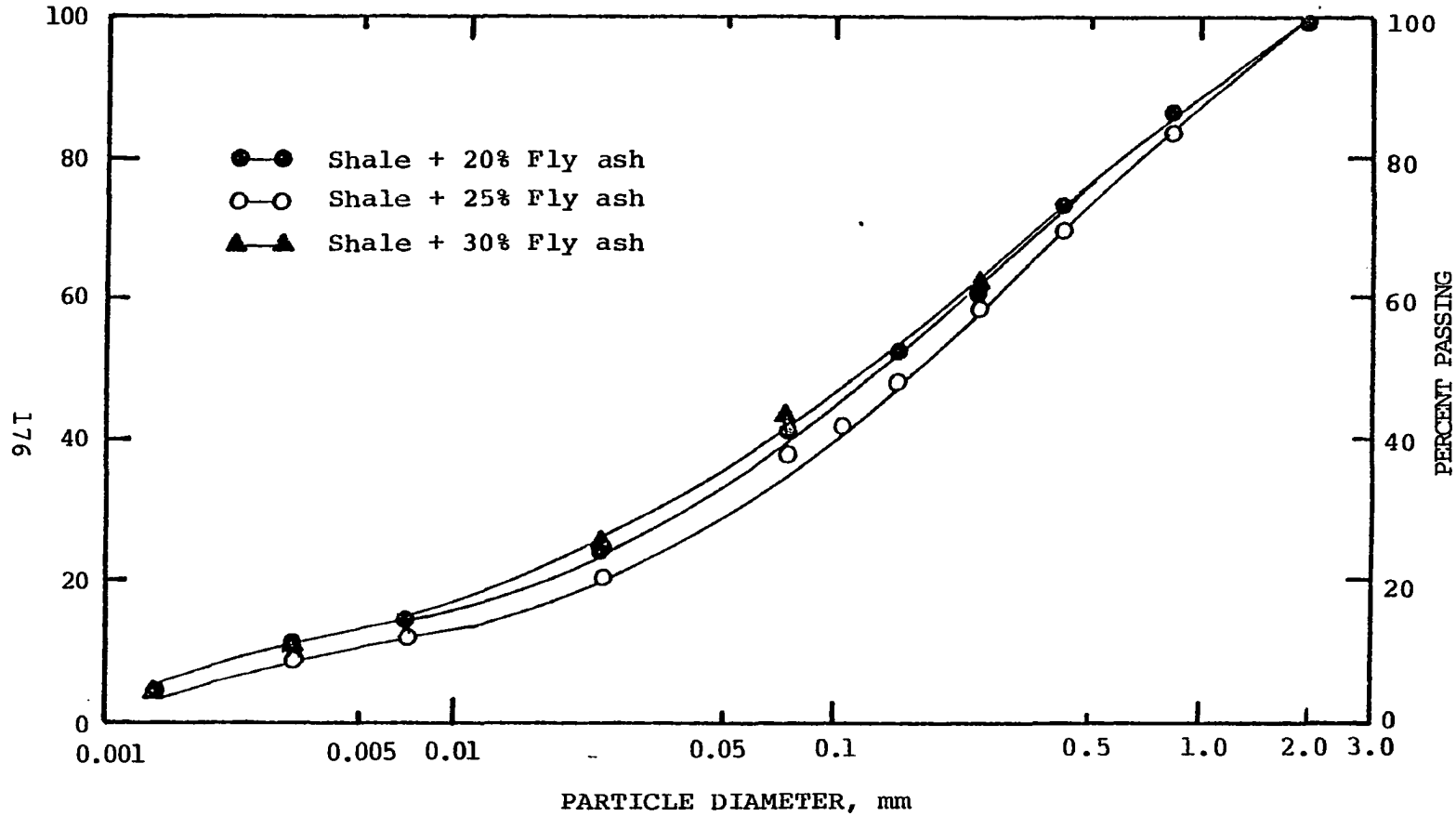

Figure B.3: Gradation curves of fly ash stabilized shale

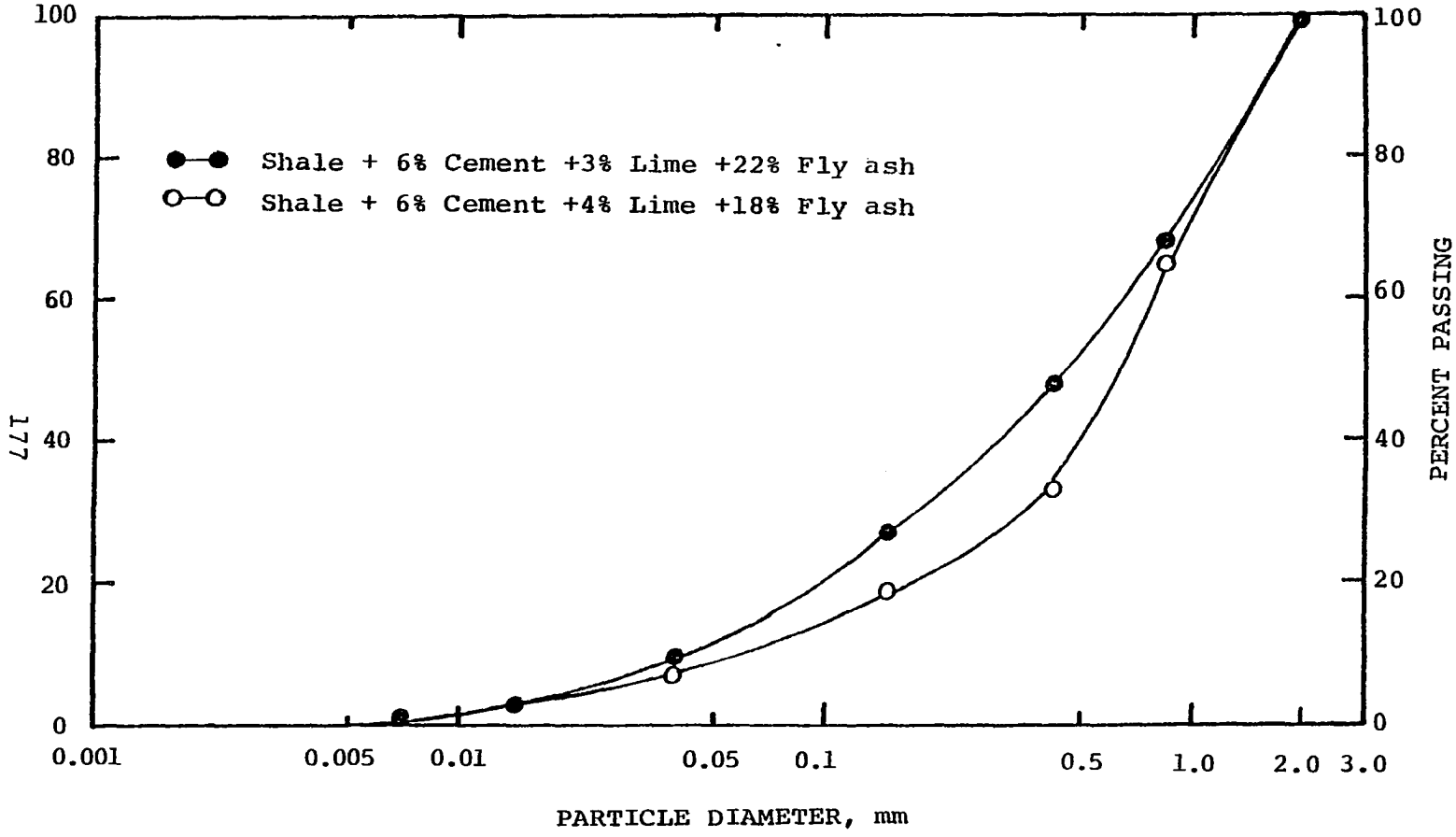

Figure B.4: Gradation curves of conjunctively stabilized shale

APPENDIX C

MOISTURE DENSITY RELATIONS

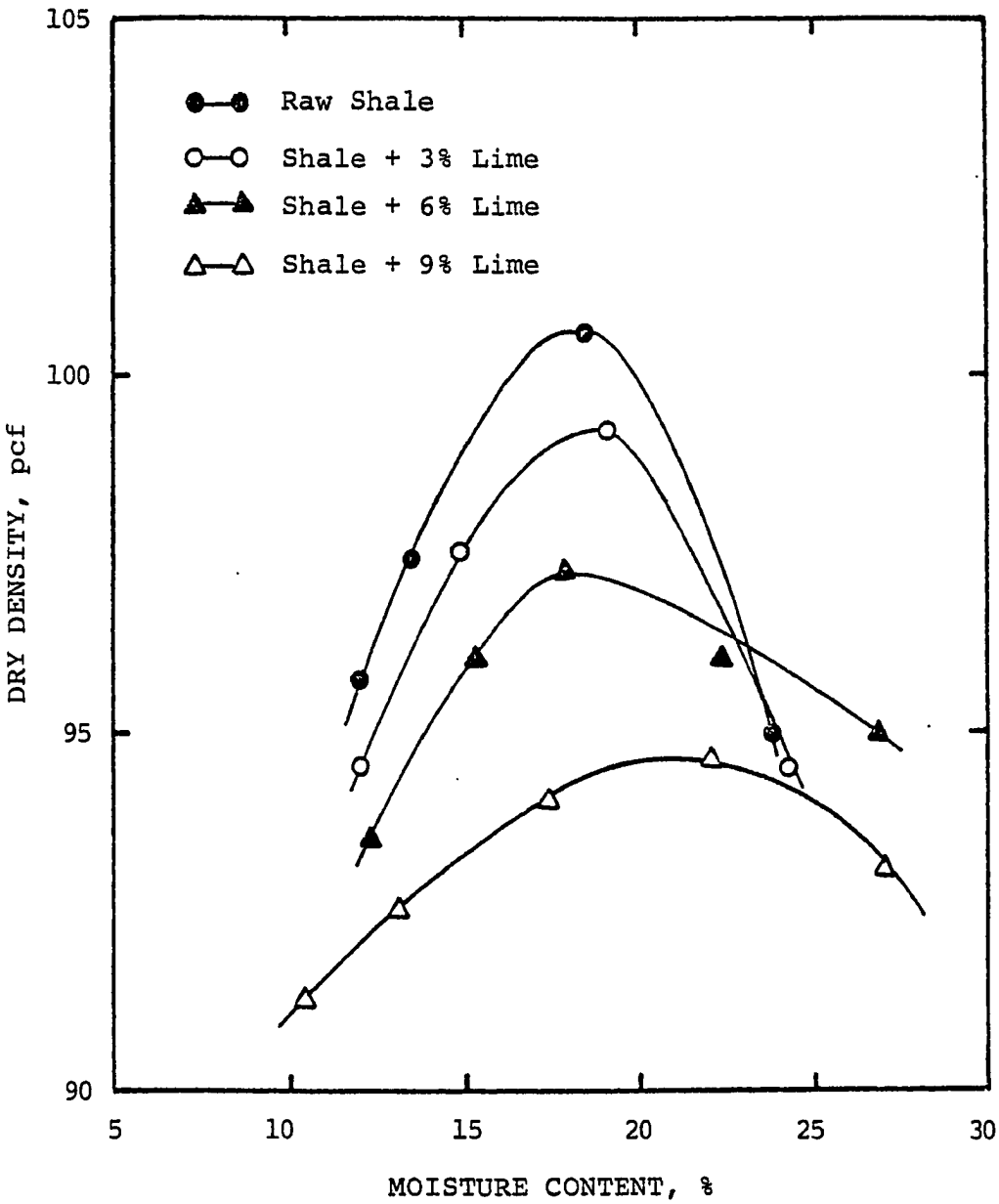

Figure C.1: Moisture density relationship of raw and lime stabilized shale

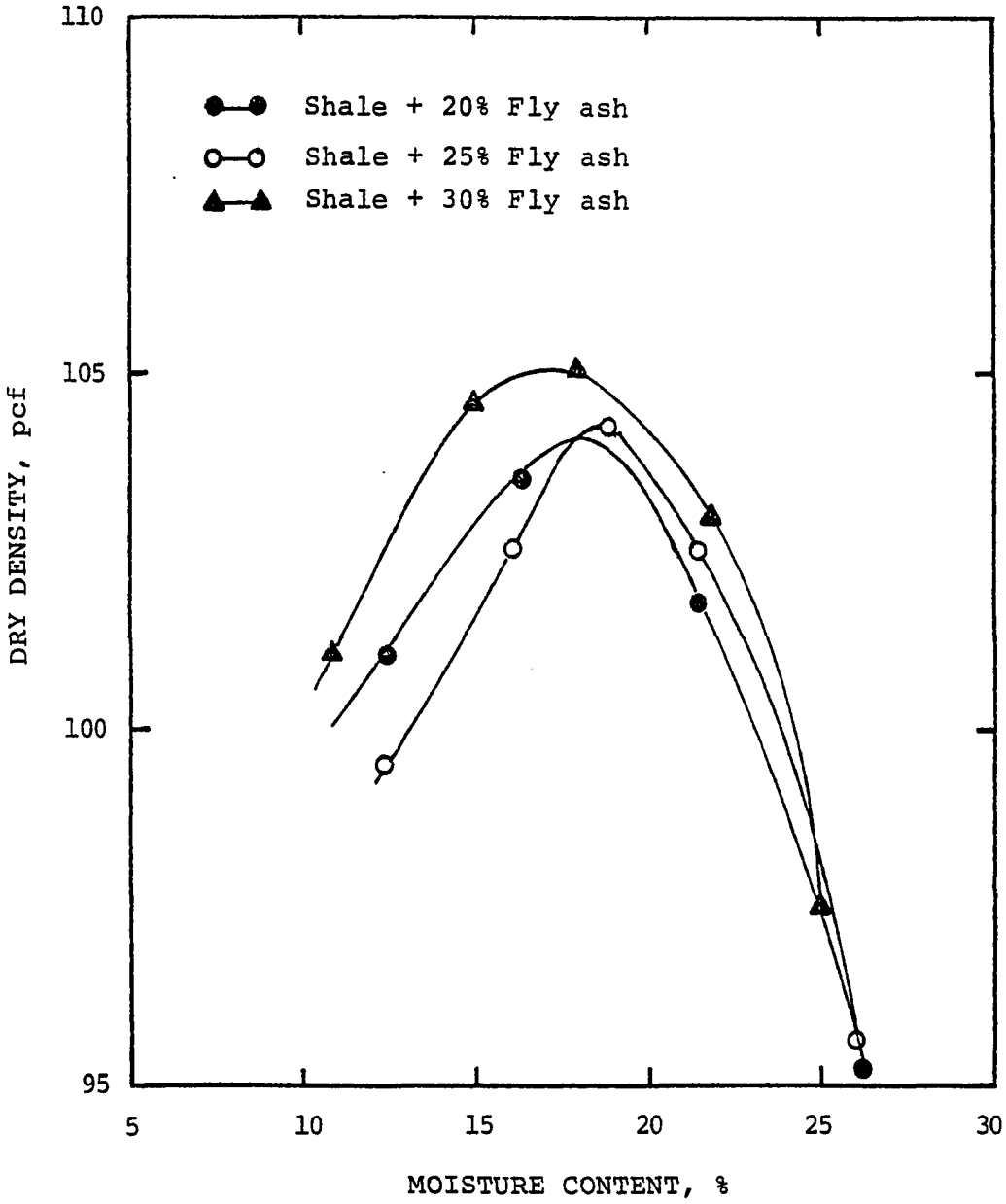

Figure C.2: Moisture density relationship of fly ash stabilized shale

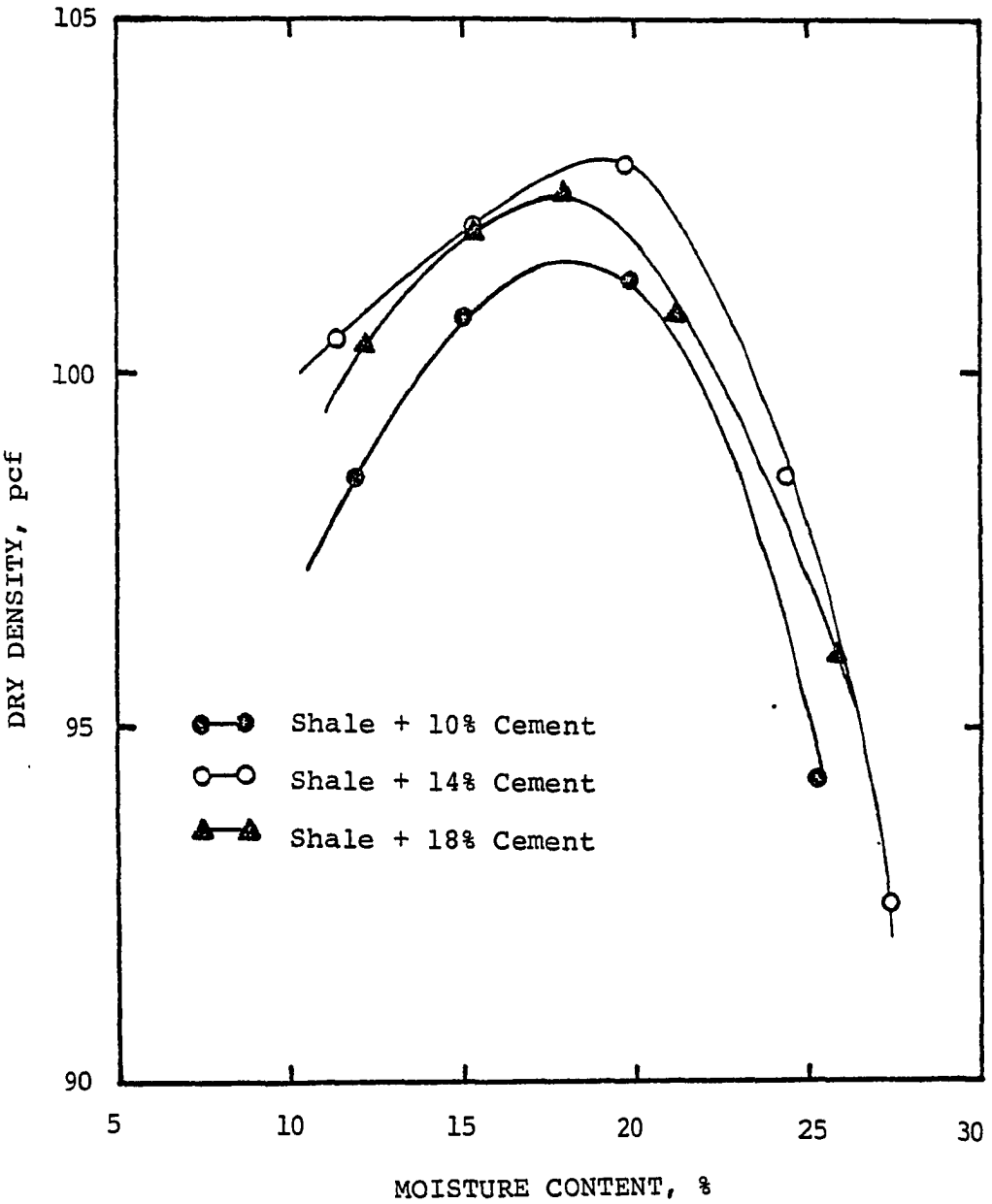

Figure C.3: Moisture density relationship of cement stabilized shale

APPENDIX D

STRENGTH TEST DATA

TABLE D.1: DRY AND IMMERSED STRENGTH OF STABILIZED SHALE CURED FOR 28 DAYS AT 70°F, 90 To 100 PERCENT RELATIVE HUMIDITY

Type of Mix	Unconfined Strength, psi	
	Dry	Immersed
Raw Shale	73	-
Shale + 3% lime	137	89
+ 5% lime	173	98
+ 6% lime	193	103
+ 9% lime	204	154
Shale + 20% fly ash	222	143
+ 25% fly ash	243	151
+ 30% fly ash	250	158
Shale + 10% cement	313	254
+ 12% cement	592	480
+ 14% cement	619	428
+ 18% cement	696	642
Shale + conjunctive		
8% cement + 3% lime + 22% fly ash	887	479
8% cement + 4% lime + 18% fly ash	469	363

TABLE D.2: DRY AND IMMERSED STRENGTH OF 6% LIME STABILIZED SHALE, CURED FOR 28, 90 AND 180 DAYS AT 70°F AND 90°F, 90 TO 100 PERCENT RELATIVE HUMIDITY

Curing Temperature, °F	Curing Time, Days	Dry Strength, psi	Immersed Strength, psi
70	28	107.6	71.4
70	90	129.3	100
70	180	209.5	126.5
90	28	116.0	74.2
90	90	187.7	167.4
90	180	289.0	140.6

TABLE D.3: DRY AND IMMERSED STRENGTH OF 25% FLY ASH STABILIZED SHALE, CURED FOR 28, 90 AND 180 DAYS AT 70°F AND 90°F, 90 TO 100 PERCENT RELATIVE HUMIDITY

Curing Temperature, °F	Curing Time, Days	Dry Strength, psi	Immersed Strength, psi
70	28	193.8	132.2
70	90	386.6	257
70	180	257	134.2
90	28	208	169
90	90	359.5	177.3
90	180	409.9	261

TABLE D.4: DRY AND IMMERSED STRENGTH OF 14% CEMENT STABILIZED SHALE, CURED FOR 28, 90 AND 180 DAYS AT 70°F AND 90°F, 90 TO 100 PERCENT RELATIVE HUMIDITY

Curing Temperature, °F	Curing Time, Days	Dry Strength, psi	Immersed Strength, psi
70	28	580	300.1
70	90	630	413.3
70	180	664.7	545.3
90	28	610	323.8
90	90	761.2	631.3
90	180	834.9	624

TABLE D.5: DRY AND IMMERSED STRENGTH OF CONJUNCTIVELY (8% CEMENT + 4% LIME + 18% FLY ASH) STABILIZED SHALE, CURED FOR 28, 90 AND 180 DAYS AT 70°F AND 90°F, 90 TO 100 PERCENT RELATIVE HUMIDITY

Curing Temperature, °F	Curing Time, Days	Dry Strength, psi	Immersed Strength, psi
70	28	476.6	437.7
70	90	749.4	565.1
70	180	755.7	721.4
90	28	490.3	419.0
90	90	817.6	710.8
90	180	958.7	777.7

APPENDIX E

LOAD DEFLECTION CURVES OF STABILIZED BEAMS

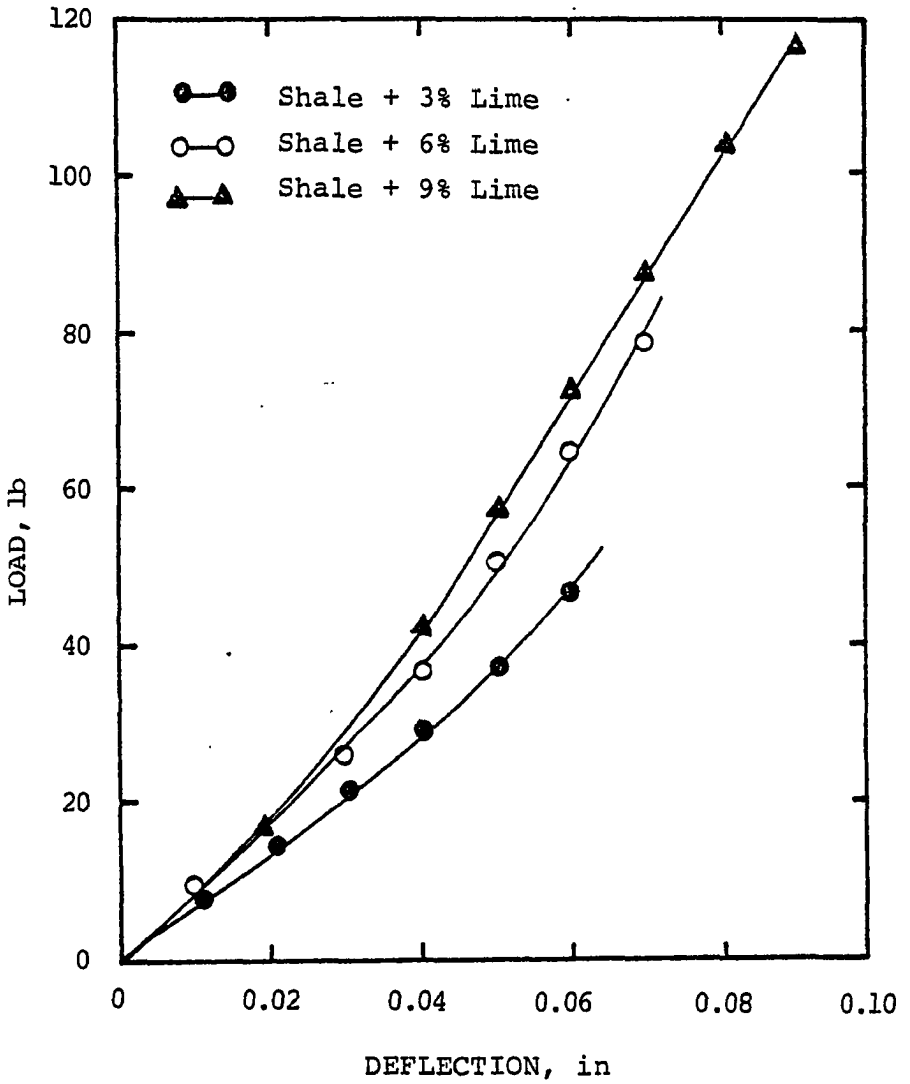

Figure E.1: Deflection patterns of lime stabilized beams

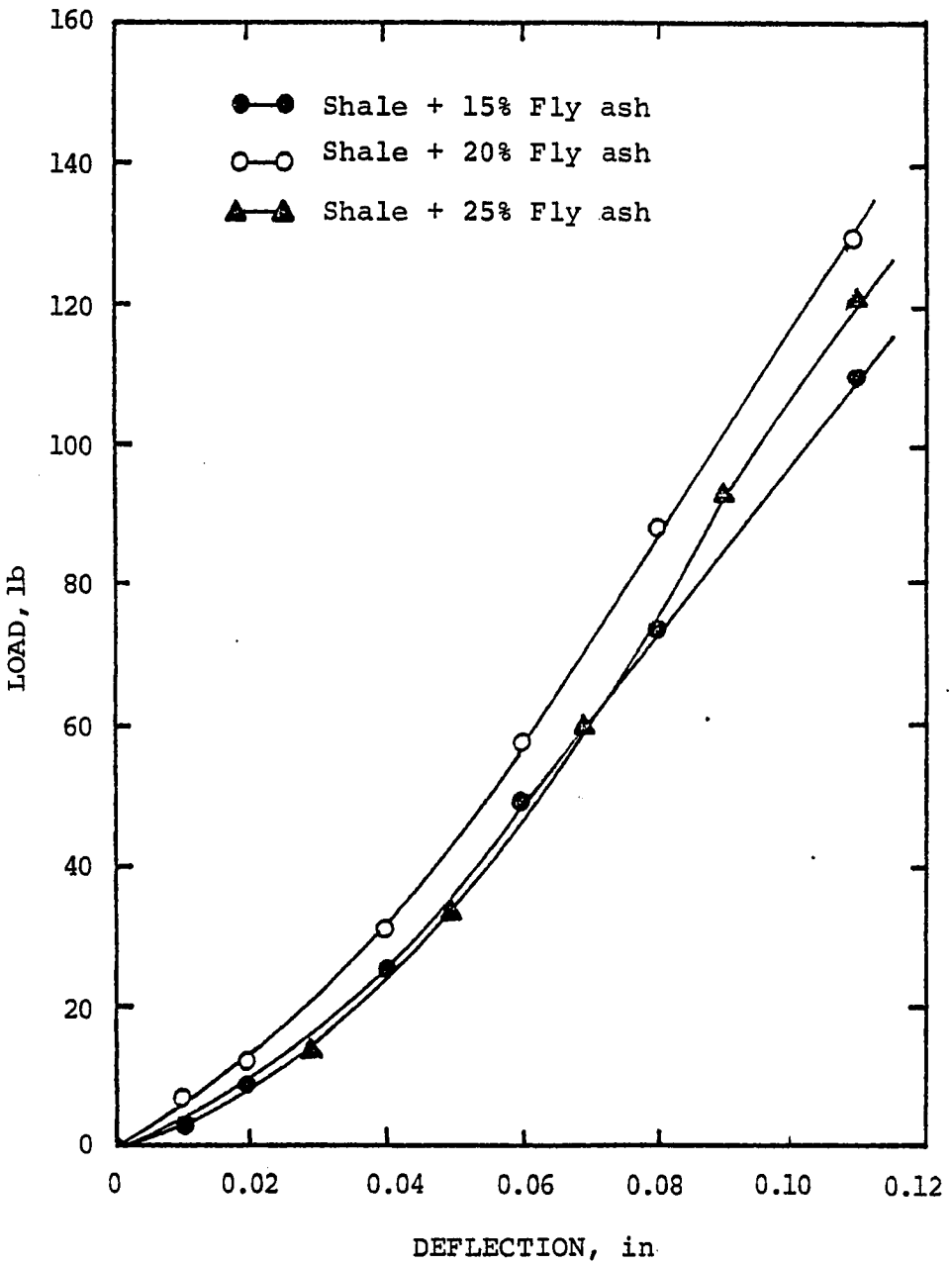

Figure E.2: Deflection patterns of fly ash stabilized beams

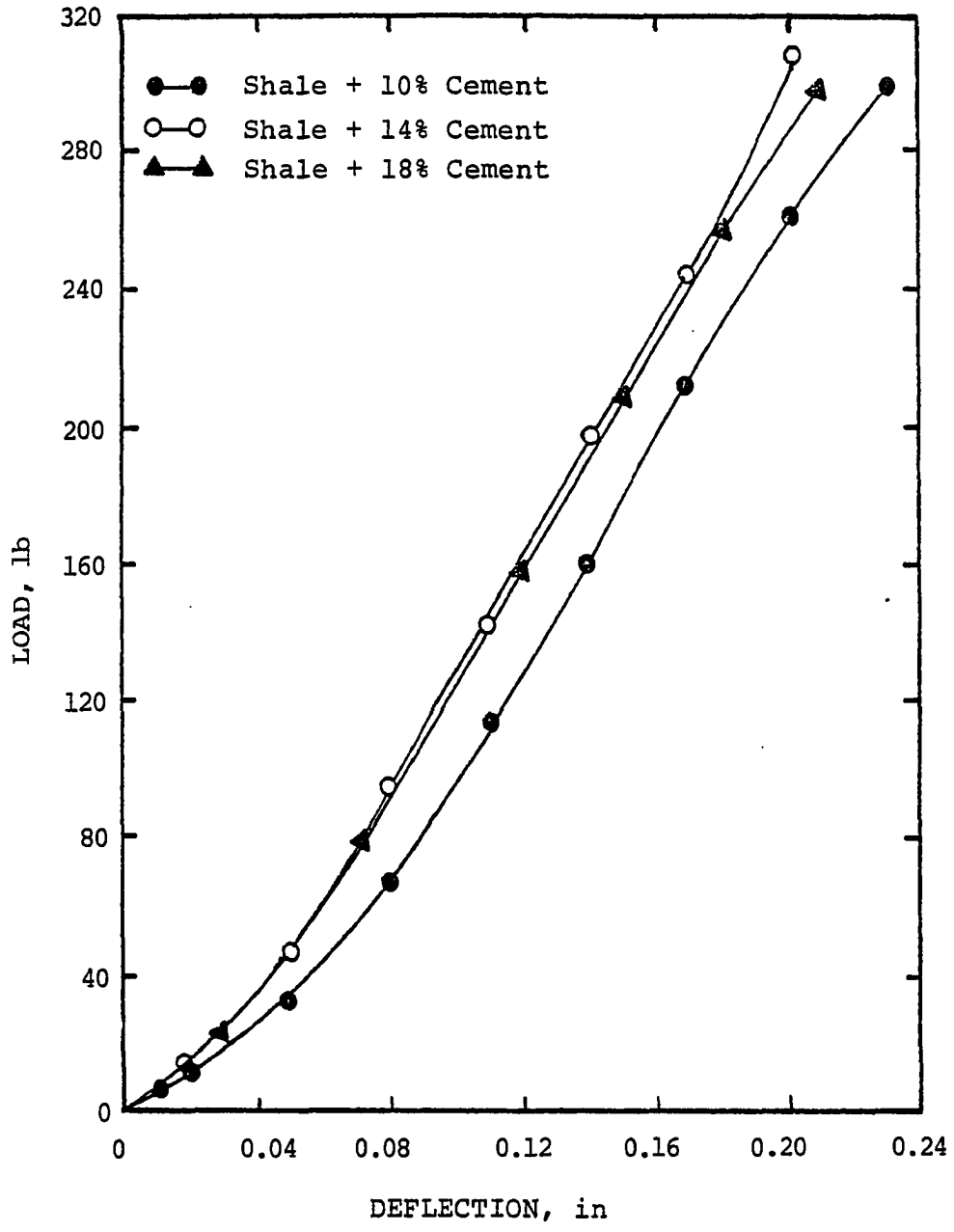

Figure E.3: Deflection patterns of cement stabilized beams

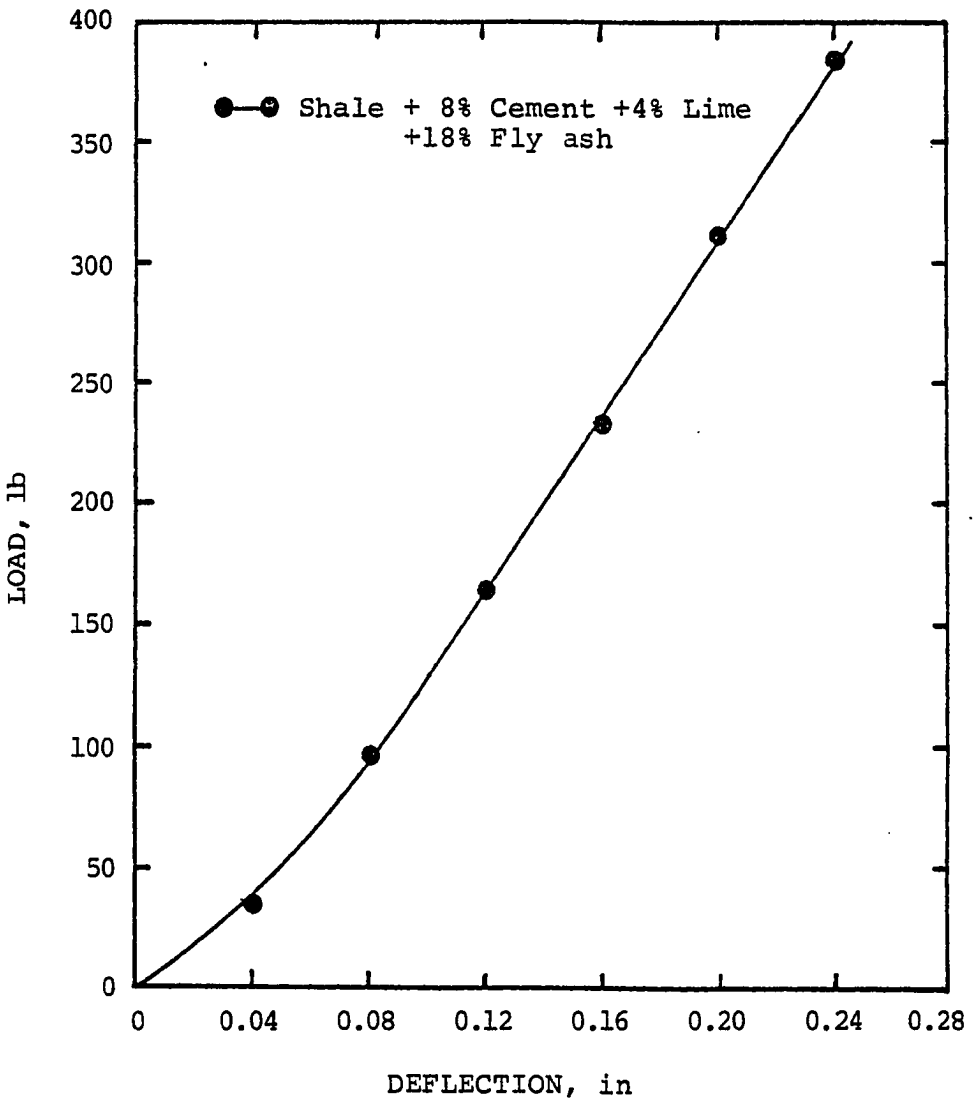

Figure E.4: Deflection patterns of conjunctively stabilized beams

APPENDIX F

X-RAY DIFFRACTOGRAMS

AND

DIFFRACTION DATA

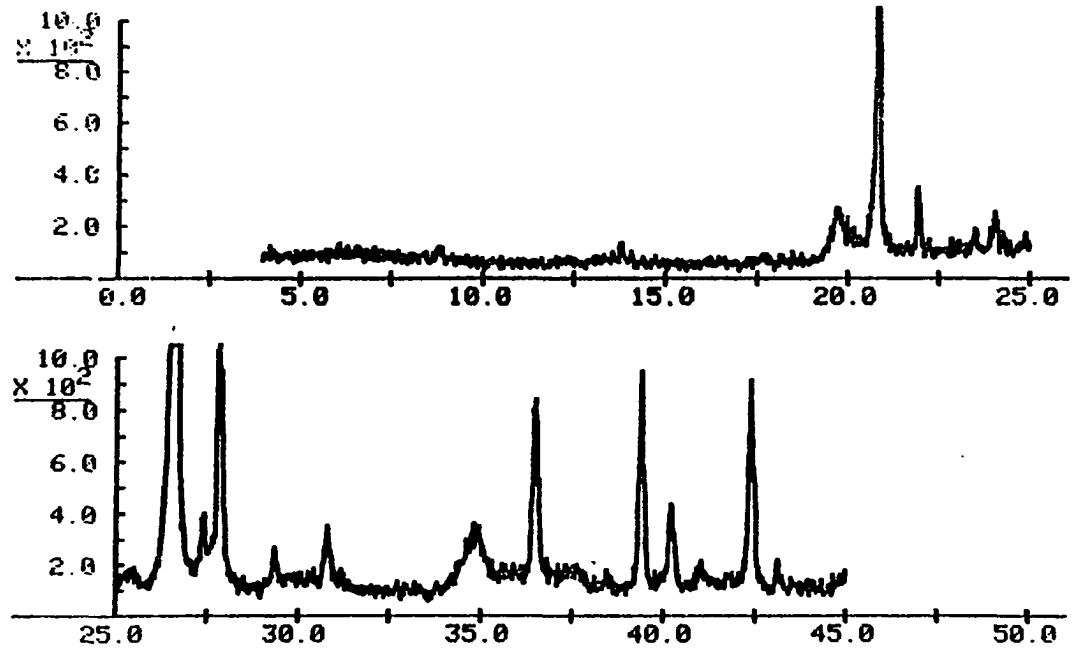

Figure F.1: X-ray diffractogram of raw shale

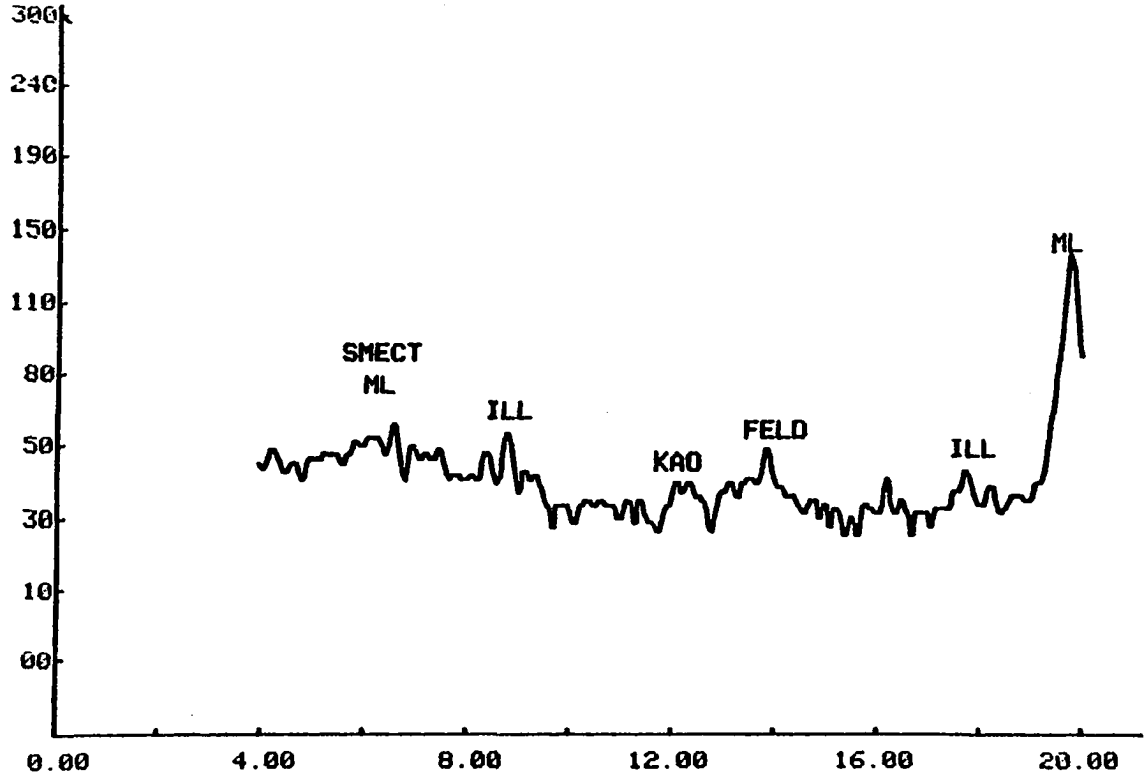

Figure F.2: Altenuated x-ray diffractogram of raw shale

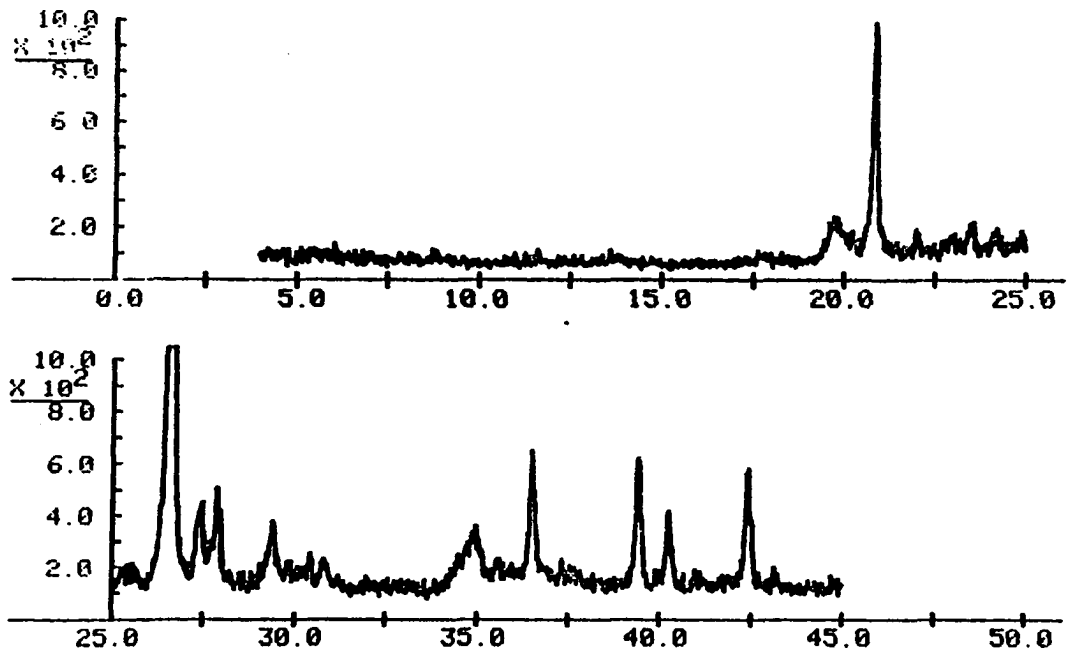

Figure F.3: X-ray diffractogram of lime stabilized shale

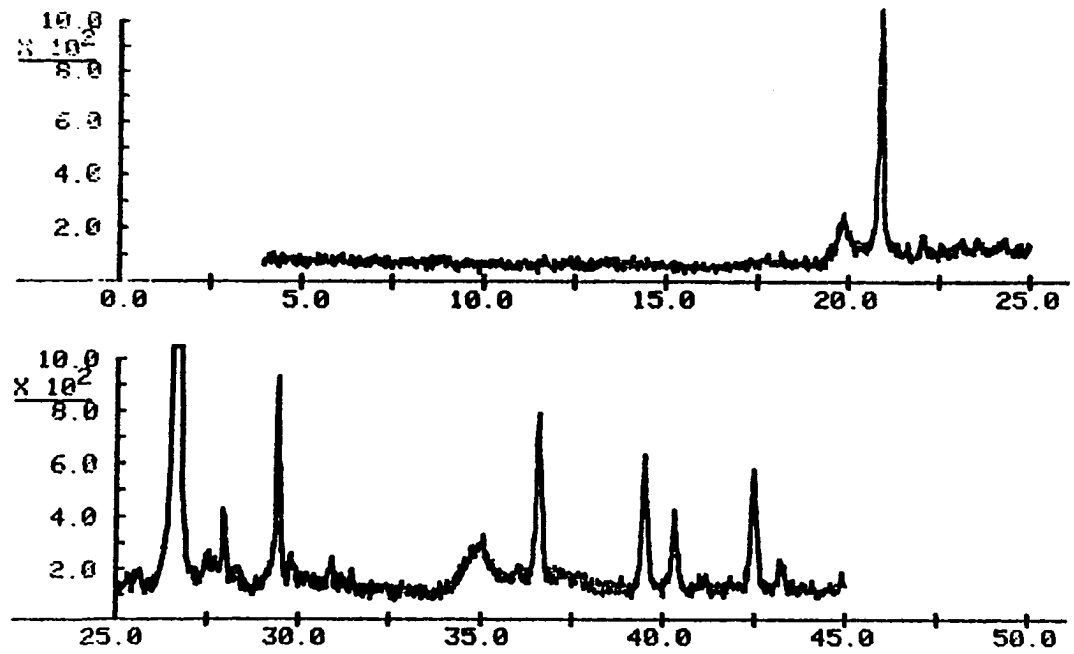

Figure F.4: X-ray diffractogram of lime stabilized shale (6%, 90°F, 28 days)

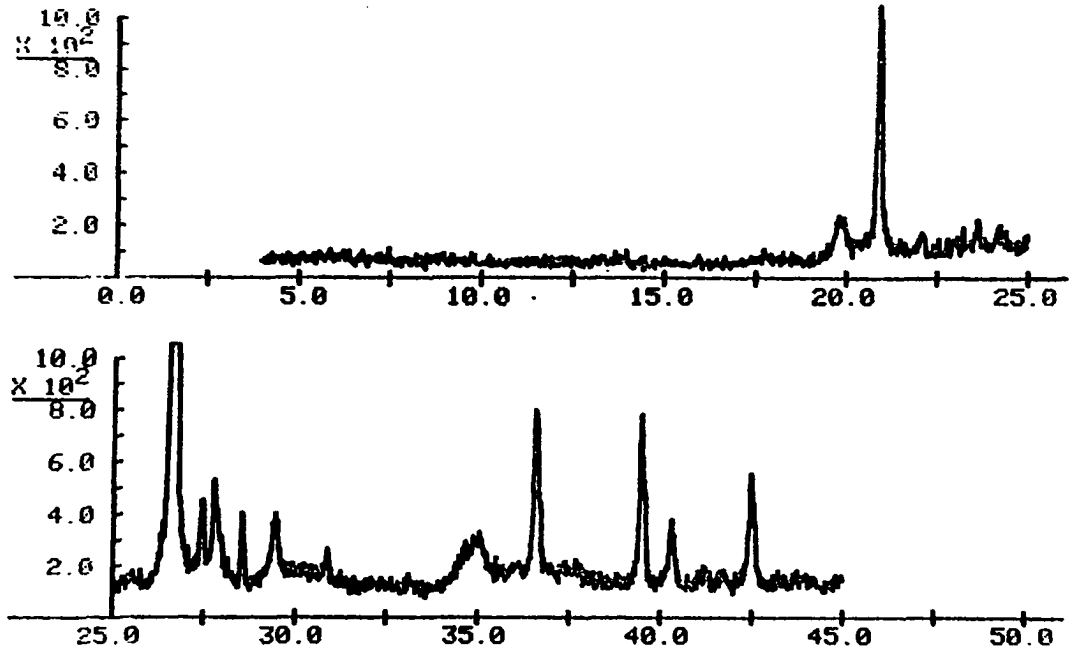

Figure F.5: X-ray diffractogram of lime stabilized shale (6%, 90°F, 90 days)

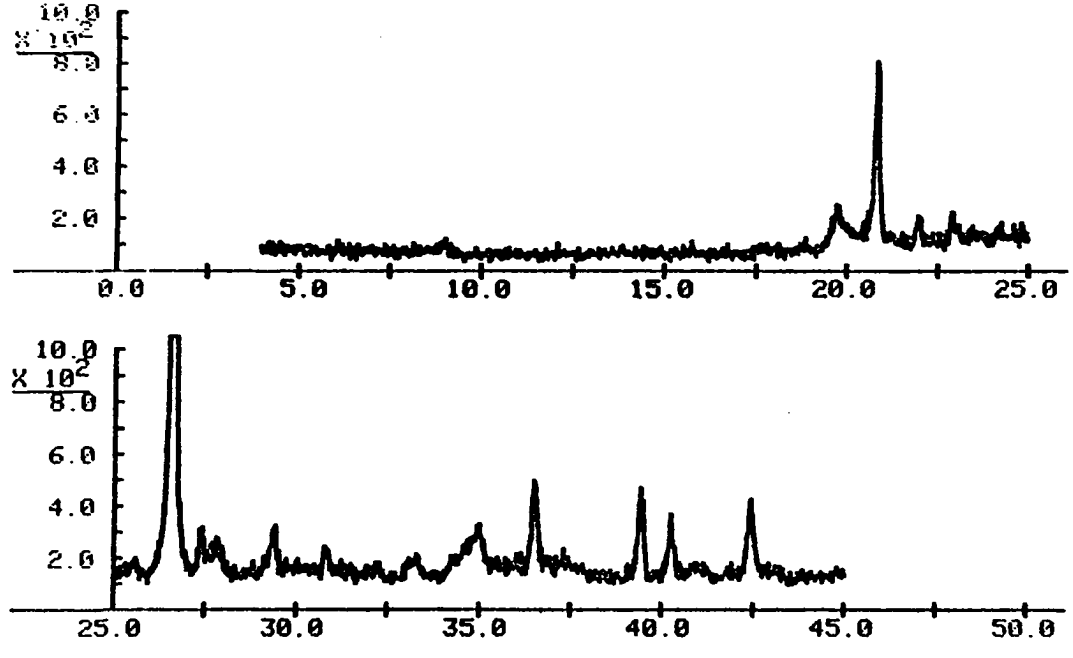

Figure F.6: X-ray diffractogram of fly ash stabilized shale (25%, 70°F, 28 days)

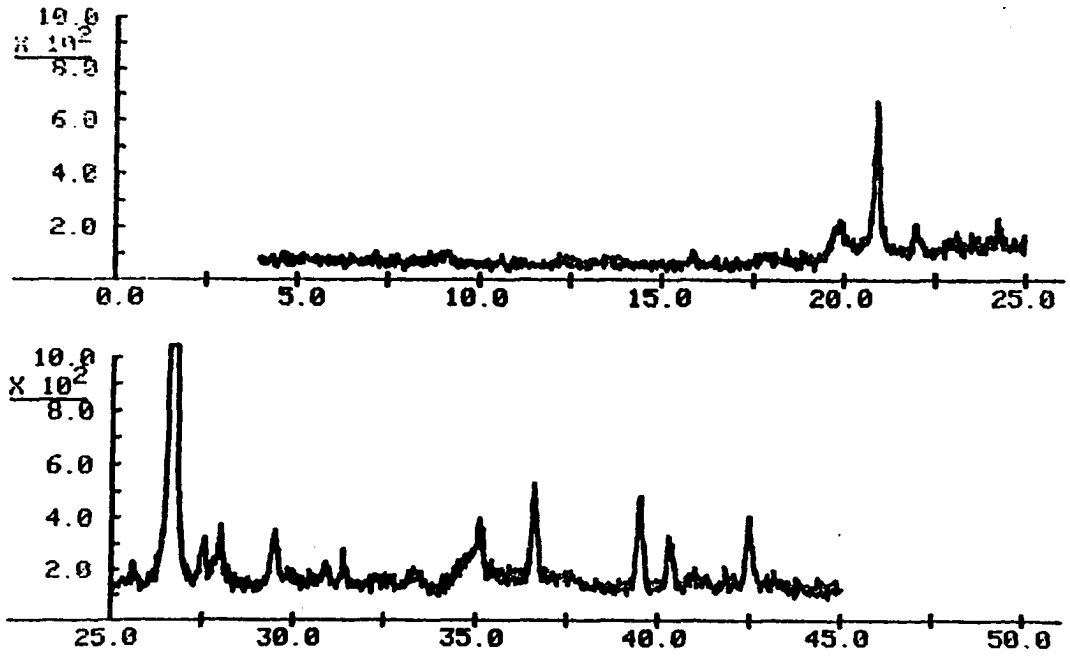

Figure F.7: X-ray diffractogram of fly ash stabilized shale (25%, 70°F, 90 days)

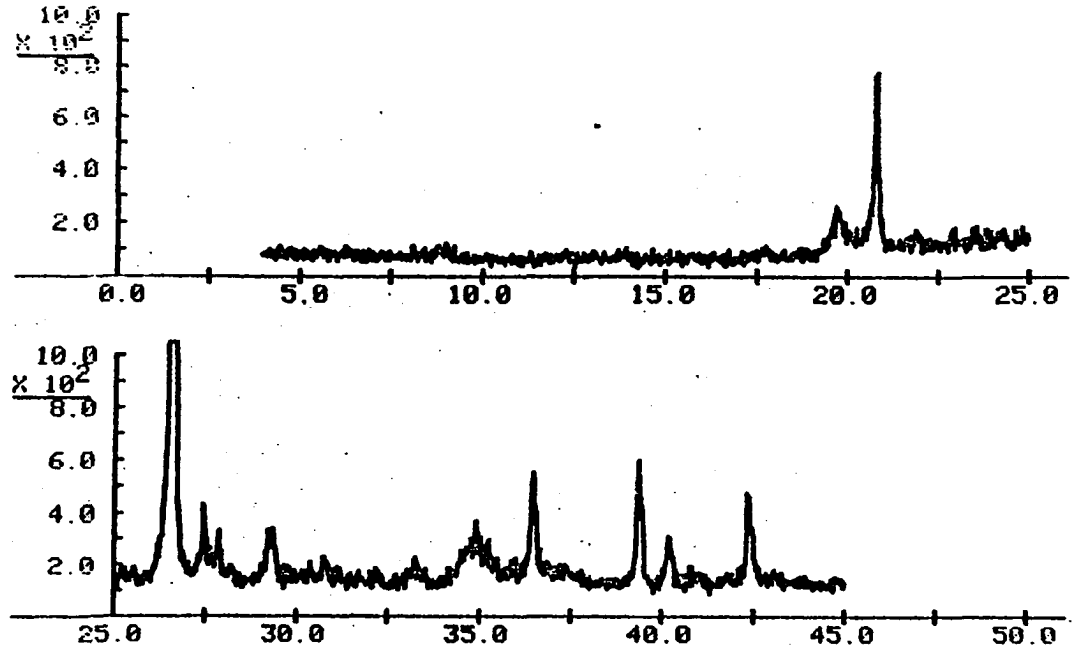

Figure F.8: X-ray diffractogram of fly ash stabilized shale (25%, 90°F, 28 days)

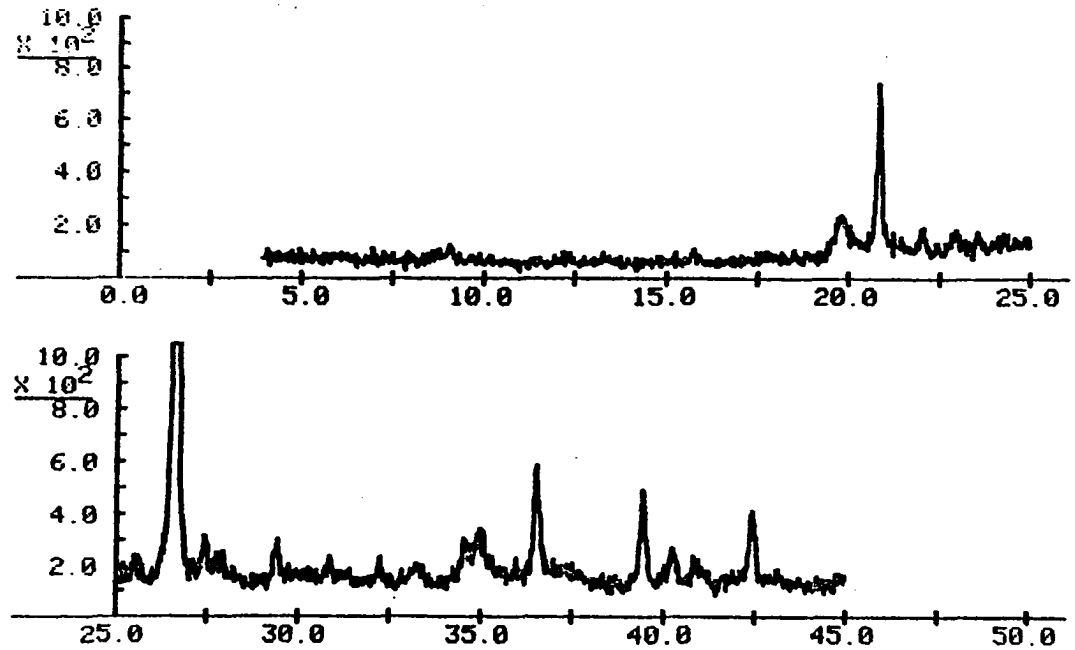

Figure F.9: X-ray diffractogram of fly ash stabilized shale (25%, 90°F, 90 days)

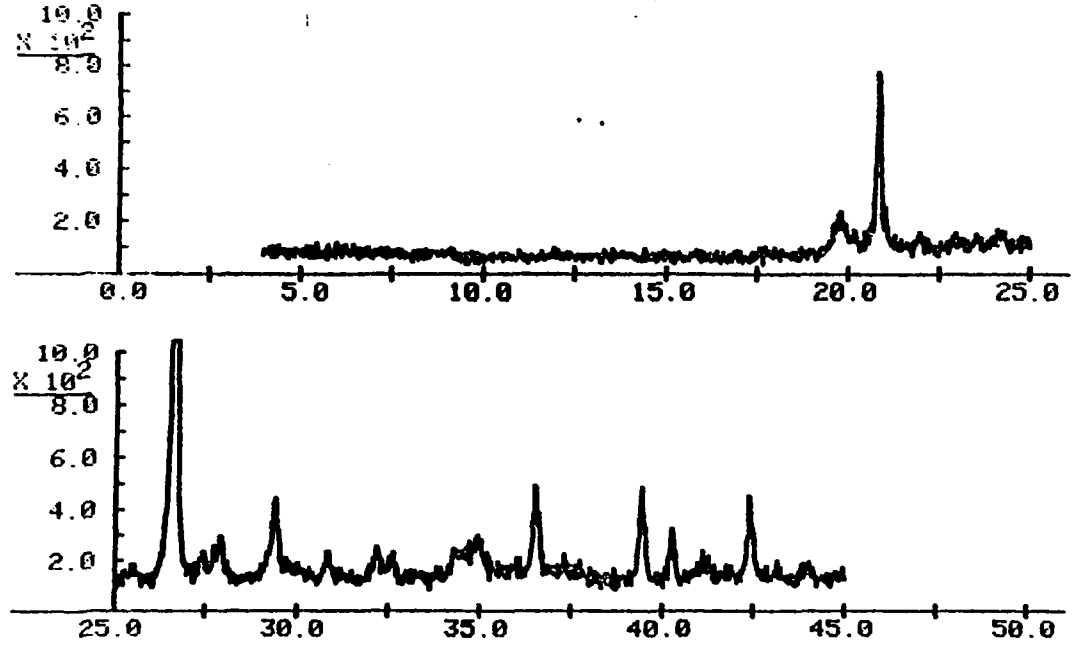

Figure F.10: X-ray diffractograms of cement stabilized shale (14%, 70°F, 28 days)

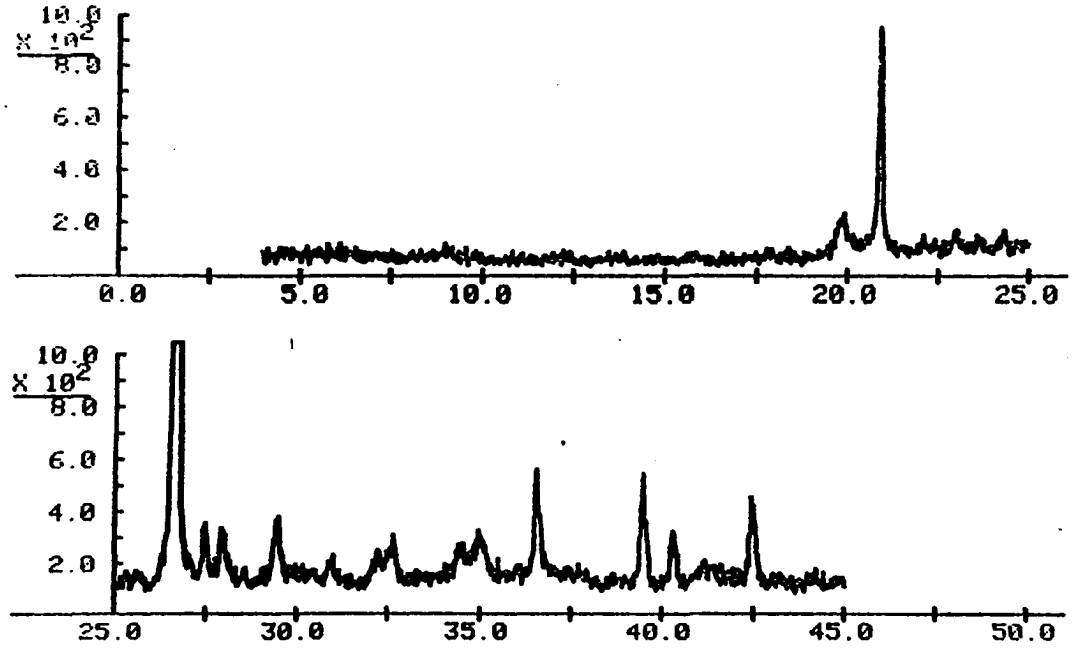

Figure F.11: X-ray diffractograms of cement stabilized shale (14%, 70°F, 90 days)

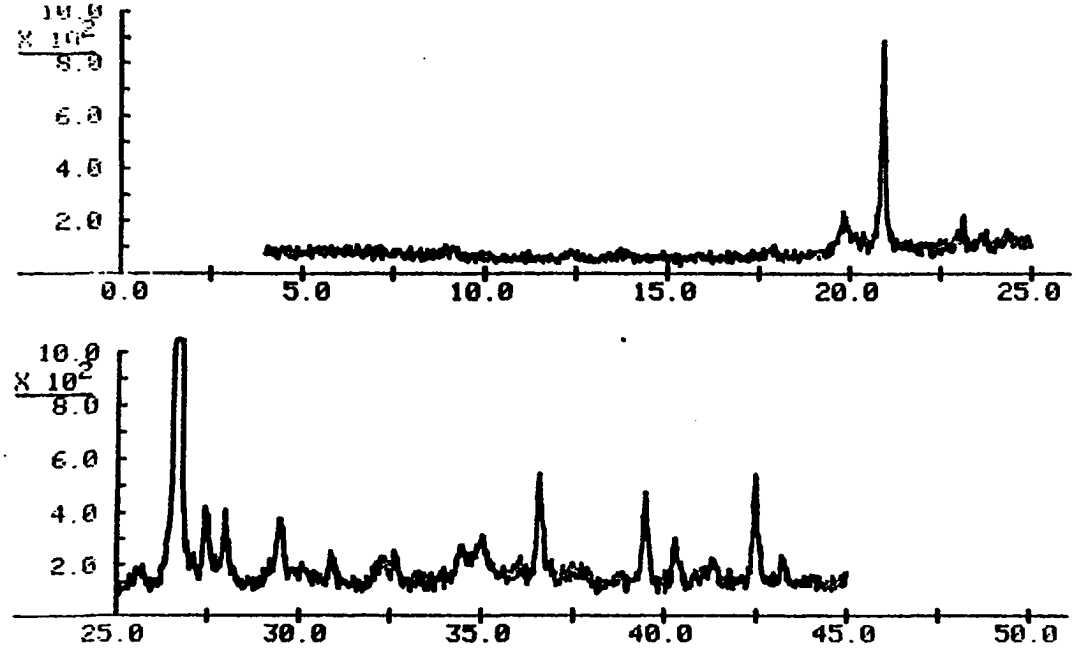

Figure F.12: X-ray diffractograms of cement stabilized shale (14%, 90°F, 28 days)

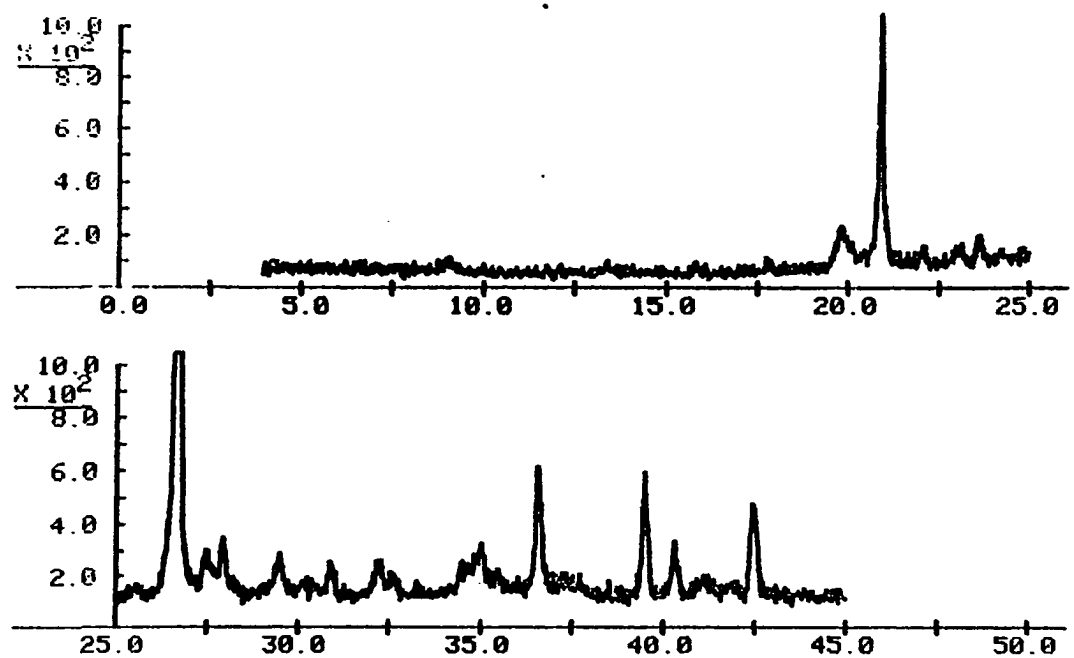

Figure F. 13: X-ray diffractogram of cement stabilized shale (14%, 90^{O}F, 90 days)

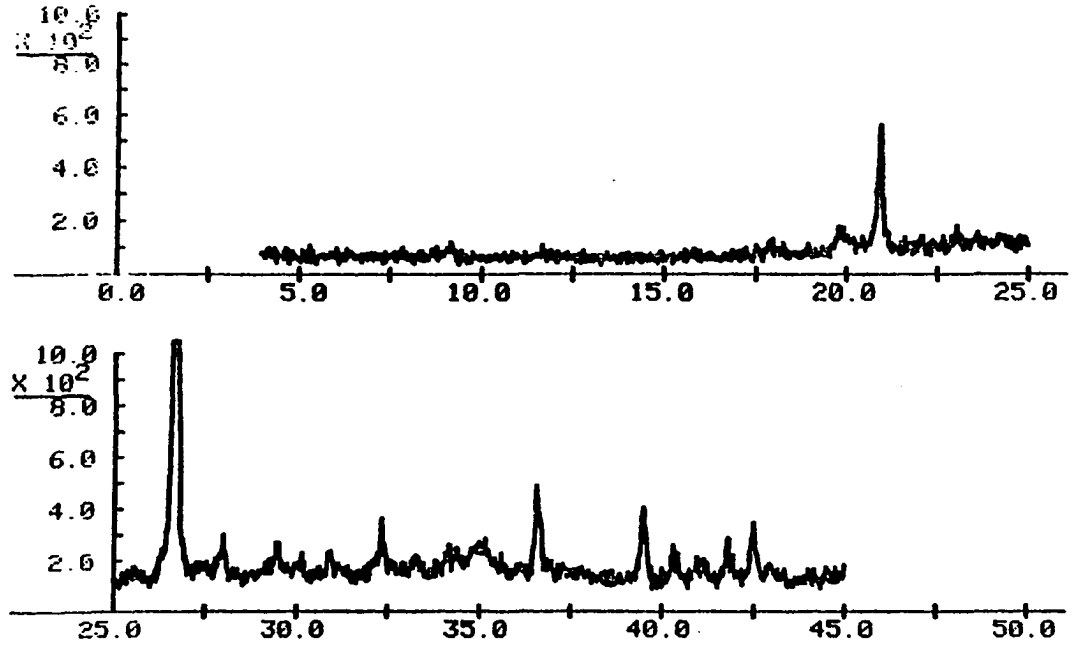

Figure F.14: X-ray diffractogram of conjunctively stabilized shale (8%c + 4%l + 18%f, 70°F, 28 days)

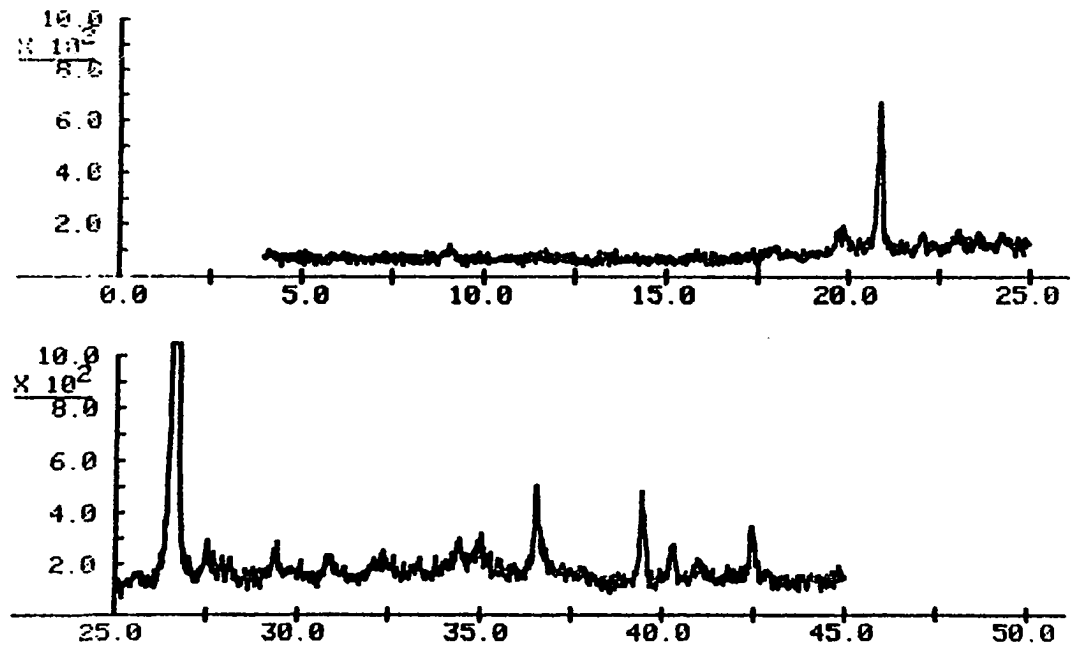

Figure F.15: X-ray diffractogram of conjunctively stabilized shale (8%c + 4%l + 18%f, 70°F, 90 days)

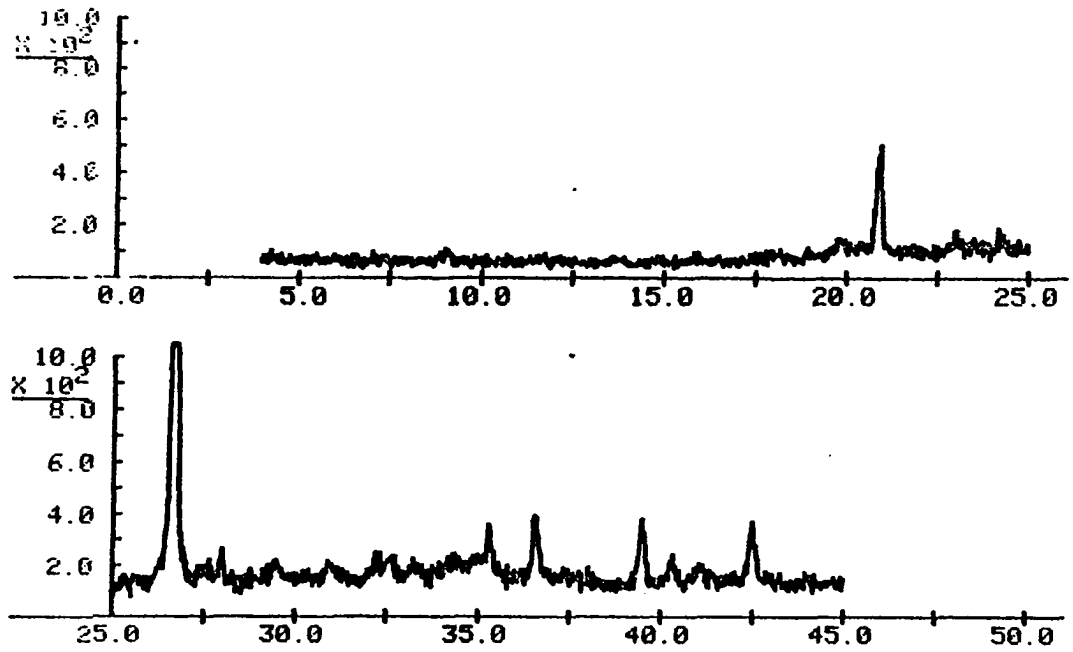

Figure F.16: X-ray diffractogram of conjunctively stabilized shale (8%c + 4%l + 18%f, 90°F, 28 days)

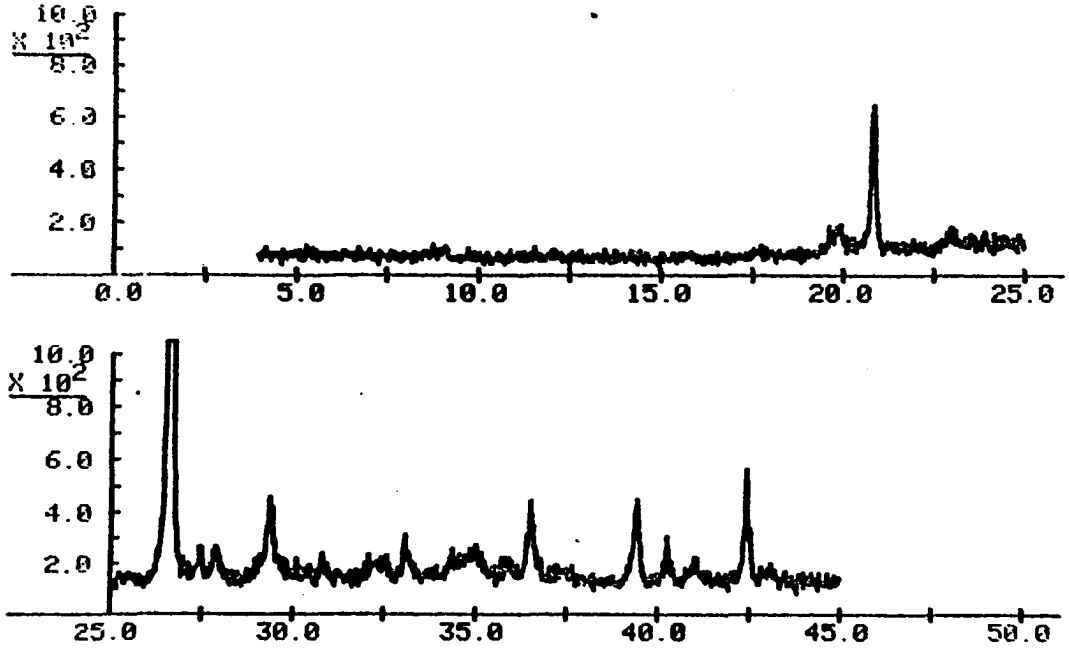

Figure F.17: X-ray diffractogram of conjunctively stabilized shale (8%c + 4%l + 18%f, 90°F, 90 days)

TABLE F.1: CRYSTALLINE DATA OF RAW SHALE

2θ Degrees	d-Spacing Angstroms	Peak Width	Peak Count	Peak Intensity%
8.81	10.02	0.31	24	0.64
13.82	6.40	0.18	35	0.93
17.70	5.01	0.30	6	0.15
19.74	4.49	0.32	83	2.22
20.82	4.26	0.13	697	18.67
21.95	4.05	0.14	112	3.01
23.46	3.79	0.20	23	0.62
24.01	3.70	0.23	49	1.31
24.29	3.66	0.13	21	0.57
25.40	3.50	0.38	30	0.81
26.60	3.35	0.16	3733	100.00
27.40	3.25	0.19	132	3.54
27.85	3.20	0.15	458	12.27
29.38	3.04	0.21	79	2.12
30.82	2.90	0.25	125	3.36
34.89	2.57	0.44	98	2.63
36.49	2.46	0.16	346	9.27
37.71	2.38	0.24	22	0.59
38.51	2.34	0.32	3	0.09
39.42	2.28	0.17	388	10.40
40.24	2.24	0.25	149	3.99
41.03	2.20	0.27	32	0.87
42.41	2.13	0.19	306	8.20
43.13	2.10	0.11	35	0.93

TABLE F.2: CRYSTALLINE DATA OF RAW SHALE STABILIZED WITH 6 PERCENT LIME CURED AT 70°F FOR 90 DAYS

2θ Degrees	d-Spacing Angstroms	Peak Width	Peak Count	Peak Intensity%
8.81	10.04	0.36	18	0.60
17.77	4.99	0.31	11	0.35
19.74	4.49	0.31	74	2.39
20.84	4.26	0.14	454	14.68
22.01	4.04	0.25	40	1.28
22.93	3.87	0.32	28	0.91
23.51	3.78	0.25	40	1.28
24.16	3.68	0.29	11	0.35
25.40	3.50	0.48	27	0.87
26.63	3.35	0.17	3091	100.00
27.40	3.25	0.17	128	4.13
27.93	3.19	0.15	146	4.74
29.38	3.04	0.25	94	3.04
30.45	2.93	0.20	59	1.92
30.87	2.89	0.24	49	1.59
34.94	2.56	0.41	86	2.80
36.54	2.46	0.20	190	6.16
39.43	2.28	0.14	225	7.28
40.26	2.24	0.16	137	4.43
41.10	2.19	0.29	4	0.14
42.40	2.13	0.12	204	6.61
43.22	2.09	0.21	6	0.20

TABLE F.3: CRYSTALLINE DATA OF SHALE STABILIZED WITH 6 PERCENT LIME CURED AT 90°F FOR 28 DAYS

2θ Degrees	d-Spacing Angstroms	Peak Width	Peak Count	Peak Intensity%
8.91	9.91	0.40	12	0.49
19.85	4.47	0.32	79	3.14
20.90	4.25	0.14	471	18.69
22.09	4.02	0.33	30	1.20
23.09	3.85	0.26	24	0.95
23.60	3.77	0.26	23	0.91
24.24	3.67	0.31	25	0.99
25.60	3.48	0.41	42	1.68
26.68	3.34	0.16	2520	100.00
27.51	3.24	0.20	72	2.87
27.99	3.19	0.15	142	5.62
28.35	3.15	0.17	42	1.68
29.45	3.03	0.12	400	15.87
29.85	2.99	0.17	50	2.35
30.90	2.89	0.24	38	1.53
31.52	2.84	0.19	32	1.29
34.96	2.56	0.53	85	3.36
36.62	2.45	0.17	279	11.07
39.51	2.28	0.23	243	9.66
40.35	2.23	0.21	142	5.62
41.09	2.19	0.32	18	0.70
42.49	2.13	0.19	213	8.46
43.24	2.09	0.25	55	2.17

TABLE F.4: CRYSTALLINE DATA OF SHALE STABILIZED WITH 6 PERCENT LIME CURED AT 90°F FOR 90 DAYS

2θ Degrees	d-Spacing Angstroms	Peak Width	Peak Count	Peak Intensity%
19.84	4.47	0.31	71	2.80
20.91	4.24	0.10	424	16.84
22.07	4.03	0.25	28	1.11
23.59	3.77	0.21	37	1.48
24.24	3.67	0.25	20	0.80
25.51	3.49	0.49	16	0.63
26.68	3.34	0.15	2520	100.00
27.47	3.24	0.14	159	6.30
27.81	3.21	0.16	199	7.89
28.57	3.12	0.12	114	4.54
29.45	3.03	0.26	125	4.98
30.90	2.89	0.25	59	2.35
35.02	2.56	0.43	76	3.00
36.59	2.45	0.18	320	12.71
39.51	2.28	0.18	234	9.29
40.33	2.23	0.23	110	4.37
41.20	2.19	0.26	16	0.63
41.74	2.16	0.23	3	0.13
42.49	2.13	0.21	185	7.34

TABLE F.5: CRYSTALLINE DATA OF SHALE STABILIZED WITH 25 PERCENT FLY ASH CURED AT 70°F FOR 28 DAYS

2θ Degrees	d-Spacing Angstroms	Peak Width	Peak Count	Peak Intensity%
9.03	9.79	0.39	14	0.66
15.75	5.62	0.31	17	0.80
19.74	4.49	0.31	69	3.30
20.84	4.26	0.14	346	16.57
21.98	4.04	0.21	44	2.09
22.90	3.88	0.15	46	2.21
25.55	3.48	0.38	27	1.29
26.63	3.35	0.16	2088	100.00
27.41	3.25	0.19	79	3.79
27.91	3.19	0.23	44	2.09
29.37	3.04	0.29	76	3.62
30.87	2.89	0.19	55	2.62
32.26	2.77	0.37	20	0.97
33.25	2.69	0.37	37	1.78
34.95	2.57	0.41	92	4.41
36.52	2.46	0.20	177	8.47
39.46	2.28	0.21	161	7.72
40.27	2.24	0.24	104	4.98
41.02	2.20	0.50	20	0.97
42.44	2.13	0.24	137	6.55

TABLE F.6: CRYSTALLINE DATA OF SHALE STABILIZED WITH 25 PERCENT FLY ASH CURED AT 70°F FOR 90 DAYS

2θ Degrees	d-Spacing Angstroms	Peak Width	Peak Count	Peak Intensity%
9.10	9.70	0.30	18	0.91
15.81	5.60	0.25	13	0.67
17.82	4.97	0.33	21	1.09
19.83	4.47	0.42	61	3.14
20.91	4.24	0.18	286	14.75
22.01	4.03	0.25	53	2.75
23.00	3.86	0.26	41	2.12
24.26	3.67	0.25	52	2.68
25.62	3.47	0.31	61	3.14
26.71	3.34	0.17	1936	100.00
27.52	3.24	0.23	98	5.06
27.99	3.19	0.21	110	5.69
29.49	3.03	0.25	121	6.25
30.90	2.89	0.28	59	3.06
31.40	2.85	0.23	77	4.00
33.36	2.68	0.42	36	1.86
35.10	2.55	0.27	137	7.07
36.62	2.45	0.21	180	9.27
39.49	2.28	0.15	149	7.69
40.34	2.23	0.24	77	4.00
40.95	2.20	0.29	17	0.87
41.90	2.15	0.30	23	1.19
42.50	2.13	0.23	132	6.83

TABLE F.7: CRYSTALLINE DATA OF SHALE STABILIZED WITH 25 PERCENT FLY ASH CURED AT 90°F FOR 28 DAYS

2θ Degrees	d-Spacing Angstroms	Peak Width	Peak Count	Peak Intensity%
8.89	9.94	0.38	10	0.50
13.89	6.38	0.38	7	0.38
17.73	5.00	0.35	10	0.53
19.77	4.49	0.25	71	3.64
20.81	4.27	0.10	296	15.28
21.92	4.05	0.40	16	0.83
22.92	3.88	0.33	27	1.40
24.24	3.67	0.26	5	0.25
26.60	3.35	0.13	1936	100.00
27.46	3.25	0.18	123	6.36
27.88	3.20	0.14	74	3.82
29.30	3.05	0.29	69	3.56
30.82	2.90	0.24	34	1.74
32.24	2.77	0.29	10	0.53
33.29	2.69	0.44	29	1.51
34.85	2.57	0.32	81	4.18
36.49	2.46	0.18	182	9.41
39.40	2.28	0.20	222	11.47
40.21	2.24	0.26	86	4.47
40.91	2.20	0.42	18	0.91
42.40	2.13	0.19	151	7.81

TABLE F.8: CRYSTALLINE DATA OF SHALE STABILIZED WITH 25 PERCENT FLY ASH CURED AT 90°F FOR 90 DAYS

2θ Degrees	d-Spacing Angstroms	Peak Width	Peak Count	Peak Intensity%
9.10	9.70	0.34	28	1.31
15.77	5.62	0.35	20	0.94
19.79	4.48	0.39	61	2.84
20.87	4.25	0.10	240	11.21
22.01	4.03	0.26	41	1.91
22.92	3.88	0.31	21	0.99
23.59	3.77	0.28	18	0.86
24.20	3.68	0.32	10	0.45
25.56	3.48	0.29	41	1.91
26.63	3.34	0.15	2144	100.00
27.46	3.25	0.19	90	4.21
27.90	3.20	0.25	45	2.09
29.41	3.03	0.23	72	3.37
30.89	2.89	0.19	44	2.03
32.26	2.77	0.42	36	1.68
33.32	2.69	0.42	29	1.36
34.59	2.59	0.21	79	3.70
34.99	2.56	0.26	99	4.57
36.56	2.46	0.23	219	10.22
39.45	2.28	0.16	161	7.52
40.28	2.24	0.25	62	2.91
40.98	2.20	0.44	18	0.82
42.49	2.13	0.14	119	5.54

TABLE F.9: CRYSTALLINE DATA OF SHALE STABILIZED WITH 14 PERCENT CEMENT CURED AT 70°F FOR 28 DAYS

2θ Degrees	d-Spacing Angstroms	Peak Width	Peak Count	Peak Intensity%
19.78	4.48	0.36	67	3.25
20.85	4.25	0.15	328	15.82
21.09	4.21	0.16	64	3.09
22.01	4.03	0.31	33	1.57
23.00	3.86	0.29	26	1.26
23.54	3.78	0.21	27	1.31
24.20	3.68	0.40	40	1.92
25.44	3.50	0.41	40	1.92
26.65	3.34	0.13	3070	100.00
27.43	3.25	0.21	64	3.09
27.91	3.19	0.32	98	4.73
29.40	3.04	0.25	172	8.29
30.87	2.89	0.25	66	3.17
32.21	2.78	0.29	77	3.74
32.65	2.74	0.23	62	3.01
34.38	2.61	0.34	66	3.17
34.96	2.56	0.39	86	4.18
36.52	2.46	0.23	177	8.54
39.46	2.28	0.21	169	8.16
40.29	2.24	0.24	98	4.73
41.15	2.19	0.41	26	1.26
42.44	2.13	0.24	135	6.50
43.20	2.09	0.33	22	1.07
43.99	2.06	0.33	18	0.89

TABLE F.10: CRYSTALLINE DATA OF SHALE STABILIZED WITH 14 PERCENT CEMENT CURED AT 70°F FOR 90 DAYS

2θ Degrees	d-Spacing Angstroms	Peak Width	Peak Count	Peak Intensity%
9.03	9.78	0.31	11	0.62
17.87	4.96	0.25	7	0.42
19.85	4.47	0.31	69	3.94
20.91	4.24	0.13	408	23.35
23.01	3.86	0.23	40	2.27
23.65	3.76	0.33	30	1.71
24.27	3.66	0.30	28	1.61
25.73	3.46	0.19	32	1.86
26.71	3.33	0.13	1747	100.00
27.51	3.24	0.13	112	6.43
27.76	3.21	0.15	55	3.13
28.01	3.18	0.23	108	6.19
29.46	3.03	0.27	112	6.43
30.96	2.89	0.25	40	2.27
32.20	2.78	0.30	48	2.72
32.65	2.74	0.26	76	4.33
34.46	2.60	0.25	58	3.31
35.09	2.56	0.25	58	3.31
36.61	2.45	0.19	132	7.57
39.52	2.28	0.20	202	11.54
40.34	2.23	0.21	102	5.84
41.16	2.19	0.57	45	2.57
42.49	2.13	0.27	146	8.38
43.23	2.09	0.31	18	1.01
44.16	2.05	0.32	9	0.52

TABLE F.11: CRYSTALLINE DATA OF SHALE STABILIZED WITH 14 PERCENT CEMENT CURED AT 90°F FOR 28 DAYS

2θ Degrees	d-Spacing Angstroms	Peak Width	Peak Count	Peak Intensity%
9.08	9.73	0.34	14	0.59
12.34	7.17	0.37	10	0.44
13.85	6.39	0.31	17	0.73
17.85	4.97	0.31	16	0.69
19.85	4.47	0.27	58	2.51
20.92	4.24	0.13	376	16.34
23.10	3.85	0.17	48	2.07
23.67	3.76	0.22	15	0.66
24.34	3.65	0.38	25	1.09
25.68	3.47	0.26	31	1.36
26.70	3.34	0.16	2304	100.00
27.15	3.28	0.19	64	2.78
27.49	3.24	0.25	119	5.16
28.01	3.18	0.19	125	5.44
29.49	3.03	0.26	108	4.69
30.93	2.89	0.24	55	2.38
32.24	2.77	0.30	30	1.31
32.68	2.74	0.20	36	1.56
34.46	2.60	0.25	71	3.06
35.01	2.56	0.36	72	3.14
36.60	2.45	0.21	196	8.51
37.84	2.38	0.37	18	0.77
39.56	2.28	0.21	172	7.45
40.35	2.23	0.26	67	2.92
41.35	2.18	0.33	41	1.78
42.49	2.13	0.12	174	7.56

TABLE F.12: CRYSTALLINE DATA OF SHALE STABILIZED WITH 14 PERCENT CEMENT CURED AT 90°F FOR 90 DAYS

2θ Degrees	d-Spacing Angstroms	Peak Width	Peak Count	Peak Intensity%
9.05	9.77	0.42	10	0.50
15.87	5.58	0.25	10	0.53
17.81	4.98	0.31	10	0.50
19.82	4.48	0.37	66	3.40
20.89	4.25	0.14	467	24.21
22.07	4.03	0.21	18	0.92
23.05	3.86	0.29	17	0.87
23.63	3.76	0.25	38	1.99
25.53	3.49	0.31	21	1.10
26.70	3.34	0.13	1927	100.00
27.51	3.24	0.24	72	3.75
27.96	3.19	0.19	106	5.50
29.49	3.03	0.29	71	3.66
30.92	2.89	0.21	69	3.57
32.24	2.77	0.26	61	3.16
34.53	2.60	0.28	27	1.40
35.01	2.56	0.30	81	4.20
36.60	2.45	0.17	225	11.67
39.54	2.28	0.20	177	9.18
40.34	2.23	0.26	83	4.30
41.08	2.20	0.44	34	1.75
42.49	2.13	0.25	161	8.37

TABLE F.13: CRYSTALLINE DATA OF SHALE CONJUNCTIVELY STABILIZED, CURED AT 70°F FOR 28 DAYS

2θ Degrees	d-Spacing Angstroms	Peak Width	Peak Count	Peak Intensity%
9.15	9.66	0.31	14	1.11
15.81	5.60	0.34	7	0.55
17.96	4.93	0.38	23	1.87
19.87	4.47	0.42	34	2.73
20.91	4.24	0.15	228	18.51
23.04	3.86	0.30	22	1.79
24.29	3.66	0.33	11	0.88
25.57	3:48	0.45	20	1.64
26.71	3.34	0.14	1232	100.00
27.96	3.19	0.27	44	3.54
29.48	3.03	0.25	66	5.33
30.13	2.96	0.25	18	1.43
30.93	2.89	0.24	49	3.98
32.35	2.76	0.27	81	6.57
33.32	2.69	0.30	29	2.37
34.24	2.62	0.35	53	4.33
35.06	2.56	0.51	49	3.98
36.65	2.45	0.15	125	10.18
39.52	2.28	0.23	139	11.30
40.37	2.23	0.25	59	4.81
41.10	2.19	0.40	19	1.57
41.76	2.16	0.19	34	2.73
42.49	2.13	0.19	104	8.44
43.05	2.10	0.35	14	1.11

TABLE F.14: CRYSTALLINE DATA OF SHALE CONJUNCTIVELY STABILIZED, CURED AT 70°F FOR 90 DAYS

2θ Degrees	d-Spacing Angstroms	Peak Width	Peak Count	Peak Intensity%
9.08	9.73	0.33	19	1.09
15.81	5.60	0.25	15	0.85
17.89	4.95	0.37	12	0.65
19.81	4.48	0.19	30	1.70
20.86	4.26	0.14	269	15.10
22.01	4.03	0.27	27	1.52
23.00	3.86	0.35	21	1.19
23.60	3.77	0.33	23	1.29
24.28	3.66	0.31	22	1.24
25.66	3.47	0.31	20	1.14
26.65	3.34	0.17	1781	100.00
27.49	3.24	0.23	61	3.42
28.13	3.17	0.25	36	2.02
29.45	3.03	0.19	48	2.67
30.88	2.89	0.31	27	1.52
32.29	2.77	0.69	15	0.85
33.32	2.69	0.31	17	0.94
34.45	2.60	0.24	62	3.50
34.99	2.56	0.37	52	2.91
36.54	2.46	0.12	161	9.06
39.49	2.28	0.21	144	8.09
39.95	2.25	0.28	17	0.94
40.29	2.24	0.24	66	3.68
41.04	2.20	0.36	32	1.82
42.49	2.13	0.20	98	5.50

TABLE F.15: CRYSTALLINE DATA OF SHALE CONJUNCTIVELY STABILIZED, CURED AT 90°F FOR 28 DAYS

2θ Degrees	d-Spacing Angstroms	Peak Width	Peak Count	Peak Intensity%
9.02	9.80	0.30	13	0.94
18.98	4.67	0.32	4	0.26
19.85	4.47	0.42	31	2.28
20.88	4.25	0.25	172	12.47
22.99	3.86	0.32	26	1.89
24.26	3.67	0.33	19	1.41
26.69	3.34	0.19	1376	100.00
27.54	3.24	0.21	25	1.82
27.99	3.19	0.20	38	2.79
29.47	3.03	0.37	34	2.44
31.00	2.86	0.31	28	2.04
32.20	2.78	0.29	40	2.88
32.65	2.74	0.31	40	2.88
33.33	2.69	0.35	27	1.96
35.33	2.54	0.19	106	7.71
36.60	2.45	0.24	106	7.71
39.51	2.28	0.23	106	7.71
40.38	2.23	0.23	38	2.79
41.07	2.20	0.38	35	2.53
42.51	2.12	0.27	119	8.63
44.05	2.05	0.42	23	1.67

TABLE F.16: CRYSTALLINE DATA OF SHALE CONJUNCTIVELY STABILIZED, CURED AT 90°F FOR 90 DAYS

2θ Degrees	d-Spacing Angstroms	Peak Width	Peak Count	Peak Intensity%
9.04	9.77	0.37	12	0.79
15.79	5.61	0.32	8	0.54
17.68	5.01	0.32	15	0.98
19.82	4.48	0.43	41	2.64
20.84	4.26	0.14	266	17.12
22.99	3.87	0.37	16	1.03
26.63	3.35	0.16	1552	100.00
27.45	3.25	0.24	40	2.56
27.90	3.19	0.26	59	3.82
29.35	3.04	0.22	135	8.67
30.86	2.90	0.24	22	1.68
32.46	2.76	0.35	29	1.88
33.15	2.70	0.32	36	2.32
34.39	2.61	0.31	46	2.98
34.99	2.56	0.40	52	3.34
36.52	2.46	0.24	135	8.67
39.44	2.28	0.19	161	10.39
40.26	2.24	0.21	76	4.88
41.01	2.20	0.43	34	2.17
42.41	2.13	0.14	207	13.36
43.06	2.10	0.26	18	1.19